Regolith-Landforms and plant biogeochemical expression of buried mineralisation targets in the Northern Middleback Ranges, ("Iron Knob South") South Australia

Louise Thomas

Geology and Geophysics, School of Earth and Environmental Science,
University of Adelaide, Adelaide SA 5005, Australia

A manuscript submitted for the Honours Degree of Bachelor of Science,

University of Adelaide, 2011

Supervised by Dr. Steven M. Hill

ABSTRACT

South of the town Iron Knob on the northern Eyre Peninsula, a tenement scale plant biogeochemical survey and regolith-landform mapping, combined to define areas with elevated Cu, Zn and Au contents that are worthy of follow-up exploration. Plant biogeochemistry was conducted within a 6 Km^2 area with 1 Km spacing between each E-W trending transect and 200 m spacing between each sample. A regolith-landform map presents the distribution of regolith materials and associated landscape processes to help constrain geochemical dispersion. A Philips XL30 SEM provided insight into how the plants uptake certain elements and distribute them within the organs structure. Two zones of elevated trace metals (e.g. Cu, Au and Zn) were defined either side of a NW-SE structure crossing over the N-S trending 'Katunga' ridge. Both targets were located on similar regolith-landform units of sheet-flood fans and alluvial plains. Copper and Zn results were best represented by the western myall species while the bluebush species was best at detecting Au. A follow up study targeting the NW-SE structure with closer sample spacing is recommended in further constraining drilling targets. For the tenement holding company, Onesteel Ltd, these results are significant as they define two new areas of interest for possible IOCG mineralisation. For research purposes the results confirm that plant biogeochemistry can be used as an effective tool for detecting mineralisation along buried structures providing the use of the right species in the area.

Key Words: Iron Knob, northern Eyre Peninsula, plant biogeochemistry, regolith-landform, Onesteel, IOCG mineralisation

Table of Contents

1.0.   INTRODUCTION

Regions in Australia with exposed bedrock have generally been well explored for mineral deposits, meaning that the areas with the greatest potential for new discovery occur beneath the less explored areas of transported cover. The Eastern Gawler Craton in South Australia is host to some of the world's largest Iron Oxide Copper Gold (IOCG) deposits (Skirrow & Davidson, 2007), however, exploration is largely impeded by the thick layer of regolith. Exploration for IOCG targets under cover has traditionally been carried out using geophysics and drilling, which so far have contributed to discovering large, buried ore bodies such as the Prominent Hill and Olympic Dam IOCG±U deposits in South Australia. Geophysical mapping of magnetic and gravity anomalies has in most cases been one of the first steps in identifying an exploration target, followed by drilling, which, however, can be a time-consuming and expensive process. Ideally, a time and cost efficient, intermediate method to test the geochemical 'fertility' of buried geophysical targets prior to drilling could reduce the risk associated with unsuccessful drilling programs. Plant biogeochemistry offers such an intermediate technique, and is a major focus of this study.

Biogeochemical methods of exploration involve the chemical analysis of plant tissues to assess the presence and nature of underlying mineralization, bedrock composition, bedrock structure (faults, joints and folds), and the chemistry of the soil, surficial sediments, and associated groundwater (Dunn 2007). Studies of the relationship between plant chemistry and mineralised rock have been recorded as far back as 1898 when the Omai gold mine in Guyana used ash samples of Baromalli (*Castostemma spp.*) and 'Ironwood' for a measure of the gold concentration (Lungwitz 1900, Dunn 2007). Well documented accounts of biogeochemistry used in exploration became more common after the 1930's with the USSR, Sweden, England, North America and United States leading the way (Brundin 1939,

Warren *et al.* 1968, Kovalevsky 1987, Dunn 2007). Within Australia, plant biogeochemistry has been less widely adopted compared to other, such as stream sediment, soil, calcrete and 'lateritic' methods of regolith geochemical exploration. Successful studies conducted throughout the Gawler Craton (Sheard *et al.* 2009), Curnamona Province (Fabris *et al.* 2009) and regions of NSW (Hill & Hill 2003) however have helped to make plant biogeochemistry a more widely recognised and accepted exploration technique.

The study area provides an ideal setting for assessing the effectiveness of biogeochemical exploration for IOCG deposits undercover. It is on the south-eastern margin of the Gawler Craton within the Cleve sub-domain in the Northern Middleback Ranges. The area is at the northern end of Onesteels tenement (EL3516) close to the town of Iron Knob and the Iron Monarch mine. The vegetation of the study area is dominated by western myall (*Acacia papyrocarpa*) with an understory of pearl bluebush (*Maireana sedifolia*). Both types of vegetation have previously been used in biogeochemical studies and have proven their use in expressing buried mineralisation. Blackoak (*Casuarina pauper*) is also found in groves throughout the study area, in particular the area over 'Katunga' ridge and has been used successfully in plant biogeochemical studies elsewhere in the Central Gawler Craton (Hill 2009).

This study aims to provide a characterisation of the three most widespread plant species in the Iron Knob South study area and then interpret these characteristics within the context of their relationship to buried mineralisation targets. As part of this interpretation, the regolith-landform context of samples will also be constrained using a regolith-landform map. Provided that the plant sampling is reasonably consistent, the major variations in biogeochemical results will largely be attributed to bedrock (including mineralisation) characteristics and the regolith-landform setting. Provided the regolith-landforms are well

constrained, then a large component of the biogeochemical characteristics will be attributed

to bedrock contributions.

2.0. STUDY AREA

2.1. Location

Iron Knob is approximately 50 km NW of Whyalla on the northern Eyre Peninsula. The area corresponds to the northern section of Onesteels tenement (EL3516) boundary in the Middleback Ranges (Figure 1). The study area is on 'Katunga' station just south of Iron Knob. The main vehicular access is via the Iron Knob - Whyalla Road and the Eyre Highway, and some further access was granted using station tracks.

2.2. Climate

Iron Knob in the Middleback Ranges is in an arid to semi-arid region. In the summer months between December and February maximum daily temperatures vary between 28°C and 29.7^{o}C with overnight minimums averaging between 15.9^{o}C and 17.7^{o}C (WeatherZone 2011). During the winter months between June and August maximum daily temperatures average between 17°C and 18.3^{o}C with overnight minimums averaging between 5.2^{o}C and 6.1^{o}C (WeatherZone 2011).The mean annual rainfall at Iron Knob is approximately 272 mm, with the majority falling in the cooler winter months (WeatherZone 2011). Prevailing winds are aligned in a generally north-south orientation with southerly winds being more common than northerly winds in all seasons except winter (Onesteel 2009).

2.3. Vegetation

Most of the vegetation in the study area, on either side of the 'Katunga ridge' is used for grazing (Figure 2). In the south of the area, close to Pine Creek, is where the vegetation is most dense. The vegetation communities in the area include both low open woodland communities and chenopod shrubland. The low open woodland communities are dominated by sugarwood (*Myoporum platycarpum*), western myall (*Acacia papyrocarpa*) and mulga

(*A. aneura*) with understoreys of pearl bluebush (*Maireana sedifolia*). The chenopod shrubland community is characterised by minimal tree cover, but with black oak (*Casuarina pauper*), mulga and rosewood (*Alectryon oleifolius*) trees in thickets across the area (Hill 2009). This community consists of pearl bluebush, bladder saltbush (*Atriplex vesicaria)* and the occasional bluebush daisy (*Cratystylis conocephala*) and on the ridges grades into a hummock grassland understorey dominated by spinifex (*Triodia irritans*).

2.4. Geology

The geology described in this paper is of the northern Middleback Ranges occurring within the Cleve Sub-domain of the south eastern margin of the Gawler Craton. The Cleve domain is a major Early to Middle Proterozoic orogenic belt or 'mobile zone' which extends down the length of eastern Eyre Peninsula and east to Yorke Peninsula (Parker & Lemon 1982). The Proterozoic belt is characterised by a sequence of highly metamorphosed and deformed sediments, including quartzite's, schists/gneisses, dolomites, iron formations and amphibolites, collectively known as the Hutchison Group (Parker & Lemon 1982). Three main sequences make up the Hutchison group: a basal quartzite sequence (Warrow Quartzite), a mixed chemical and clastic sequence (Middleback Subgroup), and an upper psammopelitic unit (Yadnarie Schist) (Schwarz 2004).

The Middleback Subgroup can be further sub-divided into four stratigraphic units: Katunga Dolomite, Lower Middleback Jaspilite, Cook Gap Schist and Upper Middleback Jaspilite.

- Katunga Dolomite: Conformably overlies the Warrow Quartzite and is a massive to poorly banded dolomitic marble with minor banded calc-silicate gneiss.

- Lower Middleback Jaspilite: Consists of five different members, from the top of the Katunga Dolomite these are: a graphitic quartzite (Poornamookinnie Member), carbonate facies banded iron formation (BIF) below a silicate BIF (Duke member), oxide facies BIF (Duchess Member), Mixed silicate and carbonate BIF (Knight member) and a mixed silicate facies BIF with schist (Long Gully Member). This unit conformably overlies the Katunga Dolomite.

- Cook Gap Schist: Consists of strongly foliated massive amphibolites, layered garnetiferous migmatite gneiss and layered medium to fine grained quartz veined garnetiferous gneiss and schist.

- Upper Middleback Jaspilite: Regularly banded mixed silicate and carbonate facies BIF with local oxide facies BIF in the Middleback Range and graphitic quartzite in western regions (Parker *et al.* 1985).

The mixed chemical and clastic metasediments of the Middleback Subgroup represent a number of cyclic transgressions and regressions of the sea either across a continental shelf or within a major basin deepening to the east (Parker & Lemon 1982, Parker *et al.* 1985). The Cook Gap Schist and Yadnarie Schist each represent a transgressive influx of deeper water clastic sediments (Parker & Fanning 1998). Conformable amphibolites in the Cook Gap Schist are of quartz tholeiite composition and probably represent either mafic volcanic extrusions or mafic sills intruded before deformation (Parker *et al.* 1985). Similar amphibolites occur in the Willyama Supergroup in Broken Hill and Olary (Parker *et al.* 1985). Unlike Broken Hill type mineralisation, the zinc-silver mineralisation however, is associated with the dolomitic carbonates and calc-silicates of the Katunga Dolomite, Lower and Upper Middleback Jaspilites and the Warrow Quartzite (Parker *et al.* 1985, Parker & Fanning 1998). Two subsequent phases of basin development followed The Hutchinson Group formation (Fanning *et al.* 1988). The first of these phases was the deformed rhyolite

and rhyodacite of the Myola Volcanics, amphibolites and interlayered mica schist and laminated quartzite (Fanning *et al.* 1988). The second phase on the eastern Eyre Peninsula was of the McGregor Volcanics consisting of a bimodal suite of rhyolitic-dacitic ash-flow tuffs and basaltic lava flows (Moonabie Formation) (Fanning *et al.* 1988).

Two major periods of complex deformation, metamorphism and plutonism have been recognised within the southern Gawler Craton (Figure 3) (Parker & Lemon 1982, Fanning *et al.* 1988). The Sleafordian Orogeny which culminated *c.* 2300 Ma ago, affecting the Archaean and early Proterozoic basement rocks, and the Kimban Orogeny, which extended from *c.* 1820-1580 Ma (Parker & Lemon 1982, Parker *et al.* 1985, Webb *et al.* 1986). A later but much weaker deformation event, the Wartaken Event is recognised locally throughout the Craton, this occurred 1500-1450 Ma (Parker *et al.* 1985). Three deformational episodes (D_1, D_2, D_3) have been recognised within the Kimban Orogeny effecting the sediments and volcanics within each of the Hutchison Group, Myola Volcanics and McGregor Volcanics sequences (Fanning *et al.* 1988). The three deformational episodes include regional metamorphism and schistosity formation (D_1), overturned isoclinal folding (D_2), and upright, open folding and mylonitisation (D_3) (Parker & Lemon 1982). The peak observed metamorphic grade of the Hutchison Group occurring at 1845-1700 Ma (Webb *et al.* 1986) is of middle to upper amphibolite facies (Parker 1978).

2.5. Previous Exploration in Area

No previous exploration for IOCG deposits has taken place in the area of Iron Knob. Exploration of the area has been purely for deposits of iron ore hosted in the metamorphosed sediments of the Hutchison Group within the Middleback Ranges. Further south of Iron Knob however has been iron-oxide copper gold exploration undertaken by Equinox Resources (1997-1998) and Helix Resources (1997-1998) using calcrete sampling

to define drill targets. More recently honours students Mitchell (2010) and Hicks (2010) renewed the datasets of Equinox and Helix by completing a biogeochemical and geochemical survey of the Project Mawson area. The Project Mawson study area is located approximately 20 Km south from the southernmost transect of the Iron Knob south study area.

2.6. Exploration Potential of the Area

The Eastern Gawler Craton is a world-class IOCG terrain hosting well known deposits such as Olympic Dam, Carrapateena, Prominent Hill and Moonta. The following points indicate as to why exploration surrounding Iron Knob is occurring.

- The Middleback Ranges are host to a large hematite formation which has been the focus of mining and exploration for the past century. Exploration for copper and gold surrounding Iron Knob has never been considered until now.

- Sulphides and Au spatially associate with abundant (>10%) magnetite and or/ hematite (Skirrow 2004). The Iron Monarch mine within the field area provides such a hematite deposit.

- Iron Knob is located on the margin of the 'premier uranium bearing' IOCG, > 500 Km-long Olympic Cu-Au-(U) province (Skirrow *et al.* 2007) and is within the Moonta Au corridor (Figure 4).

- There is a lack of deep regolith over the eastern Eyre Peninsula

- Diamond Drilling by Onesteel at the recently explored Project Mawson area, 20 Km South of Iron Knob has returned results of chalcopyrite and native copper in the core.

- The 1615-1645 Ma McGregor Volcanics possibly created both a source of heat and metals when they intruded into the area, necessary for the mineralisation of IOCG deposits.

3.0.   METHODOLOGY

This study includes four main components, therefore requiring four main methods associated with each:

1. Biogeochemistry;

2. The production of a regolith-landform map and the subsequent development of a local landscape evolution model.

3. Use of the Philips XL30 SEM; and,

4. Geochemistry

3.1. Biogeochemistry

Plant Biogeochemistry was the main method relied upon in this study to produce the analytical results. Some advantages of this technique include:

- Widespread and in some cases abundant vegetation cover across the landscape;

- easy access to samples;

- ability for plant roots to penetrate transported cover and transfer elements from depth to the surface;

- environmentally passive exploration approach, with minimal site disturbance and need for remediation; and,

- some proven exploration success and expression of buried mineralisation (Hill 2009, Sheard *et al.* 2009).

The species, western myall (*Acacia papyrocarpa*), pearl bluebush (*Maireana sedifolia)* and black oak (*Casuarina pauper*) were the targets of the biogeochemistry program.

Western myall (Figure 5) and pearl bluebush (Figure 6) were first chosen as the sample targets as they are both native to the 'Katunga' area and are both in abundance. The

blackoak species (Figure 7) was later recruited as a sample target, after finding that it was abundant over the Katunga ridge and in small groves across the study area. The wide, spreading root systems and deep penetrating sinker roots of each of these species are ideal attributes for plant biogeochemistry to be used to explore for buried mineralisation targets.

The western myall is one of South Australia's major arid zone trees, occurring in a broad belt from the Flinders Ranges to the Nullarbor Plain (Boomsma & Lewis 1981, Lange & Sparrow 1992). It grows on calcareous soils in the 150 – 300 mm rainfall zone (S.A.A.L.N.R.M.B. 2008). The western myall is a slow growing species and may reach up to 6 m before becoming recumbent (lying down) (Lange & Sparrow 1992, S.A.A.L.N.R.M.B. 2008). The canopy of the western myall tree can be used as a rough estimate of age (Figure 8), mature trees vary from 250 years to 350+ years (S.A.A.L.N.R.M.B. 2008). As for all acacias, rather than leaves, the western myall has phyllodes which appear silvery in the younger foliage and green in more mature foliage. These phyllodes are needle-like, quite rigid and are approximately 4-8 cm long (S.A.A.L.N.R.M.B. 2008).

Pearl bluebush is throughout most of this area as it is associated with regolith substrates that allow great root penetration, such as fractured bedrock or sites with calcareous soils (Hill & Hill 2003) as on the Eyre Peninsula. The pearl bluebush is reported to live at least 150-300 years and has a relatively deep tap-root system (up to 3 m) with shallow deciduous feeding roots (Cunningham *et al.* 1992, Hill 2009). It is described by Hill (2009) in (Sheard *et al.* 2009) as a multi-branched shrub, with 4-8 mm long green/greyish succulent leaves that join directly to the stem.

Black oak grows in groves within chenopod shrublands in temperate semi-arid to arid regions of New South Wales, South Australia and Western Australia (Barritt & Facelli

2001). In South Australia it typically occurs on red sands, calcareous loams of sand plains and dune swales, usually with regolith carbonate close to the surface (Hill 2009 in, Sheard *et al.* 2009). Black oak can grow up to 15 m tall and mostly grows in groves < 1 to 10 ha (Barritt & Facelli 2001). It has a dark grey fissured or scaly bark and long, jointed, slender, wiry, and grey/green branchlets that are 1-2 mm thick. The lengths of the branchlets (Figure 7) vary with each tree but are usually in the range of 15 – 55 cm.

Each of these species has been previously used for biogeochemical mineral exploration in the Gawler Craton (Thomas 2004, Sheard *et al.* 2009). Some of the sites include the Birthday Au prospect, Challenger mine, Boomerang Au prospect (Lintern 2004) and Tunkillia (Hill 2009, Sheard *et al.* 2009). The pearl bluebush, a sample target at each of the above mentioned sites has been used widely for biogeochemical surveys throughout the Gawler Craton as it favours transported cover and has had reasonable success in detecting buried mineralisation. Blackoak and bluebush were found best at expressing underlying mineralisation within an elemental suite including Au, Ce, La, Th and U on the Tunkillia prospect in the Central Gawler Craton (Hill 2009, Sheard *et al.* 2009). The western myall has not been so widely used in biogeochemistry programs as the blackoak and bluebush, however, Thomas (2004) sampled the western myall as one of the minor species in a survey at Tunkillia. Cu and Zn were found to be at 6-8 ppm and 26-28 ppm respectively.

For the plant biogeochemistry study at Iron Knob south, the phyllodes of the western myall, twigs of the bluebush and branchlets of the black oak were the selected plant organs to be sampled. Previous studies had shown that with the black oak species, branchlets were the best plant organ to sample, due to ease in collection and preparation. With the pearl bluebush, in previous studies the plant organ of choice has been the leaves, however in this

study the twigs were chosen to minimise dust contamination. As for the western myall the phyllodes were chosen for ease in collection.

The samples were collected along 6 km long E-W trending transect lines with 200 m spacing between each sample. The number of samples was dependant on whether or not there was a target plant at the planned location and providing it was not close to a contamination source (e.g. Iron Monarch mine, road/track). In total there was 6 lines, each transect line was spaced 1 km from the next to give a tenement-scale biogeochemical survey. The samples were collected using powder-free latex, gloved hands (contamination between samples is minimal) to prevent contamination by chemicals such as sunscreen on the hands. All jewellery is also removed prior to sampling. Samples were collected from a uniform canopy height (between waist and arm's reach high) and away from areas more prone to dust contamination (e.g. away from roads/tracks, drill sites and cattle feed stations). Due to the proximity of the study area to the Iron Monarch Mine, some mine dust contamination may have been unavoidable, however, no samples were taken close to mullock heaps, waste dumps or graded roads. The samples were placed in labelled brown paper bags and folded over. Brown paper bags were used as they prevent the leaves from sweating which reduces the rate of decomposition. GPS coordinates were then recorded as well as the sample bag number and anything else worth noting about the sample or its location. In total, 161 samples were collected. This included 55 western myall samples, 82 pearl bluebush samples and 24 black oak samples (Figure 9).

Once the samples are collected they are best left stored in the brown paper bags to dry out and to prevent the sample sweating and decomposing (Mitchell 2010). When back in the laboratory the samples were placed in an oven at 60°C for 48 hours to remove excess moisture. The drying process also helps to separate the plant organs as is the case with the

pearl bluebush, the leaves tend to shrivel and fall off the twigs. After all of the samples are dried they are ready to be prepared for analysis.

Sample preparation involved sorting and milling the vegetation which was carried out in a clean dust free environment. Access to ethanol, paper towel and an air compressor was also essential, as these were the tools used to sterilise the milling equipment. The sample sorting process ensures that all unwanted plant material was removed prior to milling, e.g. fruit, twigs (if not bluebush) and damaged or diseased leaves. Once the sample had been sorted it was then ready to be milled using a stainless steel, rotating blade, coffee grinder to form a fine powder. To eliminate the potential for contamination from the equipment and cross contamination from other samples, a series of sterilising processes were put in place. Once a sample had been milled, before starting another the left over powder from the coffee grinder was blown out using the air compressor, then using ethanol and paper towel the inside was cleaned out. The inside would then be dried out again using the air compressor before milling a small amount of the next sample to ensure the inside of the grinder is coated with the next sample (deliberate pre-contamination), this initially milled sub-sample was then discarded and the remainder of the sample was milled. The sample once ground up was then transferred into a small (70 x 120 mm) labelled paper envelope. In total 177 samples were milled, of these 16 were sample duplicates.

The duplicates were taken 1 every 10 samples and are used as a quality assurance and quality control (QAQC) measure so that sample representation can be assessed. The sample duplicates are marked as another sample number so that they are unknown to the laboratory. The laboratory, however, will also conduct its own set of duplicates as well as analytical blanks (flour and blanks) and standard reference materials (in this survey, vegetation standard V14) to help determine any analytical error.

Samples once prepared are sent to the ACME laboratories in Canada for analysis. The samples are further processed and then analysed by ACME for a 53 suite of elements. ACME analyse each sample by digesting 0.5 g in HNO_3 and then using Inductively Coupled Plasma – Mass Spectrometry (ICP-MS) for ultralow detection limits. It took up to a month for ACME to analyse the samples and send back the data in excel spreadsheets.

3.2. Regolith – Landform Mapping

Interpretation of an A3 sized ortho-photograph of the Iron Knob South area was the first step in creating the regolith-landform map. The colour, scanned and georectified ortho-photograph was provided by Onesteel. The imagery was high quality to enable identification of most landforms and with the help of Google Earth the colour changes were also determined and broadly related to regolith materials. The lack of a digital elevation model (DEM) and topographic map to fit the area made it difficult to determine individual units, however, a fieldtrip following initial map compilation provided the opportunity of verification.

Regolith-landform units (RLUs) were interpreted and map polygons outlined onto tracing film and then scanned and digitised using the program 'Paint.NET'. The scanned image can be found in Figure 10. Using ArcGIS the digitised image was then geo-referenced using the known coordinates of specific locations to add a coordinate system and a scale bar, north arrow and map scale were added to complete it. The RLU codes are based on the system developed by Pain *et al* (2007) in CRC LEME which uses capital letters to describe the regolith type, followed by lowercase letters for the type of landform. For example, the RLU code, 'Aed' describes an alluvial drainage depression as 'A' means alluvial sediment and 'ed' means it is a drainage depression. For subdivision of major RLUs due to subtle differences in regolith lithology, landform or vegetation, modifier numbers can be used at

the end of the code. For example, with more than one type of 'Aed' unit, the descriptors become 'Aed$_1$', 'Aed$_2$', and so on.

The regolith-landform map is important for representing and understanding where regolith materials are distributed throughout the area as well as the landscape processes associated with these materials. In particular, for when the information will be coupled with the results from the biogeochemical survey. This can potentially inform of an anomalous zone associated with *in-situ* mineralisation or if the source is transported and can be traced through the landscape sedimentary systems.

3.3. Philips XL30 SEM

To get a better understanding of how the plant organs in each species of vegetation uptake the elements and distribute them in the plant organs a Field Emission Scanning Electron Microscope (SEM), coupled with an Energy Dispersive Spectroscopy (EDS) system was used (Figure 11). The SEM uses high resolution special imaging with Oxford Cryo-transfer and fracture stage to view biological tissues and plant samples without compromising their integrity (Microscopy 2011). With the SEM close up images of the leaves and chemical composition within the structure can be represented. Four samples were prepared for analysis, and included fresh western myall samples collected on the third field trip to the area. Three of the samples had known elemental concentrations and were all high in Cu and Zn. The fourth sample had been taken close to one of the trees with high target element contents and sampled for follow up exploration and is yet to be analysed, therefore for the purposes of this method it was used as an unknown. The myall phyllodes were sliced in half using a thin blade (cleaned with ethanol) to show the inside and were then placed fresh side up onto mounts (Figure 12) provided by Adelaide Microscopy and labelled. Adelaide Microscopy then carbon coated the samples. Two different detectors were used for imaging

the samples, the secondary electron detector (SE) and the backscattered electron detector (BSE). Secondary electrons are very low energy electrons (<50 eV) emitted from the outer shell of atoms comprising the material of interest due to excitation by the primary electron beam (Wade 2010). Due to their low energy only secondary electrons from the first few atomic layers of the material (< nm) can escape, and as such SE mode reveals information on surface topography of the sample (Wade 2010). Using the SE detector, topographic highs appear as bright spots on the image and conversely the topographic lows appear as the darker regions. Backscattered electrons are high energy electrons scattered from atoms up to ~50 nm below the surface of the sample (Wade 2010). As a result BSE mode reveals information on the atomic number of the sample, regions that contain atoms with high atomic numbers are bright spots and conversely atoms with low atomic number are shown as dark regions. Chemical analysis in the SEM is performed by measuring the energy and intensity distribution of the x-ray signal generated by a focused electron beam (Goldstein *et al.* 2002), provided by the EDS system. For further information on the EDS system please refer to Goldstein (1981).

3.4. Geochemistry

Originally geochemistry was going to have as much weight in the project as the plant biogeochemistry. Due to the minimal exposure of regolith carbonate and detrital ferricrete and the lack of any previous geochemical studies in the area however, we are now only using it to help confirm the results in the biogeochemistry and regolith – landform map. In Iron Knob south small rises of detrital ferricrete can be found, two samples were taken out in the field for further study. The largest piece collected was cut in half using the rock saw to view the distribution of the rounded 0.5-2 cm clasts of hematite inside. The clasts are distributed quite evenly amongst the red iron stained clay matrix as can be seen in Figure

13. Regolith carbonate is locally abundant but not widespread in this area, however no in place profiles were found along the transect lines. Two samples of regolith carbonate were collected from *in-situ* mounds. This was not enough to conduct a study with but would be useful as a point of reference in the regolith-landform study.

4.0. RESULTS

A suite of 15 target elements have been chosen for detailed assessment based on their abundance within the study area, known association with IOCG deposits and use in previous exploration programs dealing with similar geology. The elements can be split into three groups, these are:

1. The prime commodity elements (Cu, Zn, Au),

2. the pathfinder, accessory and Rare Earth Elements (REEs) (Pb, Ag, U, Se, Y, Ce, Re, Li, La), and,

3. The elements associated with detrital contamination (Fe, Al, Zr).

Raw data sets for the 15 target elements and the associated analytical detection limits are provided in Appendix 1.

4.1. Biogeochemistry

The analysis of the samples shows some elements are typically more abundant in certain plant species more than others. This may be due to depth of root penetration, rate of water uptake, the substrate the plant prefers to grow on, size of cell wall for the element to pass through, or plant physiological processes specific to certain species. The probability plots, histograms and Spearman correlation matrices referred to in this section were created using the program ioGAS. The x-y scatter plots referred to in this section were also created using the program ioGAS, however, only eight of the elements (Cu, Zn, Au, Y, Ce, Li, Zr and La) were used as the x-axis, as these plots display the most valuable data. Table 1 provides the Spearman correlation matrix cut-off values.

As touched upon in section 3.1 QAQC measures are of particular importance in any biogeochemical surveys. In this study QAQC has been maintained throughout the sampling stage (removal of jewellery, wearing gloves, etc.), laboratory stage (standards, blanks and

duplicates) and now at the data processing stage. Calculation of the percent difference error, half relative difference and 95% confidence interval of the analytical duplicates and V14 standards have enabled us to check the quality of the results. Summary statistics for each target element and specie can be seen in Appendix 1 with some duplicate data plotted to show precision.

4.1.1. WESTERN MYALL ELEMENT ASSOCIATIONS

A correlation matrix for western myall can be viewed in Table 2. X-Y scatter plots referred to are in Figures 14-21.

A total of 55 western myall samples were collected and analysed, making this species the second most abundantly sampled in the area. The highest recorded Cu value in the western myall was 13.65 ppm, which was the highest recorded Cu value from all three species. The highest Zn detected was at 33 ppm, also the highest out of the three species. The highest recorded Au value was at 1.6 ppb. The Pearson correlation matrix, shows a slight correlation between the Cu and Zn commodity elements ($r^2 = 0.53$), the x-y scatter plots (Figure 14 & 15) also support the correlation as they display a widely distributed scatter with very little linear structure. Au has a slight correlation to both Zr and Al at $r^2 = 0.53$ and $r^2 = 0.55$ respectively. Abundant levels of both Zr and Al are typical indicators of detrital contamination in plants. This may mean there is weak detrital contamination where Au is abundant in western myall. Gold has only minor elevated values and is not well correlated with many other elements whereby the scatter plots produced (Figure 16) are mostly data striped (indicating values at or near analytical detection limit). In the REEs there is a very strong correlation between the elements Ce, Y and La, this is also expressed in the x-y scatter plots (Figure 19 & 21). Lithium has a slight correlation to both Y and Ce as does Pb. Aluminium has a moderate to strong correlation to Zr which is useful in determining that

they are both indicators of contamination and not in-situ. Pb also has a moderate to strong correlation to Li which is interesting and is expressed in the x-y scatter plot in Figure 18. Ag, U, Se and Re have weak to negative correlations to all elements.

4.1.2. PEARL BLUEBUSH ELEMENT ASSOCIATIONS

A correlation matrix for pearl bluebush can be found in Table 3. X-Y scatter plots referred to are in Figures 14-21.

The pearl bluebush was the most abundantly sampled species with 82 samples analysed. The highest recorded Cu value in the pearl bluebush species was 8.38 ppm, highest Zn was 21.5 ppm and highest Au was at 3.3 ppb, which was the highest recorded value out of all the species. Copper and Zn show a surprisingly weak correlation ($r^2 = 0.39$) that is also expressed in the x-y scatter plots that show a widely scattered plot indicating weak correlation. REEs and heavy metals, U, Y, Ce, Li, La, Fe, Pb, Zr and Al however have all recorded a very high correlation to each other in the BB with La and Ce recording a perfect correlation that is also expressed in the x-y scatter plots. Selenium and Re show weak correlation against all of the other elements and Au displays a negative correlation with majority of the bluebush elements. The x-y scatter plots for Au display prominent data banding against all elements except Cu and Zn. This may be due to the data approaching the analytical detection limit or not enough data points.

4.1.3. BLACK OAK ELEMENT ASSOCIATIONS

A correlation matrix for black oak can be found in Table 4. X-Y scatter plots referred to are in Figures 14-21.

A total of 24 Black oaks were sampled, making this the least sampled species of the three. The highest Cu value recorded in the blackoak was 5.03 ppm, highest Zn was at 16.3 ppm

and the highest Au was at 0.6 ppb. The correlation between Cu and Zn is best in the BO species with a correlation of $r^2 = 0.61$. The x-y scatter is still widely distributed but is closer to linear than the bluebush and western myall. This however, could be due to only having a small sample size. Cu and Zn have very weak to negative correlations with all other elements. There is a very strong correlation between the REEs, Ce, Y and La and then moderate to strong relationships between Fe, Pb, Zr, Al and the above REEs. X-y scatter plots of the REEs display the correlations well. The most interesting relationship would be the moderate correlation between Au and Re ($r^2 = 0.67$), however this again may be a result of the small sample size. Ag, U, Se, Li and Re in every other element except Au have very weak to negative correlations with the rest of the elements.

4.1.4. SPATIAL ASSOCIATION

The location of the species sampled in the field area is displayed in Figure 9. The commodity element concentration maps for each specie are displayed in Figures 22-30 and the concentration maps for the rest of the chosen element suite can be found in Appendix 1. For orientation, the biogeochemical transects have been numbered 1-6 with 1 as the northernmost transect and 6 as the southernmost transect.

<u>Western Myall:</u>

Western myall were sampled on each of the six transects, with majority of the samples located to the western area of the ridge. Figures 22-24 display the recorded sample points and analysed concentration data for Cu, Zn and Au in western myall. How closely each element is associated with another is discussed in section 4.1.1.

Copper and Zn are the most anomalous elements out of the target element suite and are detected best through western myall. High Cu values have been interpreted as

concentrations above 7.65 ppm, average range is from 4.4 – 7.65 ppm and the lowest values were interpreted as anything below 4.4 ppm. Interpretation of the concentration ranges was aided by the histogram and probablility plots found in Appendix 1. The highest prospective Cu values in WM are located at the eastern end of transect six and at the western end of transects 4, 3 & 2. These two areas have been targeted as prospective due to there being more than several high values at that location. Copper also appears to be picking up a NW-SE trending structure through the gap between the north and south ridge. This structure has been mapped out by the Geological Survey of South Australia in the Roopena 1:100,000 map in Figure 31. The location of the structure intersecting the transect 6 high values is also marked by pitted quartz lag in the field (Figure 32), which is evidence for silica fluids and sulphide movement through the structure. Zinc in the western myall species is spatially associated with Cu values, therefore the same areas are of interest, however, Zn is detected higher on the western side of transects 4, 3 and 2, than at the eastern end of transect 6. The prospective zone on the west side of the ridge is positioned over an alluvial plain, sheet-flood fan and sheet-wash depositional plain. The eastern end of transect 6 has similar characteristics positioned over an alluvial plain and sheet-flood fan. As they are both in proximity to an alluvial plain there is the possibility that both of these prospective zones contain transported mineralisation. The Au in WM returned only two results of average value (0.58-1.1 ppb) along transect 3, along transect 6 however, results of (1.1-1.6 ppb) were returned in the same location of high Cu and Zn, making this the most prospective area for the commodity elements using western myall. For the remaining elements, Ag, U, Fe and Zr display very low to detection limit concentrations in the western myall. Yttrium, Ce, La and Pb are generally found in low to average concentration throughout the WM samples except for two samples either side of the ridge in transect 3, that appear high in all

of these elements. Selenium, Li and Re have detected the structure through the north and south ridges similar to the commodity elements.

Pearl Bluebush:

  Pearl Bluebush were sampled along all 6 transects and above the northernmost transect at an outcropping quartz vein. Figures 25-27 display the concentration maps for Cu, Zn and Au in bluebush samples. As BB was sampled where WM and BO could not be located the distribution is very sporadic, however, the bulk of samples are on the eastern side of 'Katunga' ridge. Majority of the Cu concentrations are in the range of 4.4-7.65 ppm, the highest three samples are located at the eastern end of transects 1, 2 and 3. As these three samples are seperated by a kilometer further exploration is needed to gauge prospectivity. The majority of Zn concentrations are in the range of low to average (4.4-16.5 ppm) concentration. The highest detected concentration of Zn within BB is at 21.5 ppm and is located next to the mine in transect 3. Gold is detected very well within the BB species and has returned average to very high (0.58-2.4 ppb) results along transect 6 either side of the high results in the WM species. Transect 4 shows a concentration of 1.5 ppb close to where Cu and Zn in the WM had high results possibly due to the NW-SE structure through the ridges. The highest Au result is located at the eastern end of transect 3 with a concentration of 3.3 ppb. The high Au concentrations along transect 6 are located on sheet-flood fans and sand plains. The concentration of 3.3 ppb is located over an alluvial deposition plain and the 1.5 ppb result is located over a sand plain close to a sheet-flood fan. Silver, Ce, Y, La, Pb, U, Fe, Zr and Al all recur along the eastern end of transects 1-4 with sporadic distributions of high concentration. As the concentration levels of Zr, Al and Fe are higher than any other area this may be a depositional area of airborne contamination from the mine. Rhenium has some very sporadic highs surrounded by low concentrations and Se has

average to high concentrations along transects 1 and 2. As the two northernmost transects cross over many different regolith-landform units the concentrations of Se may be due to the lithology of the underlying bedrock. The element Li is found only in very low concentrations within the BB.

Black oak:

Black oak has only been sampled along 5 of the 6 transects and in a small grove above the northernmost transect at an outcropping quartz vein. Figures 28-30 display the concentration maps for Cu, Zn and Au in blackoak samples. The majority of the samples were taken where the transects crossed over 'Katunga' ridge and the smaller southern ridge. Unfortunately majority of the Cu values in the BO are very low with the highest value at 5.07 ppm and a similar case with Zn. One tree however detected Zn at 23.2 ppm and was located in the small grove north of the study area. Three average (0.58-0.6 ppb) values of Au were detected within BO, one is located along transect 6, close to high values of Au in the BB. The other two are located either side of 'Katunga' in transects 3 and 4. The transect 3 value is close to similar concentrations of Au within WM, located over an aeolian sand plain. The transect 6 concentrations are located over a sheet-flood fan and sand plain. The remaining REEs, heavy metals and contaminant indicators are generally all low in concentration over the ridge except for one location. Transect 3 has two samples that have recurring average to high concentrations in Y, Pb, Zr, Al, Ag and Ce. One sample appears to be on a small alluvial fan located next to outcropping ironstone and the other close by is on an erosional rise dominated by ironstone lag.

4.2. Regolith – Landform Map

The completed regolith-landform map (Figure 33 & Appendix 1) includes the Iron Knob south transect area and approximately an extra 2 kilometres east of the transect area and 3

km west. 20 units in total were inferred using the ortho-photograph of the area and confirming it in the field. A table of the regolith-landform unit codes can be found in Appendix 1 along with a full legend to the regolith-landform map. The major landforms in this map are depositional and erosional plains, alluvial depressions and plains and different sheet-wash fans. The 'Katunga' ridge as the highest point in the topography has many depressions that are eroding out valleys through the ridge. The channels flow east off the side of the ridge creating sheet-flow and alluvial fan deposits as the surface becomes level on the flanking plains. The smaller channels then flow south towards swamps and the larger Pine Creek channel. On the eastern side of the ridge plains are mostly dominated by alluvial deposition and sheet-flood fans. On the western side of the ridge the plains are more dominated by alluvial and sheet-flood deposition with a greater aeolian input. More detailed descriptions of the RLUs are below.

4.2.1. TRANSPORTED REGOLITH

Alluvial sediments– A

Alluvial sediments are transported through a system by water confined at some stage to a channel or valley system. The area has a main alluvial drainage depression that heads south along the west side of 'Katunga' ridge (possibly following a structure) then changes course close to the bottom of the transect and runs east. Due to the drainage depression that is 'Pine Creek' much of the area is shaped by depositional and alluvial plains, however with the ridge as a high topographic point there is room for a diverse number of units. Alluvial landforms include: flood plains (af), alluvial plains (ap), alluvial swamps (aw), drainage depressions (ed), alluvial fans (fa) and depositional plains (pd). Topographically the flood plains, plains, swamps and depressions make up the lowest parts of the area. The alluvial plains and flood plains are dominated by open chenopod shrubland and are distinguished by

different sediments. The lithology of the depressions, fans and depositional units coming off the east side of the 'Katunga' ridge are dominated by ferruginous lag (Figure 34) that is coarse and angular becoming finer and better sorted towards more distal settings. The alluvial swamps form at the lowest parts in the topography where the system naturally drains into, the dark clay/loam sediments are generally covered in native grasses and the larger open woodland trees are usually close by.

<u>Sheetwash sediments – CH</u>

Sheetflow deposits are deposited where there are fewer obstructions, therefore relatively flat land surfaces with minimal vegetation cover. Five main types of sheetflow deposit were interpreted on the regolith-landform map, these are: erosional plains (ep); erosional low hills (el); erosional rises (er); sheet-flood fans (fs); and, depositional plains (pd). The erosional rises and hills create the framework for the east dipping slope on the side of the ridge. The lithology is almost completely made up of angular ironstone and BIF lag which has eroded off the *in-situ* outcrops higher up. Spinifex, red mallee trees and small pearl bluebush shrubs prefer the inclined slopes of the ridge. Sheet-flood fans form at the base of high topography preferring level to gently inclined landforms. The fans are mostly composed of colluvium with the lithology of the Middleback Sub-group. The differences in the fan units is due to the density of vegetation, the units derived from the smaller ridge to the south are within aeolian units and have much denser vegetation and regolith carbonates. $CHfs_2$ is a secondary fan system covered in open chenopod shrubland that is made up of distal finer sediments in which small incised channels are cut. The final sheet-flood fan is more proximal to the sources of colluvium and as a result has more surface lag, this unit occurs close to the ridge and coming off the mine site. A hardpan regolith carbonate occurs

just below the surface of most of the alluvial units especially the fans coming off the ridge (Figure 35).

<u>Aeolian sediments – IS</u>

Aeolian sediments cover a majority of the mapping area but only form their own discrete landform units in the centre of the mapping area where the west side of the 'Katunga' ridge trapping these sediments. The sand plains (ps) form a very distinct unit as they consist of well rounded and sorted, fine red-brown quartz sands. These RLUs are generally densely vegetated by both low open woodland communities and chenopod shrubland (Figure 36). These RLUs are typically underlain by hardpan regolith carbonate with quartz and ironstone lag.

4.2.2. IN-SITU REGOLITH

<u>Slightly weathered bedrock – SS</u>

The bedrock in the area is split into different groups depending on the degree of weathering and the topography. Two main areas include exposed *in-situ* bedrock, both are on the highest points of each hill. The exposed rock is slightly weathered. The landform units include low hills (el) that are 30 – 90 m above the plains, and hills (el) that are landforms of high relief being 90 – 300 m above the plains. The lithology of the slightly weathered bedrock is of Iron formations (Figure 37) and Upper Middleback Jaspilite of the Middleback Sub-group. Botryroidal hematite was also found around the outcrops (Figure 38).

4.3. Philips XL30 SEM

Figures 39-44 display some of the images and charts created using the SEM. The main aim was to see if it was possible to view crystals of the commodity elements within the

structure of the plant organ. Images have been taken of the inner structure of a western myall phyllode (Figure 39), calcium oxalate crystals (Figure 40 & 41), iron oxide crystals (Figure 42 & 43) and salt crystals. It was made possible to analyse the make-up of each crystal selected by using an energy dispersive microanalysis system (EDS) so that mineralogy could be identified. The charts created using the EDS system display peaks in kilo-electron volts (KeV) that correspond to certain elements. The EDS system enables the user to collect data and then identify individual peaks that stand out above the rest. As discussed in section 3.3, regions containing bright spots in SE mode correspond to topographic highs and bright spots in BSE mode correspond to atoms with high atomic numbers. The leaf matter in BSE and SE modes is displayed as a topographic low with low atomic number, the EDS system distinguished high peaks at the beginning of the spectrum that were identified as C and O. Sample 197 that was a duplicate of an anomalous tree along transect 6 had iron oxide crystals, salt crystals and a potential quartz identified within the prepared phyllode. The continuous high peak of C throughout the spectrums is due to carbon coating of the sample. Sample 183 was of unknown elemental concentrations and was the only sample in which clays were identified with high peaks of Mg, Si, Al, K and O (Figure 44 & 45). Unfortunately no elements of value to this report were identified using the SEM, and probably would not be identified in the leaf matter unless the concentration was extremely high throughout the entire plant or there was a small nugget of Au on the leaf (very unlikely). However it is still a useful tool in understanding the distribution of elements in the leaf.

5.0. DISCUSSION

5.1. Landscape Evolution

Weathered Bedrock:

The age constraints on weathering of the bedrock in the Iron Knob south and surrounding areas are generally poor. This is due to a lack of dated sediments in the area to give a relative context to the weathering. The youngest dated weathered bedrock in the area is the banded iron formations of the Middleback Sub-group which make up part of the Paleoproterozoic Hutchison Group (2000 – 1850 Ma) (Schwarz 2004). The only further potential constraints on the area's weathering history may be derived from extrapolation of the flanking sedimentary basins. The main basin that flanks the Eastern Gawler Craton is the Cainozoic Pirie Basin, of which this study area occurs in the western hinterland of the basin. The main sedimentary units residing in the Pirie Basin are the Kanaka Beds and the Melton Limestone (Alley & Lindsay 1995). Kanaka Beds are a late Eocene – early Oligocene succession of carbonaceous siltstone, shale and sand with minor conglomerate, quartz and kaolin (Alley & Lindsay 1995). Melton Limestone is a late Oligocene – early Miocene unit consisting of carbonates with little detrital input (Alley & Lindsay 1995). It is likely that weathering would have been going during the deposition of these sedimentary units. It is possible that some of the kaolin and quartz in the early Tertiary Kanaka Beds may be derived from erosion of pre-Tertiary (Mesozoic?) weathering profiles, but the inputs of this detritus is not great, and so therefore may not be highly significant.

Alluvial:

The oldest alluvial systems relating to the long-term landscape evolution are related to the detrital (channel fill) ferricretes that extend broadly north-south to the west of the Katunga

ridge. Based on the remnant outcrop patterns these are likely to represent a former north to south flowing paleo-valley system that has since been topographically inverted. These represent the first recognition and description of detrital ferricrete, iron ore accumulations in the Iron Knob area, however their limited preservation make them too small to be an economic resource (such as the Robe pisolites that are mined for iron oxide in the Pilbara region of Western Australia). Unfortunately the age constraints on these detrital ferricretes are unknown, other than that they pre-date the contemporary drainage system. For the iron oxides to precipitate and form the cement that binds ferricrete, Fe must be mobilised as Fe^{2+} (Taylor 2009). The Fe^{2+} must be moved in water to the site of its precipitation and then encounter oxidising conditions to form Fe^{3+} (Taylor 2009). The detrital ferricrete clasts mostly include weathered ironstone of the Middleback Sub-group, that in this area are likely to have been derived from parts of the Katunga ridge and its continuation to the north (just south of Corunna homestead).

Sheetflow:

Many of the fans that come off of the Katunga ridge are sheetflow fans. To have sheetflow the vegetation needs to be sparse, implying that the climate was arid at the time. Therefore formation of the sheetflow units most likely occurred since the Miocene becoming more prominent in the Quaternary and most likely during sheetflow runoff associated with the high intensity low frequency shallow overflow to be expected during the times of the glacial maxima during the Quaternary. Due to the vegetation removal due to grazing, these conditions are still in effect today.

Aeolian:

Aeolian sands cover a large part of the field area, with the source from dune fields to the west in the Lake Gilles area. Similar to the sheetflow units, aeolian units require sparse

vegetation to form an arid climate. The Katunga ridge provides an impediment to their transport which is the reason why the aeolian sand plains are predominantly on the east side of the ridge.

Made land:

Before mining commenced in Iron Knob, in 1854 the land was originally purchased as a pastoral lease for grazing (Association 2009). Grazing is still in effect today on the Corunna station to the north of Iron Knob and Katunga station property to the south.

Small mining operations begun after the area was discovered around the same time the pastoral lease for Corunna was purchased (Association 2009). The mining lease for the area exchanged hands twice before being taken up by BHP after 1896, they started mining the first iron ore out of the Iron Knob mine in 1899 (Community 2004). Next to the town are three deposits of iron ore, Iron Monarch is the largest and is in the field area, Iron Knob is in the middle of the town and Iron Princess is on the northern outskirts of town. More than 150 tonnes of iron ore was mined out of the deposits and after 100 years of operation the mining ceased in 1999 (Community 2004).

5.2. Relationship between Plant Species

In an ideal biogeochemistry survey only plants of the same species would be sampled so that the results would be easily comparable. Ideal sample areas, however, are difficult to come by and to fill in each transect for this study the three different species of plant were required. To make the results comparable however we can compare the results of different species taken at the same location.

When collecting the samples for the biogeochemistry survey, two samples where possible would be taken from the same site from two of the different species. A total of 16 samples from 8 different sites were collected, four of the graphs compare western myall to the

bluebush and the other four graphs compare blackoak to bluebush. All 8 graphs can be found in Appendix 1. Unfortunately the blackoak could not be compared to western myall as they generally do not grow at the same sites.

Western myall vs. Bluebush

Western myall typically has a much higher Zn content than BB with Cu contents as the next largest disparity. Western myall appears as a more reliable species for the uptake of Cu and Zn than any other species, it also typically has high concentrations of Li. Whether these consistent differences between species are due to fundamental physiological processes within the plants or due to different rooting depths and geochemical access of these plants, would warrant further study.

At two sites BB have Au concentrations higher than adjacent WM samples. Bluebush also appears to have consistently higher levels of Ag, though this element is often unreliable in its analysis. With the REEs, WM and BB are quite comparable. Cerium and La are variable between species (i.e. sometimes higher in BB and sometimes higher in WM). This may mean the elements uptake in the plant is related to the substrate the plant grows on. Rhenium in three of the graphs was detected at the same level and then in one of the graphs WM detected it at a much higher level than BB. Once again this may be due to the substrate the plant grows on rather than the plant having an affinity with the element.

Blackoak vs. Bluebush

Generally the relationships here are highly variable; however, the most reliable relationship is that BB is detecting Ag at higher concentrations than BO except for one of the figures where the concentration is the same. In two graphs BB has detected Zn higher than BO and in the other two graphs BO has detected it better. In majority of the graphs Cu has been detected better by bluebush but only marginally. For the REEs Re was best

detected by bluebush however one graph had BO better than BB but not as high a concentration. Cerium was also regularly detected higher in bluebush.

5.3. Trace Element Associations, Dispersion and Residence

As discussed in sections 4.1.1-4.1.2 the strongest element associations were found between the REEs and heavy metal contaminants, these were:

- Cerium, La and Y, and,

- Aluminium and Zr

Cerium, La and Y are the most abundant elements in the REE group and are commonly associated with each other as has been noted in work by Dunn (2007). The three elements have many similar chemical properties that often cause them to be found together in geological deposits (Long *et al.* 2010). In areas where the REEs have been found highest there is a high correlation with Fe. Iron is found at low concentrations and close to the detection limit throughout most of the study area. The highest concentration (1.425 %) is located next to the mine on the east side along transect 2, and is likely mine contamination. Iron uptake is generally good in plants as it is essential for the formation of chlorophyll, so it is common to be present at concentrations above detection. As the background levels of Fe are in the range of 0.005 – 0.085 % anything greater than this is likely to be due to factors other than the required plant uptake. The source of Fe could either be from alluvial transported or windblown weathered material from the Ironstones on 'Katunga' ridge and material from Iron Monarch mine, though it could possibly be due to the underlying bedrock too. Elevated Fe results in plants are usually indicative of underlying ultramafic to mafic rocks (Dunn 2007), possibly the amphibolites of the Cook Gap Schist group. The high REEs and Fe are located on the eastern end of transects 3 & 4 though where alluvial

drainage depressions off the ridge flow into the area as well as a sheet-wash depositional plain from the direction of the mine, therefore it is still most likely contamination.

Aluminium is a common constituent of plants but is usually present at concentrations close to detection limits (Dunn 2007), isolated anomalous values occurring in the field should be suspected as contamination first. As aluminium makes up a decent component of clays and the alluvial parts of the landscape in the field area contain mostly clay soils, many of the Al highs recorded throughout the area may be a result of wind-blown contamination. Similar to Al, the availability of Zr to plants is low so concentrations are usually below 0.1 ppm (Dunn 2007) and high values should be suspected as airborne dust contamination. As Zr is a common element in sand and aeolian red sands cover majority of the study area it is reasonable to assume that this is the source of high results. The Zr and Al highs occur mostly in the bluebush species which is likely due to the BB species growing so close to the ground, unlike the blackoak and western myall trees.

Copper and zinc are important micronutrients in plants used for reproductive growth and regulating consumption of sugars respectively. As they are important elements in plants they are usually found at levels higher than the detection limit. As mentioned in the results Cu and Zn appear to have a strong association with underlying fault structures. The large NW-SE structure that cuts through the area is intersected by two NNE-SSW faults also identified in the Roopena 1:100,000 map that happen to intersect at the two areas located for possible IOCG mineralisation. This indicates mineralisation may not only be lithologically controlled by the underlying bedrock but also structurally controlled. As previous studies in the south have also shown a similar relationship between the commodity elements and fault structures as well as a drill hole south of the study area returning results of chalcopyrite and native copper, natural high plant results can also be ruled out.

Unlike Cu and Zn, Au may not only be associated with the fault structures. It has been recorded either side of the fault as with Cu and Zn, however, it is picked up in high concentrations along majority of transect 6 that is independent of the faults. The area is highly vegetated and regolith-landforms intersected include, aeolian sand plains and sheet-flood fans coming off the smaller south ridge. 'Pine Creek' is also situated close to the southernmost transect. The concentration of Au along transect 6 does not appear sporadic which supports the theory that it is probably not transported mineralisation. Further study is required.

Other interesting trace elements include Se, Li and Re as they have also picked up the major fault structure with high concentrations. Selenium can be harmful to plants in high concentrations but can be useful in low concentrations (Germ *et al.* 2007). Selenium unlike all the other elements has average to high (0.43-1.0 ppm) concentrations along both transects 1 & 2 positioned either side of the mine. As Se is a major contaminant in mine drainage water (Germ *et al.* 2007), this may mean run-off from the mine has affected soils either side of the mine causing the highs in Se. Lithium follows the trend of Cu with high concentration in most of the same places. Lithium is a minor component in nearly all igneous rocks so high concentrations other than in the fault zone may be due to underlying volcanics or amphibolites of the Cook Gap Schist. Rhenium is of interest in this study as concentrations of up to 7 ppm were recorded. As mentioned in the results section Au in both western myall and bluebush species is spatially associated with the concentration highs for Re. The two zones that have been identified as being potentially mineralised (transect 6 and the west side of the ridge) are also the two areas Re is consistently high. East of the ridge concentration highs appear as 'random' peaks, therefore are not reliable. There are no known controls of Re with concentrations above the detection limit of 1 ppb (Dunn 2007).

The remaining elements Ag, U and Pb provided no new insights into the study. Silver concentration highs are irregular and were discarded as irrelevant after finding no significant associations with the trace and commodity elements. The U concentration was so low that the samples were irrelevant although the concentrations were spatially distributed with the same pattern as Fe. As for Pb it follows a similar trend to the elemental contaminants.

5.4. Future of Exploration in the Target Area

Recent studies completed in 2010 by honours students C. Mitchell and C. Hicks at Onesteels Project Mawson tenement found that high Cu mineralisation detected using biogeochemistry was able to express underlying fault structures across the area. The faults were generally trending N-S which was ideal for the E-W trending transect lines to intersect them. In this study both D. Tanti working in the area of Iron Knob North and myself have found similar trends where high commodity element concentrations (mainly Cu and Zn) detected by biogeochemistry, express underlying fault structures.

The two zones either side of the ridge in the mapping area have been specifically looked at in more detail due to the high levels of concentration from commodity elements, the position of the zones in respect to locations of known and suspected structures, the similarities of the RLUs and low resolution ground magnetics provided by Onesteel (Figure 46). The two areas were revisited and sampled again with closer sample spacing (50 m) and will be sent off for sample analysis. Figure 47, is a map showing all of the analysed sample data, locations of the most recent samples to be analysed and suspected major fault structures.

As this project was conducted at a tenement scale the next step would be to revisit areas that have been targeted as prospective in the tenement scale (1 Km between transects, 200m

spacing between samples) and re-sample those areas with a prospect scale survey (50m spacing between samples). An E-W prospect scale survey would allow for detailed chemistry as well as defining the spatial extents of any buried mineralisation. As one of the most prospective areas in Iron Knob south is along the southernmost transect, it would be worth doing a follow-up survey with closer sample spacing to the south of the study area, giving extra attention to any identified N-S, NNE-SSW and NW-SE trending structures. With more detailed data and spatial constraints of the possible mineralisation, drillhole data can then be sought to provide information on depth of mineralisation, lithology and buried structures.

6.0.   CONCLUSION

The primary function of this study was to demonstrate the exploration potential of biogeochemistry with the aid of regolith-landform mapping to define and constrain a zone of mineralisation within the Onesteel Northern Middleback Range tenement.

This study has shown that out of the three sample mediums, western myall and pearl bluebush species were best at expressing underlying chemical signatures, with western myall the most reliable for Cu and Zn signatures and bluebush having a greater affinity with Au. The pearl bluebush however is also more prone to contamination (e.g. high Fe, Zr, Al) due to its proximity to the ground. Therefore western myall with its ability to penetrate deeply through the regolith is possibly the best sample medium. With most plant biogeochemical surveys the issue however, is not necessarily what species to sample but rather the availability and distribution of the sample in the required target area.

Construction of the regolith-landform map enabled an understanding of the distribution and dispersion of elements in the study area particularly helping to identify areas of local contamination. Certain landforms have also influenced the distribution of the target species, with western myall preferring the sandy soils of the aeolian sand plains and blackoak preferring the colluvium and sheet-wash slopes of the ridge.

Two zones of elevated commodity elements were defined either side of a NW-SE structure crossing over the N-S trending 'Katunga' ridge. Each zone is intersected by further NNE-SSW trending structures which have been identified in the Roopena 1:100,000 map. As stated by Williams *et al.* (2005) "IOCG deposits have strong structural and/or stratigraphic controls with mineralisation often localised on fault bends and intersections, in breccia bodies, shear zones, or at geological contacts". Follow up sampling of the two mineralised zones has been conducted and the samples will be sent off for analysis to

further constrain the target areas. Along with the structural similarities the targets were both located on similar regolith-landform units of sheet-flood fans and alluvial plains with only low levels of contaminants detected. As mentioned above, with more biogeochemical data to constrain the spatial extent and perhaps geophysical data to understand the fault systems, drillhole data can then be sought to provide information on depth of mineralisation, lithology and further buried structures.

ACKNOWLEDGEMENTS

REFERENCES

ALLEY N. F. & LINDSAY J. M. 1995. The Geology of South Australia, Vol. 2, The Phanerozoic. *In:* Drexel J. F. & Preiss W. V. eds., *South Australia, Geological Survey, Bulletin 54*, pp 153-176.

ASSOCIATION I. K. P. 2009. History of Iron Knob <http://www.ironknob.org/>. (retrieved 21/09 2011).

BARRITT A. R. & FACELLI J. M. 2001. Effects of Casuarina pauper litter and grove soil on emergence and growth of understorey species in arid lands of South Australia. *Journal of Arid Environments* **49**, 569-579.

BOOMSMA C. D. & LEWIS N. B. 1981. *The Native Forest and Woodland Vegetation of South Australia. South Australian Woods and Forests Department* Adelaide.

BRUNDIN N. 1939. *Method of locating metals and minerals in the ground*. **Patent 2, 158, 980**, U.S.

COMMUNITY I. K. 2004. *Iron Knob what a hole! All 150 million tonnes of it!* Iron Knob community tourist centre.

CUNNINGHAM G. M., MULHAM W. E., MILTHORPE P. L. & LEIGH J. H. 1992. Plants of western New South Wales. *Inkata Press*.

DUNN C. E. 2007. *Biogeochemistry in Mineral Exploration* (Handbook of Exploration and Environmental Geochemistry, Vol. 9). Elsevier, Amsterdam.

FABRIS A. J., KEELING J. L. & FIDLER R. W. 2009. Surface geochemical expression of bedrock beneath thick sediment cover, Curnamona Province, South Australia. *Geochemistry: Exploration, Environment, Analysis* **9**, 237-246.

FANNING C. M., FLINT R. B., PARKER A. J., LUDWIG K. R. & BLISSETT A. H. 1988. REFINED PROTEROZOIC EVOLUTION OF THE GAWLER CRATON, SOUTH-AUSTRALIA, THROUGH U-PB ZIRCON GEOCHRONOLOGY. *Precambrian Research* **40-1**, 363-386.

GERM M., STIBILJ V. & KREFT I. 2007. Metabolic Importance of Selenium for Plants. *The European Journal of Plant Science and Biotechnology* **1**, 91-97.

GOLDSTEIN J., NEWBURY D., JOY D., FIORI C., ECHLIN P. & LIFSHIN E. 1981. *Scanning Electron Microscopy and X-Ray Microanalysis: A Text for Biologists, Material Scientists, and Geologists*. Plenum Press New York and London.

GOLDSTEIN J., NEWBURY D., JOY D., LYMANN C., ECHLIN P., LIFSHIN E., SAWYER L. & MICHAEL J. 2002. *Scanning Electron Microscopy and X-ray Microanalysis* (3rd edition). Springer-Verlag, New York.

HICKS C. B. 2010. The Regolith Expression of Cu-Au mineralisation within the northern region of the Project Mawson area, NE Eyre Peninsula, South Australia. Bachelor of Science with Honours thesis, Geology and Geophysics, University of Adelaide, Adelaide (unpubl.).

HILL S. M. 2009. Vegetation sampling in the Gawler Craton. *CRC LEME*.

HILL S. M. 2011. *Photos taken in the Northern Middleback Ranges for Iron Knob Biogeochemical projects*. Hill, S.M.

HILL S. M. & HILL L. J. 2003. SOME IMPORTANT PLANT CHARACTERISTICS AND ASSAY OVERVIEWS FOR BIOGEOCHEMICAL SURVEYS IN WESTERN NEW SOUTH WALES. *CRC LEME - Advances in Regolith*, 191.

KOVALEVSKY A. L. 1987. Biogeochemical Exploration for Mineral Deposits. *VNU Press, Ultrecht*, 224.

LANGE R. & PURDIE R. 1976. Western Myall (Acacia sowdenii), its survival prospects and management needs. *The Rangeland Journal* **1**, 64-69.

LANGE R. T. & SPARROW A. D. 1992. Growth rates of western myall (Acacia papyrocarpa Benth.) during its main phase of canopy spreading. *Australian Journal of Ecology* **17**, 315-320.

LEXI 2011. *Philips XL30 FE SEM with EDS system. lexi.eng.uci.edu*.

LINTERN M. J. 2004. The South Australian Regolith Project. *CRC LEME* **156**.

LONG K. R., VAN GOSEN B. S., FOLEY N. K. & CORDIER D. 2010. The Principal Rare Earth Elements Deposits of the United States *USGS Scientific Investigations Report* **2010-5220**.

LUNGWITZ E. E. 1900. The lixiviation of gold deposits by vegetation and its geological importance. *Mining Journal (London)* **69**, 500-502.

MICROSCOPY A. 2011. Scanning electron microscopes <http://www.adelaide.edu.au/microscopy/services/instrumentation/sem.html>. (retrieved 21/09 2011).

MITCHELL C. 2010. *The Regolith Expression of IOCG mineralisation within the southern region of the Project Mawson area, NE Eyre Peninsula, South Australia*. University of Adelaide.

ONESTEEL 2009. North-SMR Development Proposal, Regulatory Application.

ONESTEEL 2011. Data package provided by Onesteel.

PAIN C. F., CHAN R., CRAIG M., GIBSON D., KILGOUR P. & WILFORD J. 2007. RTMAP Regoith Database Field Book and Users Guide. *CRC LEME Open File Report 231*.

PARKER A. J. 1978. Structural, stratigraphic and metamorphic geology of Lower Proterozoic rocks in the Cowell/Cleve district, eastern Eyre Peninsula. Ph.D thesis, Geology and Geophysics, University of Adelaide (unpubl.).

PARKER A. J. & FANNING C. M. 1998. *WHYALLA, South Australia 1:250,000 Geological Series - Explanatory Notes*. Primary Industries and Resources South Australia, Geological Survey of South Australia.

PARKER A. J., FANNING C. M. & FLINT R. B. 1985. Geology. *In:* Twidale C. R., Tyler M. J. & Davies M. eds., *Natural History of the Eyre Peninsula*, Royal Society of South Australia Inc.

PARKER A. J. & LEMON N. M. 1982. RECONSTRUCTION OF THE EARLY PROTEROZOIC STRATIGRAPHY OF THE GAWLER CRATON, SOUTH-AUSTRALIA. *Journal of the Geological Society of Australia* **29**, 221-238.

S.A.A.L.N.R.M.B. 2008. *Biodiversity: WESTERN MYALL DIEBACK AND WESTERN MYALL WHITEFLY*. *Government of South Australia*, Australia.

SCHWARZ M. 2004. *Gawler Craton Geological Framework*. PIRSA**:** 4. Government of South Australia, South Australia.

SHEARD M. J., KEELING J. L., LINTERN M. J., HOU B., MCQUEEN K. G. & HILL S. M. 2009. A guide for mineral exploration through the regolith of the central Gawler Craton, South Australia. *CRC LEME c/o CSIRO Exploration and Mining.*

SKIRROW R. G. 2004. Iron oxide Cu-Au deposits: An Australian perspective on their unifying characteristics. 17th Australian Geological Convention, Hobart, Tasmania (unpubl.).

SKIRROW R. G., BASTRAKOV E. N., BAROVICH K., FRASER G. L., CREASER R. A., FANNING C. M., RAYMOND O. L. & DAVIDSON G. J. 2007. Timing of Iron Oxide Cu-Au-(U) Hydrothermal Activity and Nd Isotope Constraints on Metal Sources in the Gawler Craton, South Australia. *Economic Geology* **102**, 1441-1470.

TAYLOR G. 2009. Landscape and Regolith. *In:* Scott K. M. & Pain C. F. eds., *Regolith Science*, pp 31-43, CSIRO Publishing, Melbourne.

THOMAS M. 2004. *Biogeochemical Data Ranges from Tunkillia Prospect, Central Gawler Craton, South Australia*. *Regolith***:** 362-364. CRC LEME.

WADE B. 2010. *Philips XL30 Scanning Electron Microscope operating instructions***:** 6-7. Adelaide Microscopy, Adelaide.

WARREN H. V., DELAVAULT R. E. & BARAKSO J. 1968. The arsenic content of Douglas-fir as a guide to some gold, silver and base metal deposits. *Canadian Mining and Metallurgy* **61**, 860-867.

WEATHERZONE 2011. Whyalla Ap Climate <http://www.weatherzone.com.au/climate/station.jsp?lt=site&lc=18120>. (retrieved 23 May 2011).

WEBB A. W., THOMSON B. P., BLISSETT A. H., DALY S. J., FLINT R. B. & PARKER A. J. 1986. GEOCHRONOLOGY OF THE GAWLER CRATON, SOUTH-AUSTRALIA. *Australian Journal of Earth Sciences* **33**, 119-143.

WILLIAMS P. J., JOHNSON D. A., BARTON M. D., FONTBOTE L., DE-HALLER A., MARK G., OLIVER N. H. S. & MARSCHIK R. 2005. Iron Oxide Copper-Gold Deposits: Geology, Space-Time Distribution, and Possible Modes of Origin. *Economic Geology* **100th Anniversary Volume**, 371-405.

TABLE CAPTIONS

1. Pearson Correlation Matrix cut-off values
2. Pearson Correlation Matrix for western myall
3. Pearson Correlation Matrix for pearl bluebush
4. Pearson Correlation Matrix for blackoak

FIGURE CAPTIONS

1. Location of Onesteels tenement, Middleback Ranges (Onesteel 2009)
2. Aerial photo of Iron Knob South
3. Tectonic evolution of geological units on WHYALLA: 250,000 (Parker & Fanning 1998)
4. Map of the Gawler Craton within South Australia highlighting (in red) the Olympic Cu-Au province as well as Moonta and OD mineralised corridors (edited from (Skirrow *et al.* 2007))
5. Western myall tree (photo by Dr Steven M. Hill (2011))
6. Pearl bluebush (Hill 2011)
7. Blackoak tree with sampled branchlets inset
8. Growth stages of western myall as defined by Lange and Purdie (1976)
9. Location of plant species sampled in the field area
10. Scanned copy of the hand drawn regolith-landform map
11. Philips XL30 FE SEM with EDS system (LEXI 2011)
12. Mounted SEM specimens (all western myall species)
13. Detrital ferricrete in field (Hill 2011) and inset the same rock sliced in half showing large hematite clasts in clay matrix.
14. x-y scatter plots created in ioGAS with Cu as the x-axis
15. x-y scatter plots created in ioGAS with Zn as the x-axis
16. x-y scatter plots created in ioGAS with Au as the x-axis
17. x-y scatter plots created in ioGAS with Y as the x-axis
18. x-y scatter plots created in ioGAS with Ce as the x-axis
19. x-y scatter plots created in ioGAS with Li as the x-axis
20. x-y scatter plots created in ioGAS with Zr as the x-axis
21. x-y scatter plots created in ioGAS with La as the x-axis

TABLES

Table 1

r2 Value	Value Association
< 0.45	Weak/ Non
0.45 – 0.6	Slight
0.6 – 0.7	General
0.7 – 0.9	Strong
> 0.9	Very Strong

Table 2

Spearman Correlation Matrix for Western myall

Correlation	Cu_ppm	Zn_ppm	Au_ppb	Ag_ppm	U_ppm	Se_ppm	Y_ppm	Ce_ppm	Re_ppm	Li_ppm	La_ppm	Fe_pct	Pb_ppm	Zr_ppm	Al_pct
Cu_ppm	1	0.53	0.095	0.16	-0.18	0.0072	0.39	0.39	0.18	0.39	0.37	-0.08	0.2	0.25	0.18
Zn_ppm	0.53	1	-0.17	0.21	-0.1	0.019	0.23	0.23	0.15	0.32	0.19	-0.045	0.22	0.094	0.039
Au_ppb	0.095	-0.17	1	-0.11	-0.073	-0.19	-0.031	-0.083	0.032	0.013	-0.066	0.33	0.065	0.53	0.55
Ag_ppm	0.16	0.21	-0.11	1	-0.057	0.03	0.034	0.054	-0.14	-0.056	0.065	0.011	0.033	-0.019	-0.008
U_ppm	-0.18	-0.1	-0.073	-0.057	1	-0.033	-0.096	-0.02	-0.044	-0.073	-0.077	-0.022	-0.1	-0.075	-0.11
Se_ppm	0.0072	0.019	-0.19	0.03	-0.033	1	-0.13	-0.14	0.13	-0.019	-0.16	-0.028	0.0039	-0.05	-0.18
Y_ppm	0.39	0.23	-0.031	0.034	-0.096	-0.13	1	0.98	0.19	0.67	0.95	0.24	0.65	0.26	0.2
Ce_ppm	0.39	0.23	-0.083	0.054	-0.02	-0.14	0.98	1	0.15	0.67	0.93	0.2	0.66	0.19	0.15
Re_ppm	0.18	0.15	0.032	-0.14	-0.044	0.13	0.19	0.15	1	0.21	0.16	0.087	0.042	0.21	0.13
Li_ppm	0.39	0.32	0.013	-0.056	-0.073	-0.019	0.67	0.67	0.21	1	0.45	0.33	0.86	0.41	0.38
La_ppm	0.37	0.19	-0.066	0.065	-0.077	-0.16	0.95	0.93	0.16	0.45	1	0.15	0.45	0.12	0.084
Fe_pct	-0.08	-0.045	0.33	0.011	-0.022	-0.028	0.24	0.2	0.087	0.33	0.15	1	0.49	0.62	0.74
Pb_ppm	0.2	0.22	0.065	0.033	-0.1	0.0039	0.65	0.66	0.042	0.86	0.45	0.49	1	0.36	0.39
Zr_ppm	0.25	0.094	0.53	-0.019	-0.075	-0.05	0.26	0.19	0.21	0.41	0.12	0.62	0.36	1	0.81
Al_pct	0.18	0.039	0.55	-0.008	-0.11	-0.18	0.2	0.15	0.13	0.38	0.084	0.74	0.39	0.81	1

Table 3

Spearman Correlation Matrix for Bluebush

Correlation	Cu_ppm	Zn_ppm	Au_ppb	Ag_ppm	U_ppm	Se_ppm	Y_ppm	Ce_ppm	Re_ppm	Li_ppm	La_ppm	Fe_pct	Pb_ppm	Zr_ppm	Al_pct
Cu_ppm	1	0.39	0.044	0.37	0.26	0.29	0.24	0.22	0.06	0.25	0.22	0.28	0.23	0.25	0.25
Zn_ppm	0.39	1	-0.026	0.6	0.5	0.41	0.3	0.24	-0.091	0.18	0.25	0.5	0.41	0.27	0.24
Au_ppb	0.044	-0.026	1	0.049	-0.042	-0.26	-0.02	-0.0082	-0.17	0.022	-0.0025	-0.028	-0.027	-0.0094	0.011
Ag_ppm	0.37	0.6	0.049	1	0.86	0.2	0.75	0.7	0.035	0.65	0.72	0.88	0.85	0.71	0.69
U_ppm	0.26	0.5	-0.042	0.86	1	0.15	0.87	0.81	-0.022	0.74	0.83	0.98	0.96	0.8	0.77
Se_ppm	0.29	0.41	-0.26	0.2	0.15	1	0.084	0.068	0.14	0.035	0.069	0.14	0.13	0.074	0.045
Y_ppm	0.24	0.3	-0.02	0.75	0.87	0.084	1	0.99	-0.02	0.91	0.99	0.85	0.95	0.98	0.96
Ce_ppm	0.22	0.24	-0.0082	0.7	0.81	0.068	0.99	1	-0.01	0.92	1	0.79	0.91	0.99	0.97
Re_ppm	0.06	-0.091	-0.17	0.035	-0.022	0.14	-0.02	-0.01	1	0.044	0.007	-0.029	0.0023	-0.014	-0.005
Li_ppm	0.25	0.18	0.022	0.65	0.74	0.035	0.91	0.92	0.044	1	0.92	0.72	0.85	0.93	0.94
La_ppm	0.22	0.25	-0.0025	0.72	0.83	0.069	0.99	1	0.007	0.92	1	0.82	0.93	0.99	0.97
Fe_pct	0.28	0.5	-0.028	0.88	0.98	0.14	0.85	0.79	-0.029	0.72	0.82	1	0.95	0.79	0.76
Pb_ppm	0.23	0.41	-0.027	0.85	0.96	0.13	0.95	0.91	0.0023	0.85	0.93	0.95	1	0.91	0.88
Zr_ppm	0.25	0.27	-0.0094	0.71	0.8	0.074	0.98	0.99	-0.014	0.93	0.99	0.79	0.91	1	0.99
Al_pct	0.25	0.24	0.011	0.69	0.77	0.045	0.96	0.97	-0.0053	0.94	0.97	0.76	0.88	0.99	1

Table 4

Spearman Correlation Matrix for Blackoak

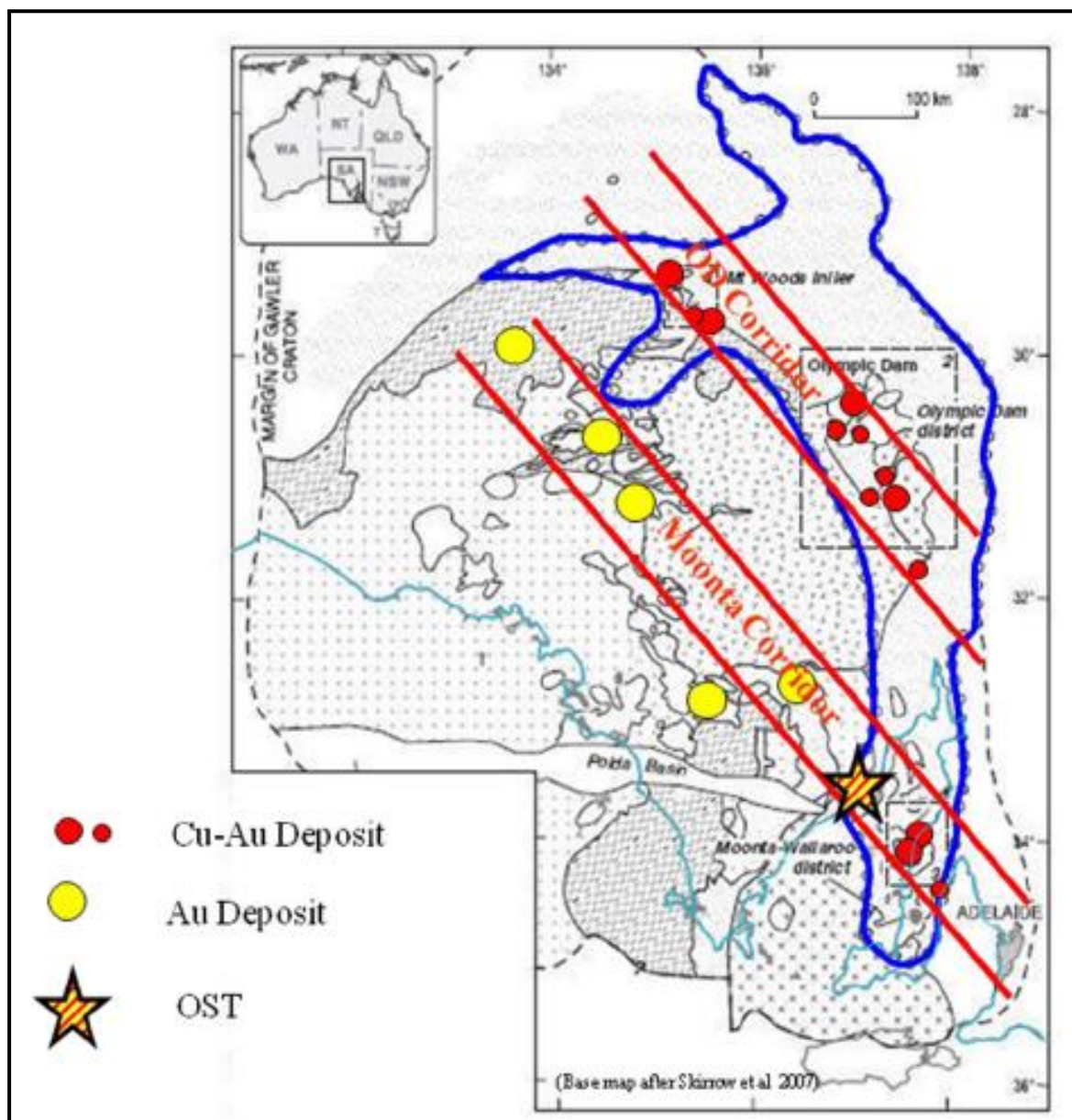| Correlation	Cu_ppm	Zn_ppm	Au_ppb	Ag_ppm	U_ppm	Se_ppm	Y_ppm	Ce_ppm	Re_ppm	Li_ppm	La_ppm	Fe_pct	Pb_ppm	Zr_ppm	Al_pct
Cu_ppm	1	0.61	-0.33	0.45	-0.17	0.37	0.011	-0.03	-0.25	-0.28	0.015	-0.02	0.083	-0.0094	-0.21
Zn_ppm	0.61	1	-0.33	0.069	-0.22	0.36	-0.0097	-0.0099	-0.013	-0.31	0.0033	0.15	0.19	0.11	-0.12
Au_ppb	-0.33	-0.33	1	-0.14	0.28	-0.41	-0.21	-0.25	0.67	0.037	-0.16	-0.16	-0.2	-0.1	-0.11
Ag_ppm	0.45	0.069	-0.14	1	0.16	0.11	-0.31	-0.35	-0.27	-0.17	-0.3	0.018	-0.22	-0.13	-0.21
U_ppm	-0.17	-0.22	0.28	0.16	1	-0.1	0.19	0.17	0.069	0.47	0.24	0.22	0.27	0.39	0.36
Se_ppm	0.37	0.36	-0.41	0.11	-0.1	1	0.23	0.2	-0.12	0.0041	0.17	0.26	0.22	0.24	-0.095
Y_ppm	0.011	-0.0097	-0.21	-0.31	0.19	0.23	1	0.96	-0.084	0.095	0.97	0.66	0.46	0.74	0.77
Ce_ppm	-0.03	-0.0099	-0.25	-0.35	0.17	0.2	0.96	1	-0.13	0.11	0.94	0.63	0.5	0.72	0.78
Re_ppm	-0.25	-0.013	0.67	-0.27	0.069	-0.12	-0.084	-0.13	1	0.097	-0.028	0.049	-0.038	-0.0083	-0.005
Li_ppm	-0.28	-0.31	0.037	-0.17	0.47	0.0041	0.095	0.11	0.097	1	0.17	0.15	0.49	0.25	0.2
La_ppm	0.015	0.0033	-0.16	-0.3	0.24	0.17	0.97	0.94	-0.028	0.17	1	0.67	0.52	0.76	0.79
Fe_pct	-0.02	0.15	-0.16	0.018	0.22	0.26	0.66	0.63	0.049	0.15	0.67	1	0.61	0.86	0.74
Pb_ppm	0.083	0.19	-0.2	-0.22	0.27	0.22	0.46	0.5	-0.038	0.49	0.52	0.61	1	0.73	0.57
Zr_ppm	-0.0094	0.11	-0.1	-0.13	0.39	0.24	0.74	0.72	-0.0083	0.25	0.76	0.86	0.73	1	0.79
Al_pct	-0.21	-0.12	-0.11	-0.21	0.36	-0.095	0.77	0.78	-0.0054	0.2	0.79	0.74	0.57	0.79	1

FIGURES
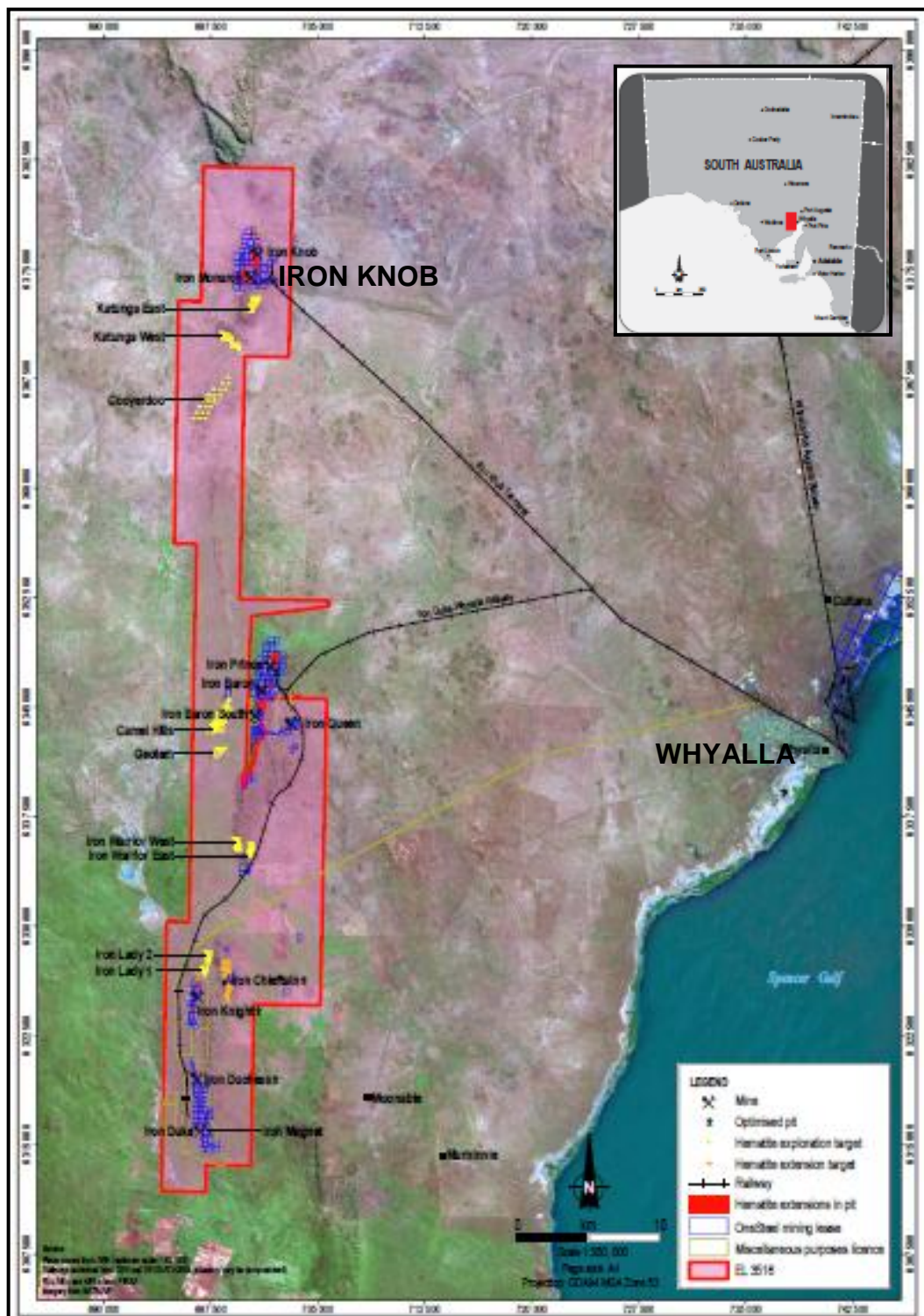
Figure 1

Aerial photo of Iron Knob south
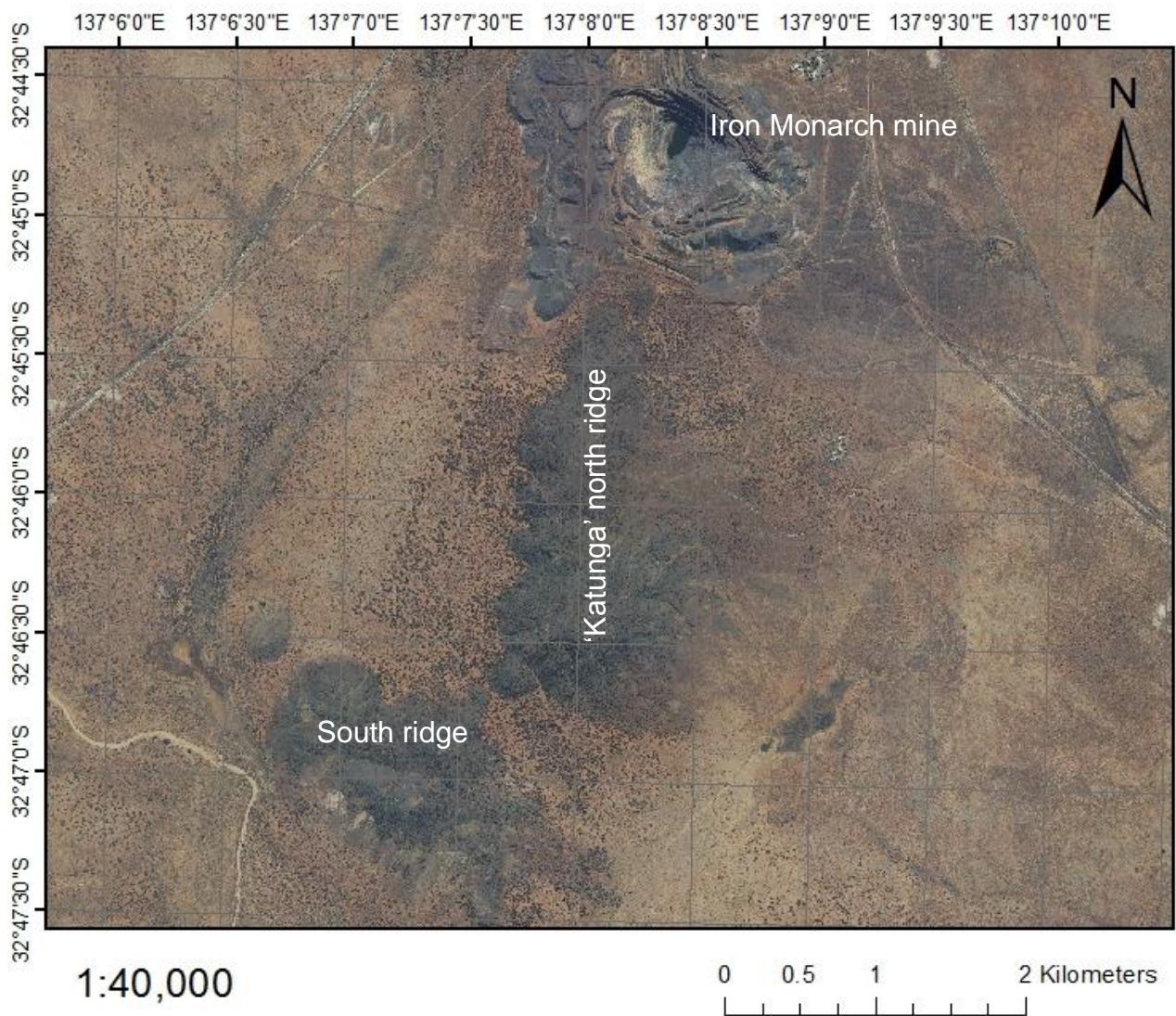
Figure 2
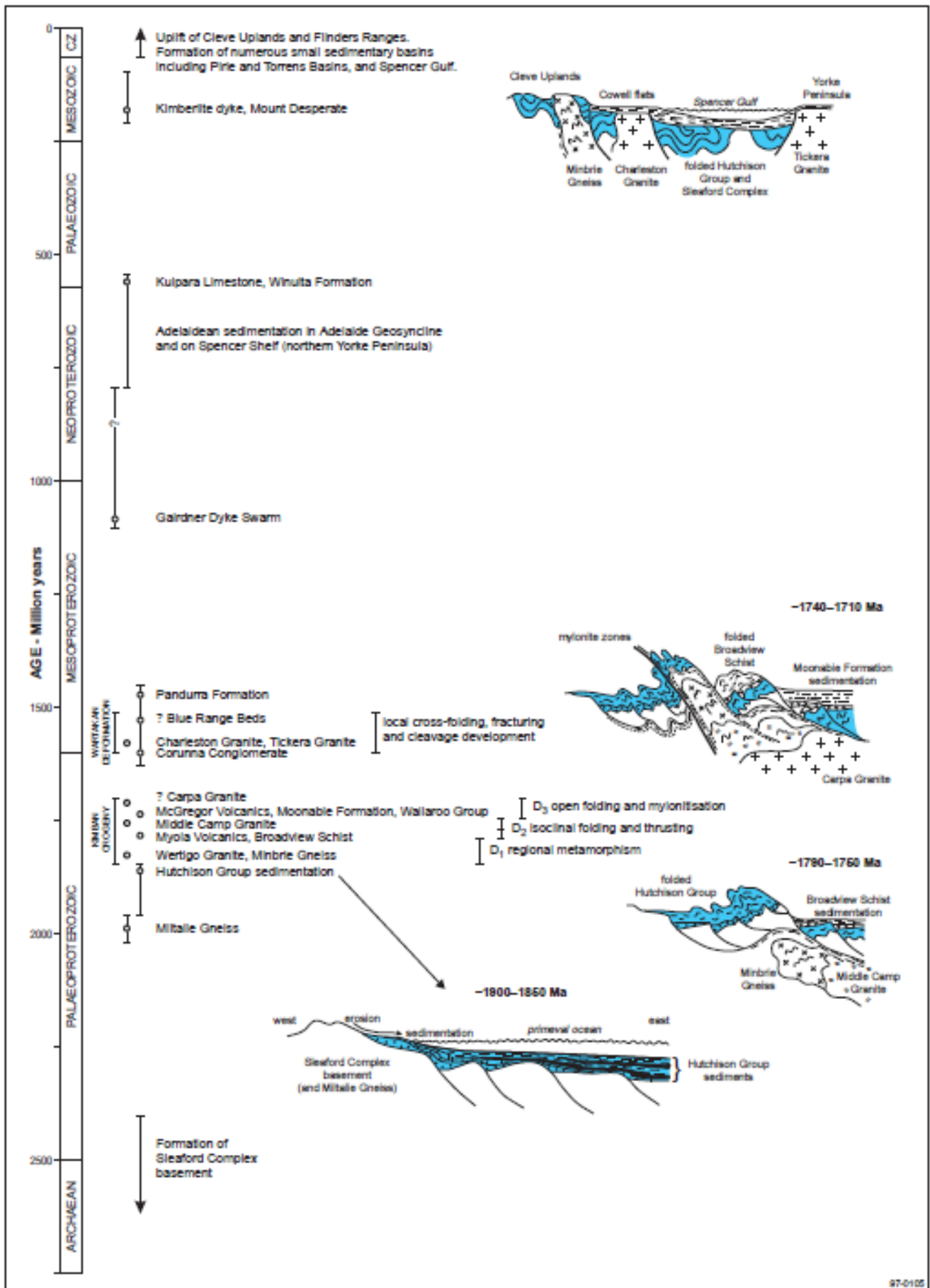
Figure 3

Figure 4

Figure 5

Figure 6

Figure 7

Figure 8

Location of Western Myall, Pearl Bluebush and Blackoak Samples

Figure 9

Figure 10

EDS system

Sample chamber with BSE, X-ray and SE detectors
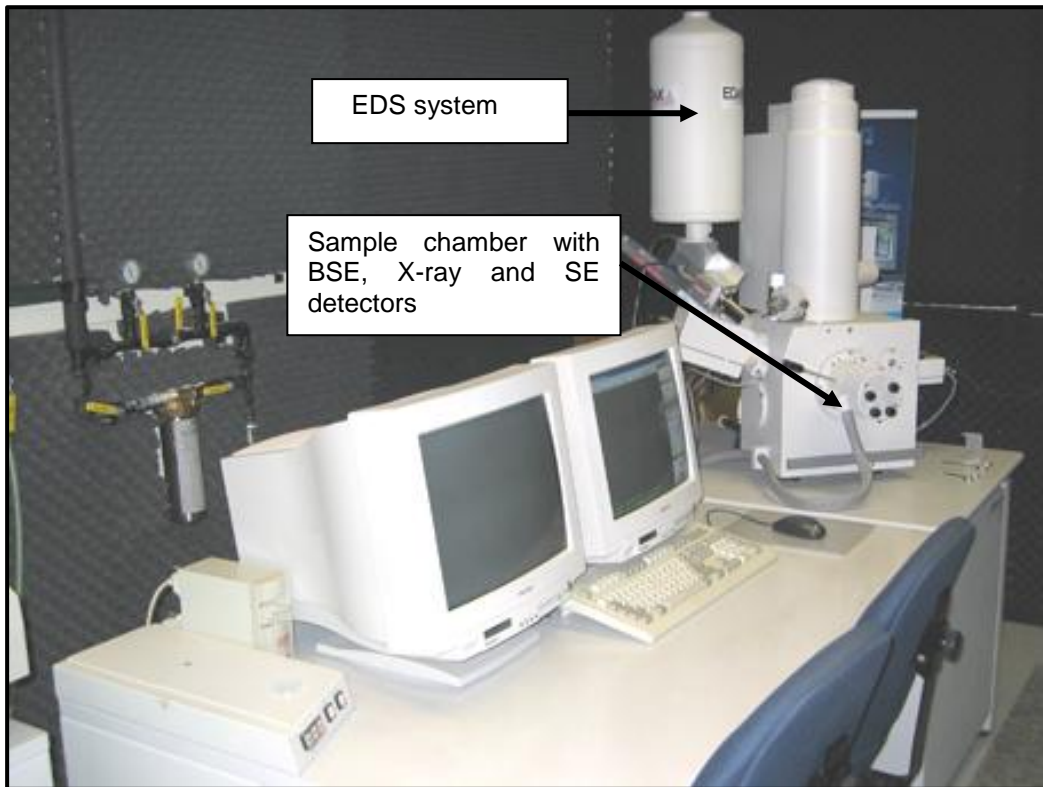
Figure 11

2 cm

Figure 12

7 cm
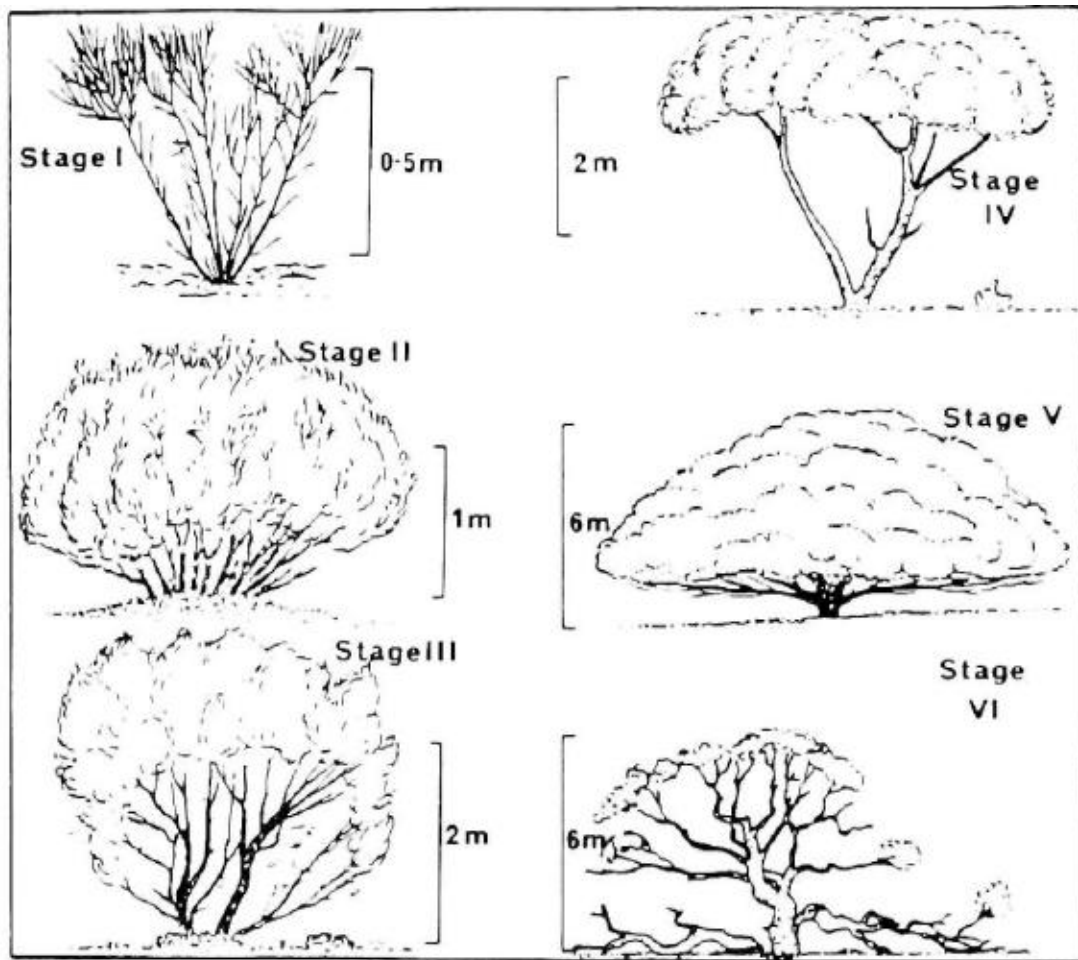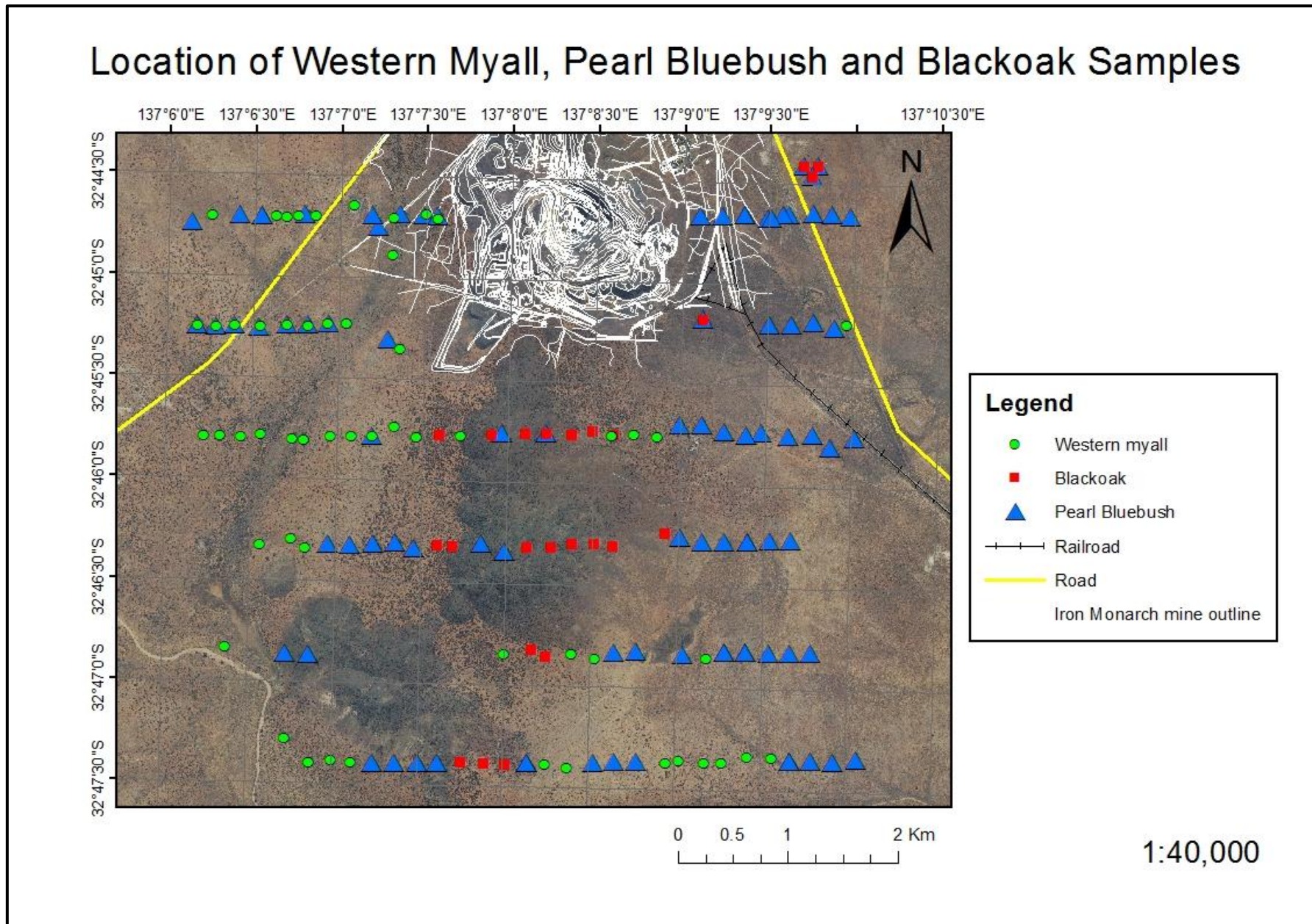
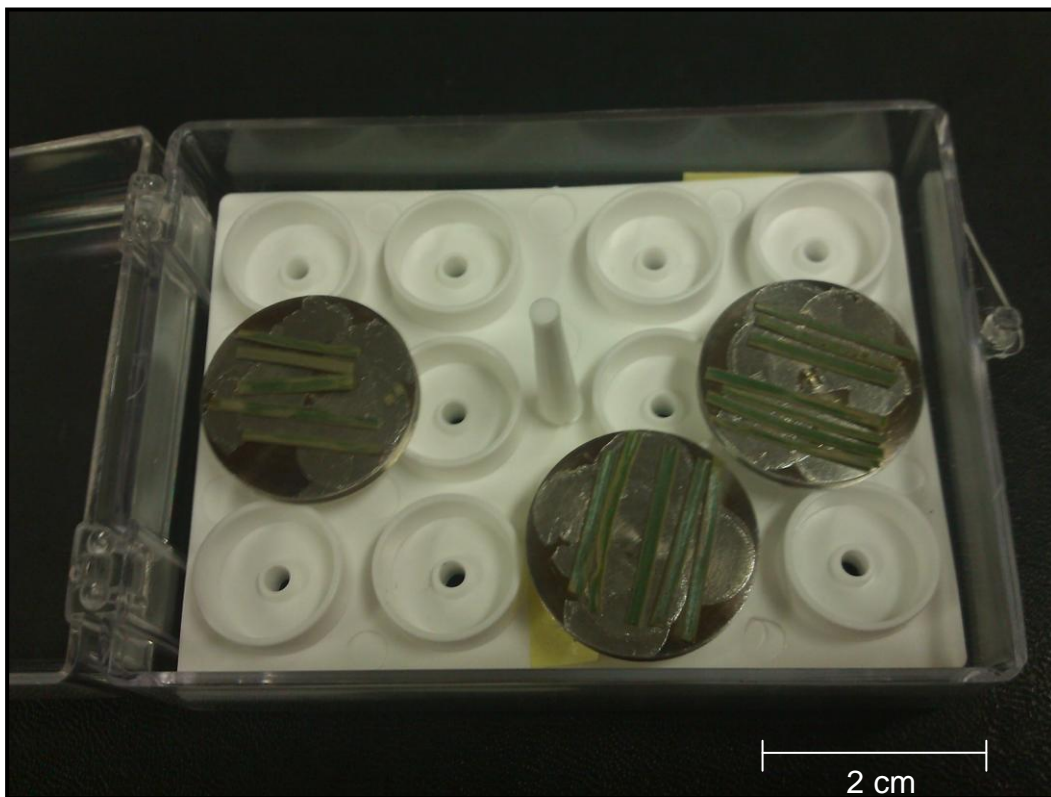**Figure 13**

X-Y Scatter Plots (created in ioGAS) – Bluebush (Blue), Black Oak (Red), Western Myall (Green)
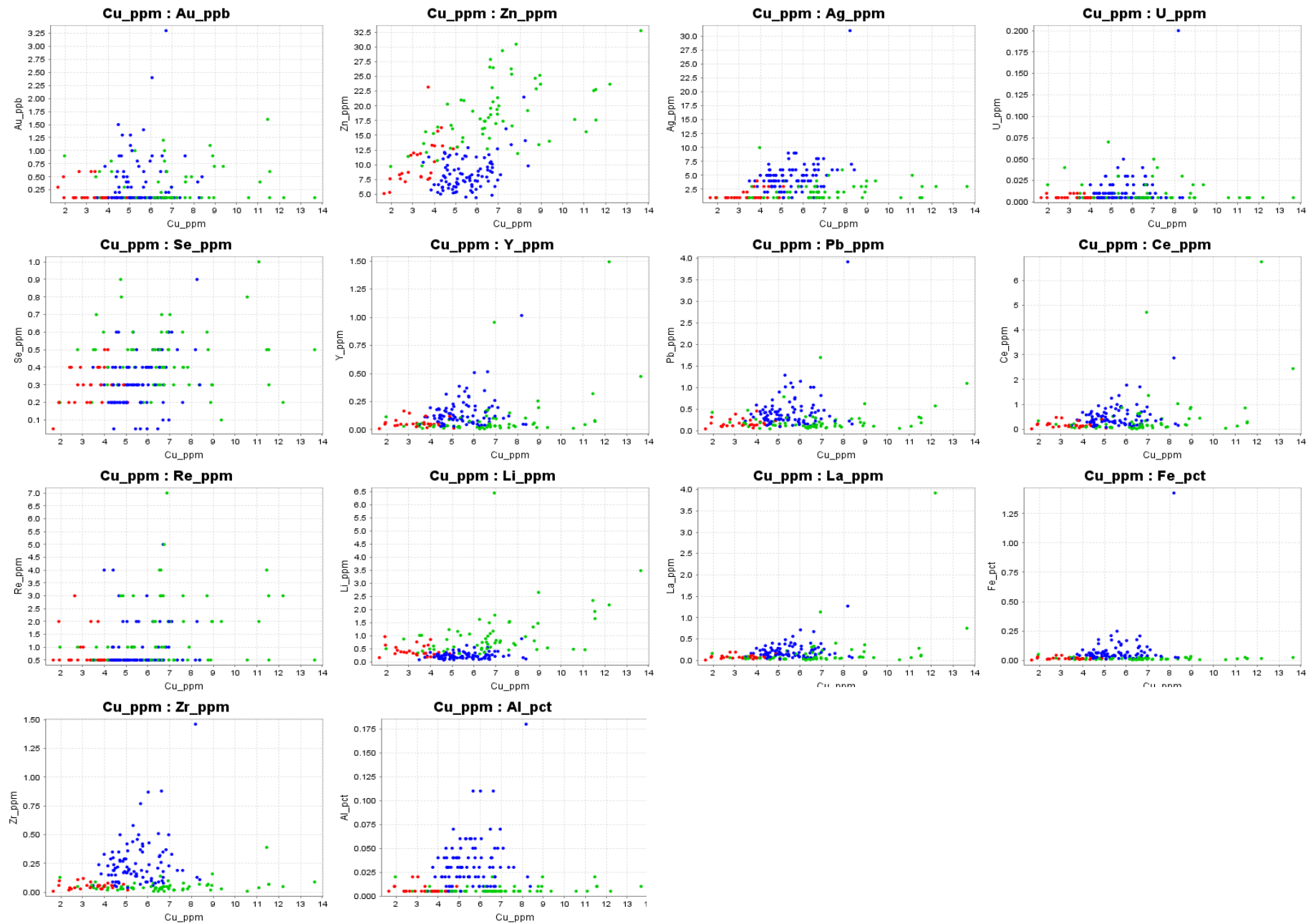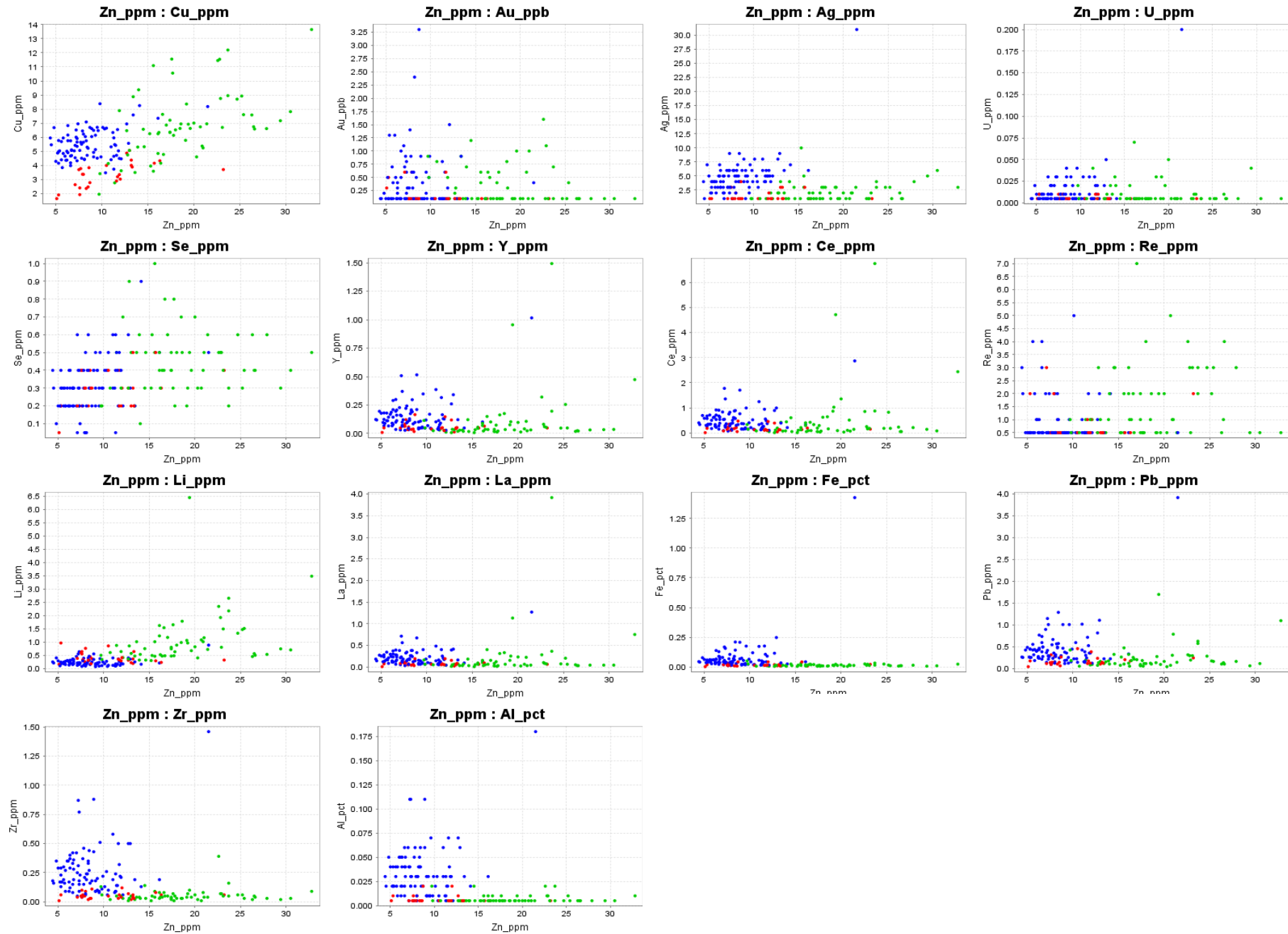

Figure 14

Figure 15
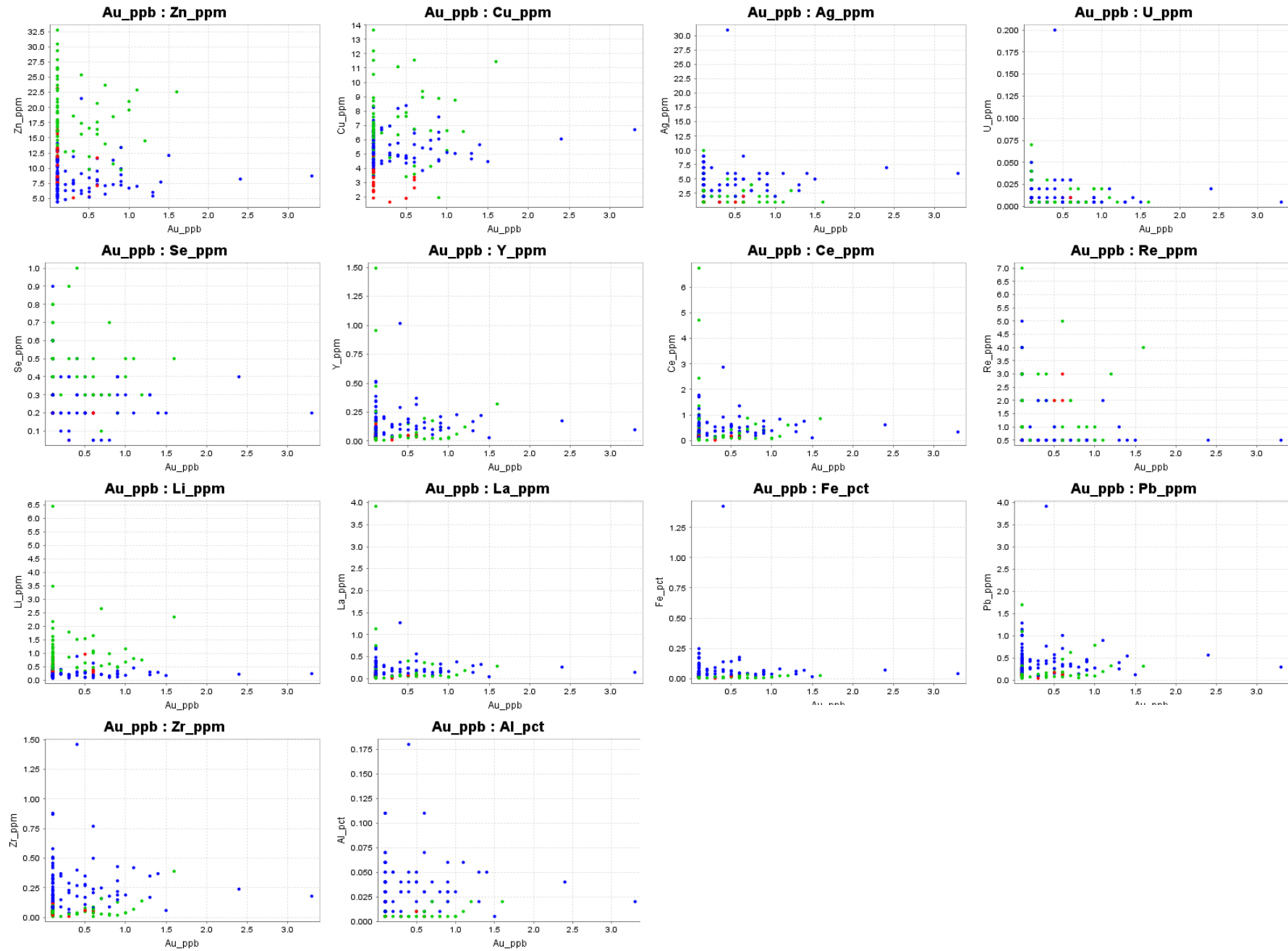
Figure 16
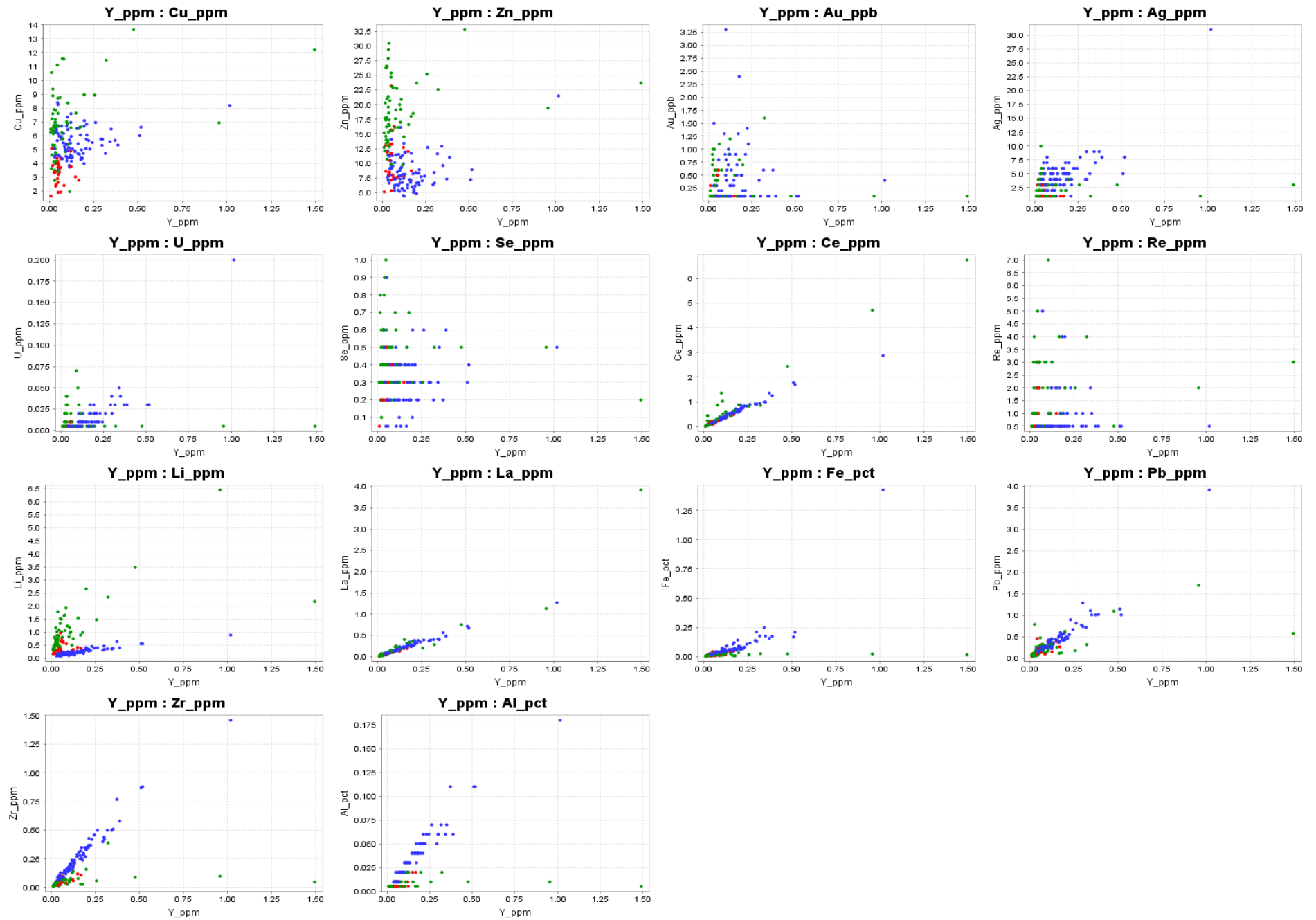
Figure 17
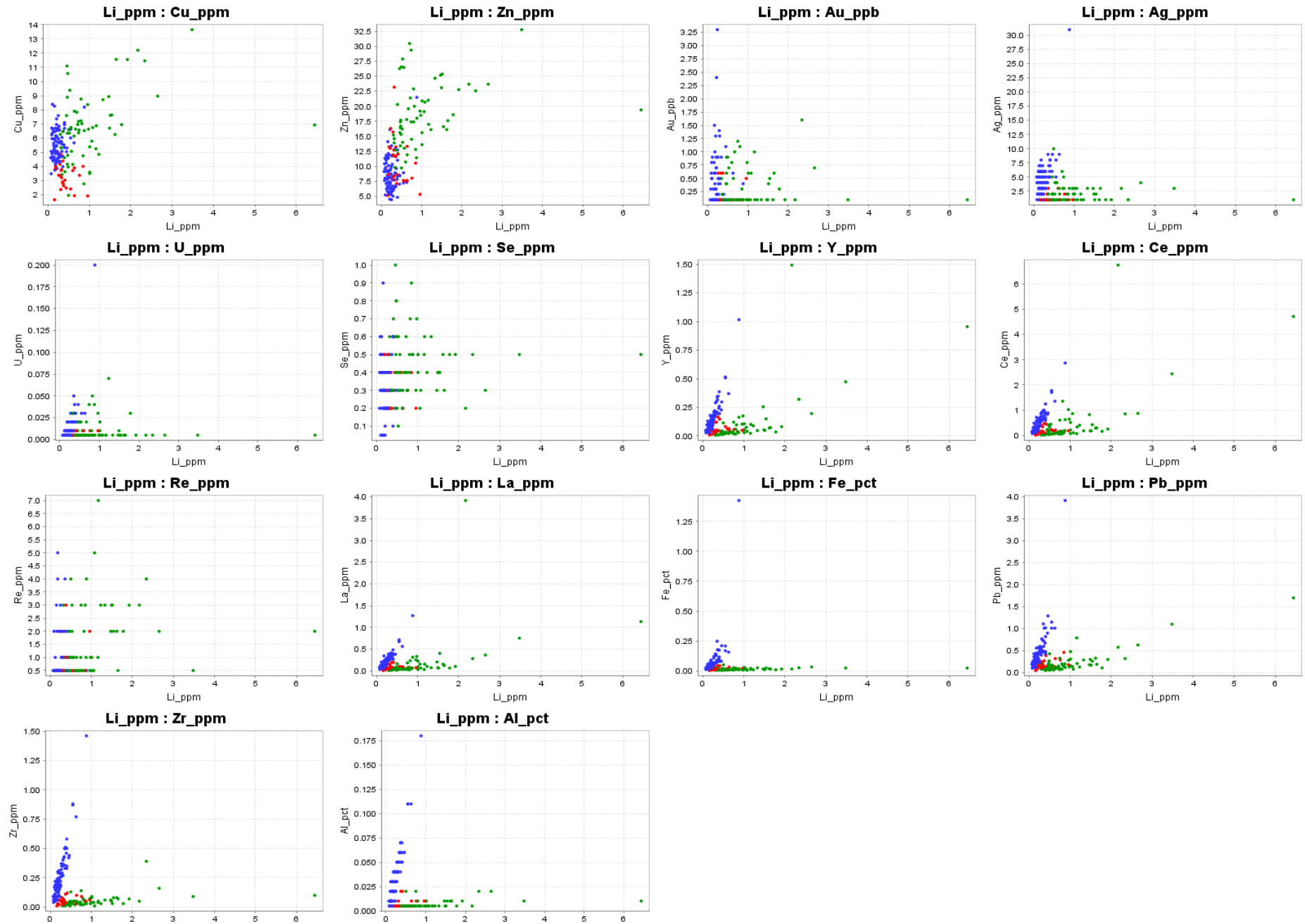
Figure 18
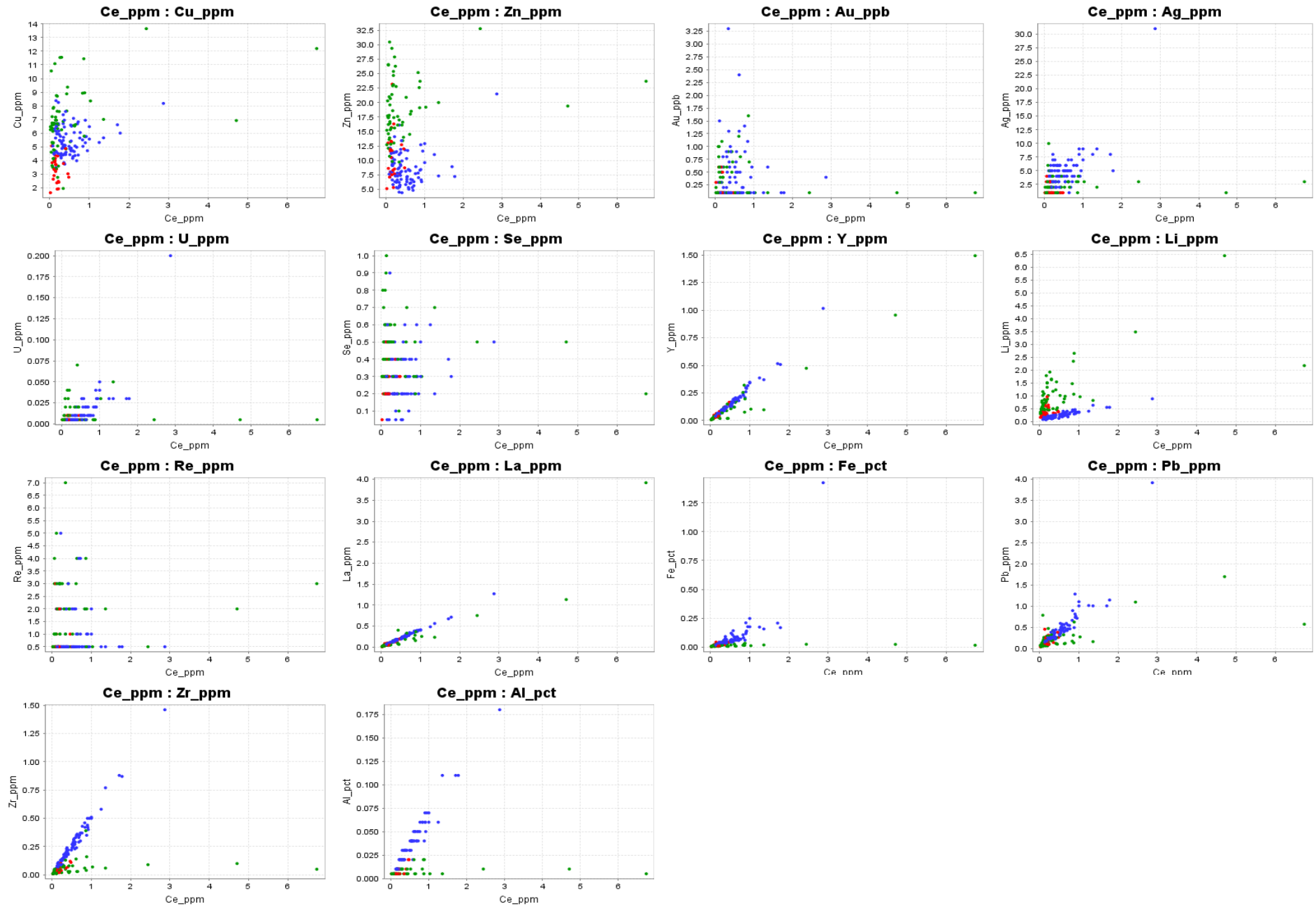
Figure 19

Figure 20

Figure 21

Cu concentration in Western Myall
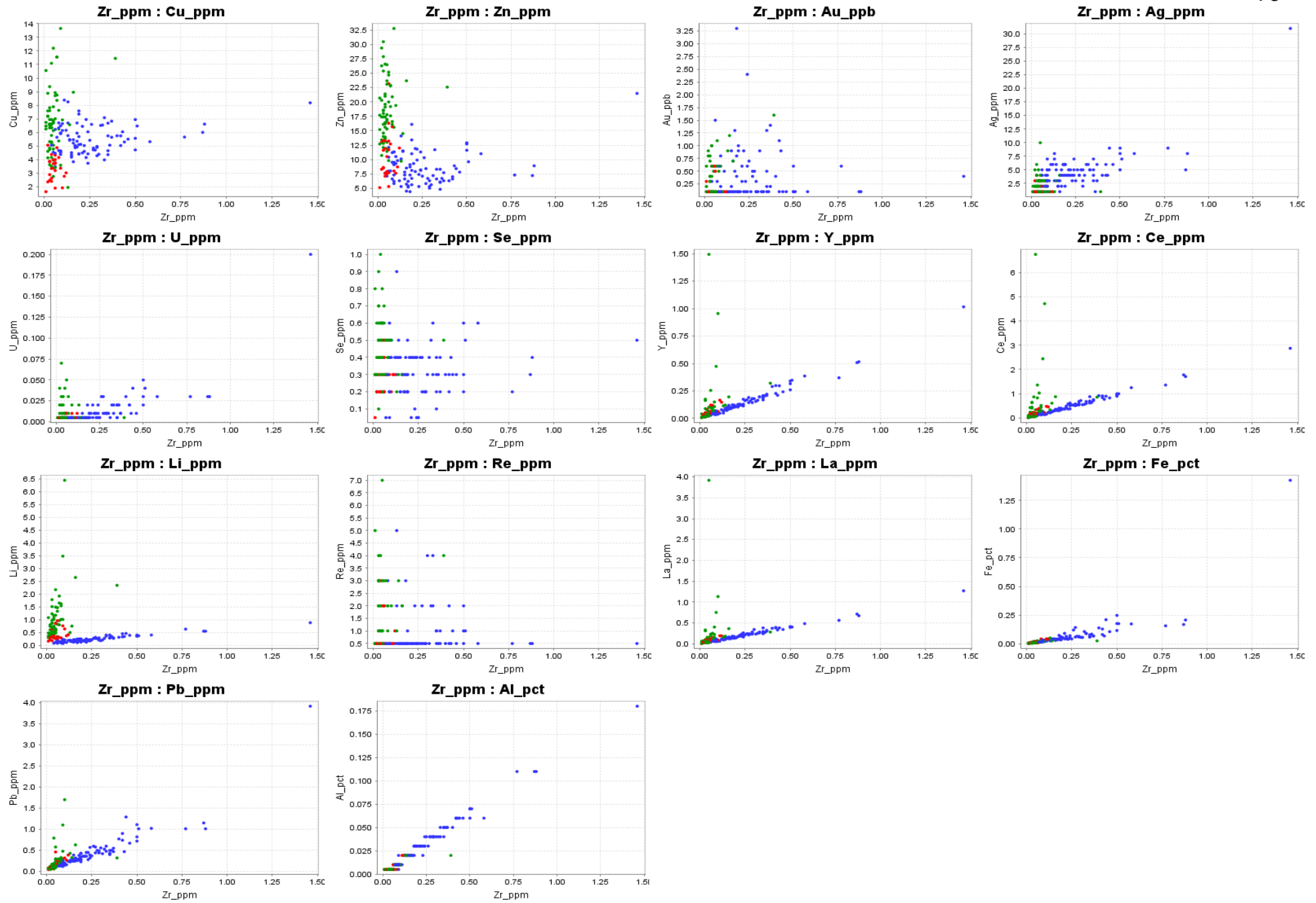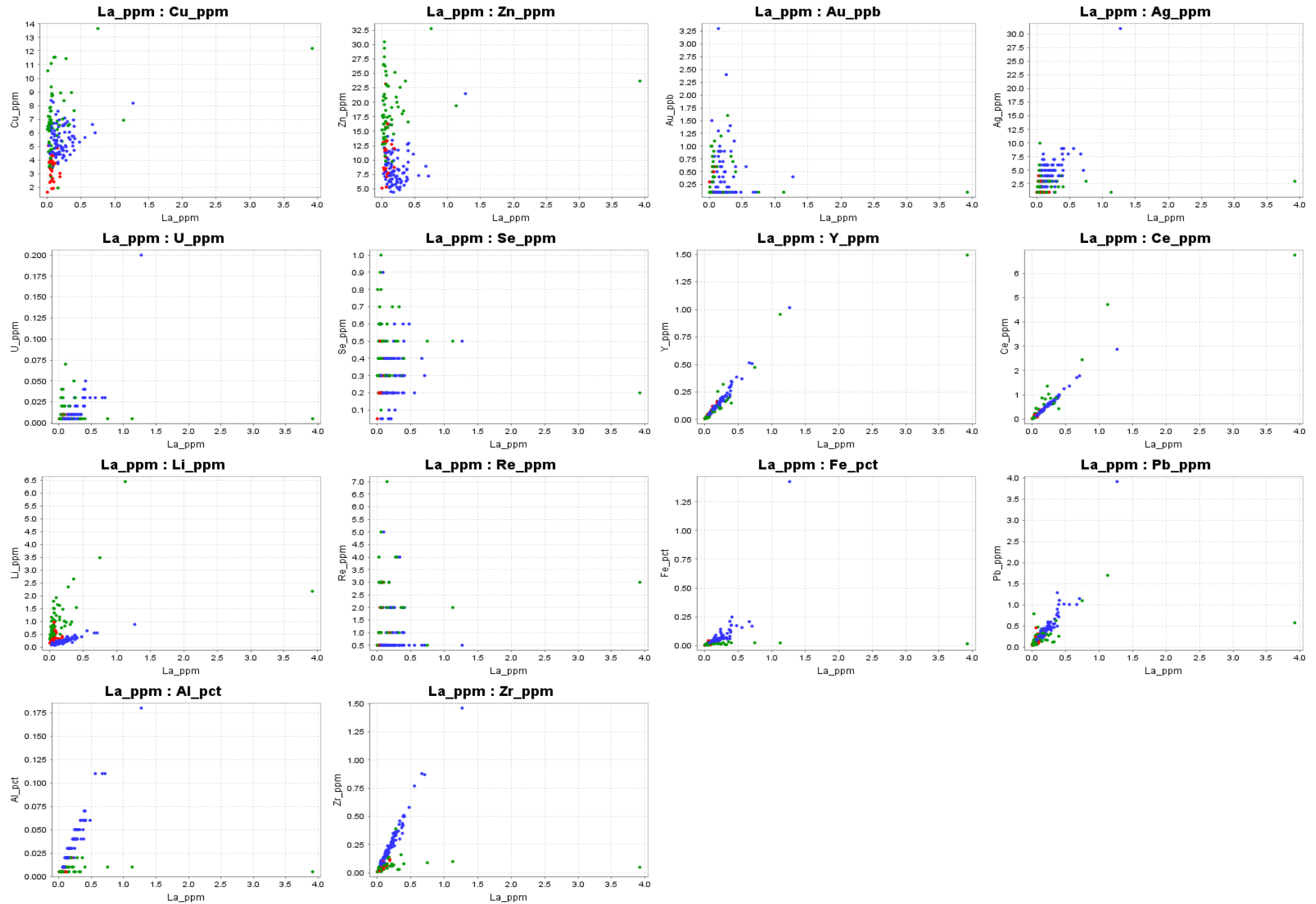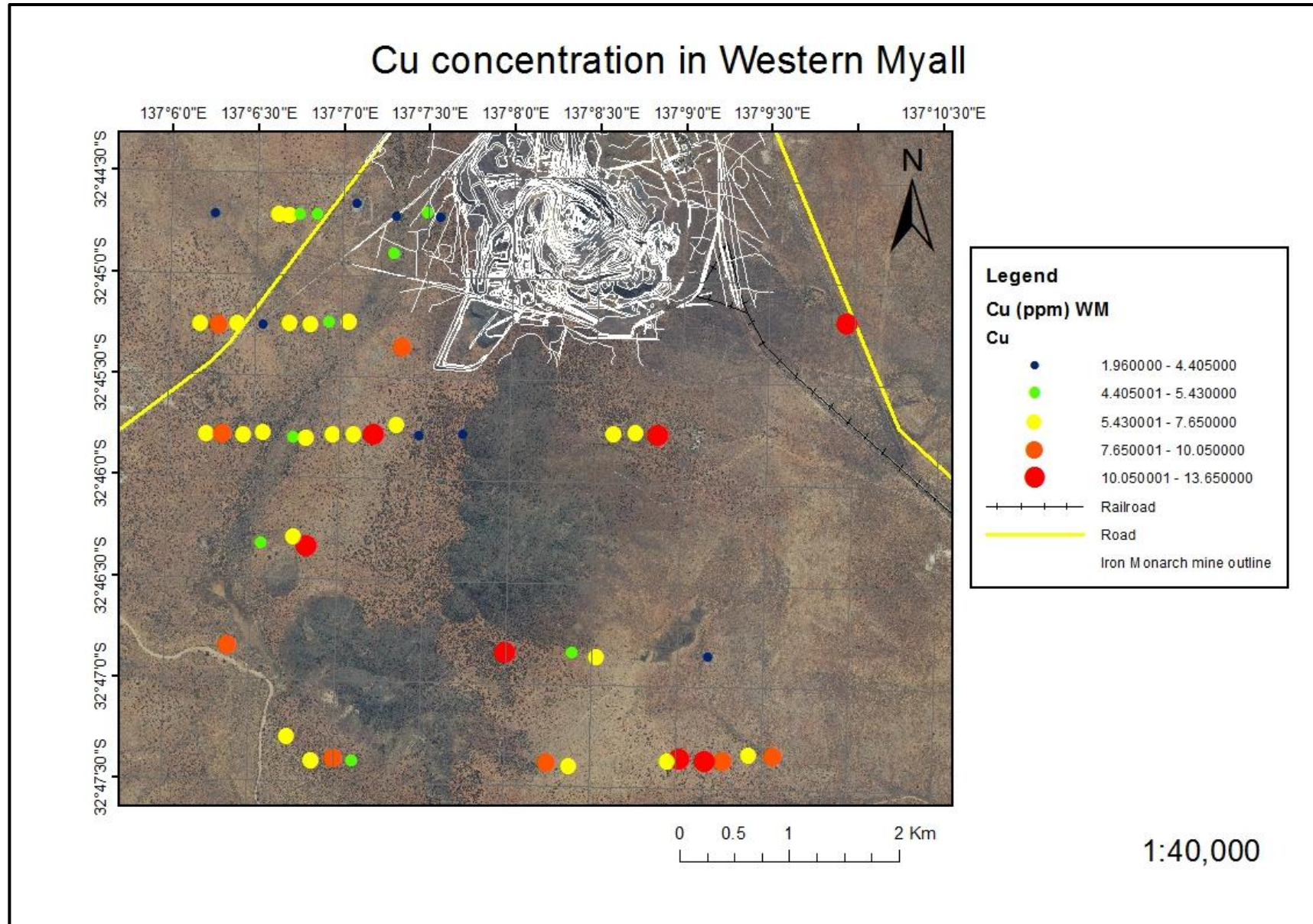
Figure 22

Figure 23

Figure 24

Figure 25

Zn concentration in Pearl Bluebush
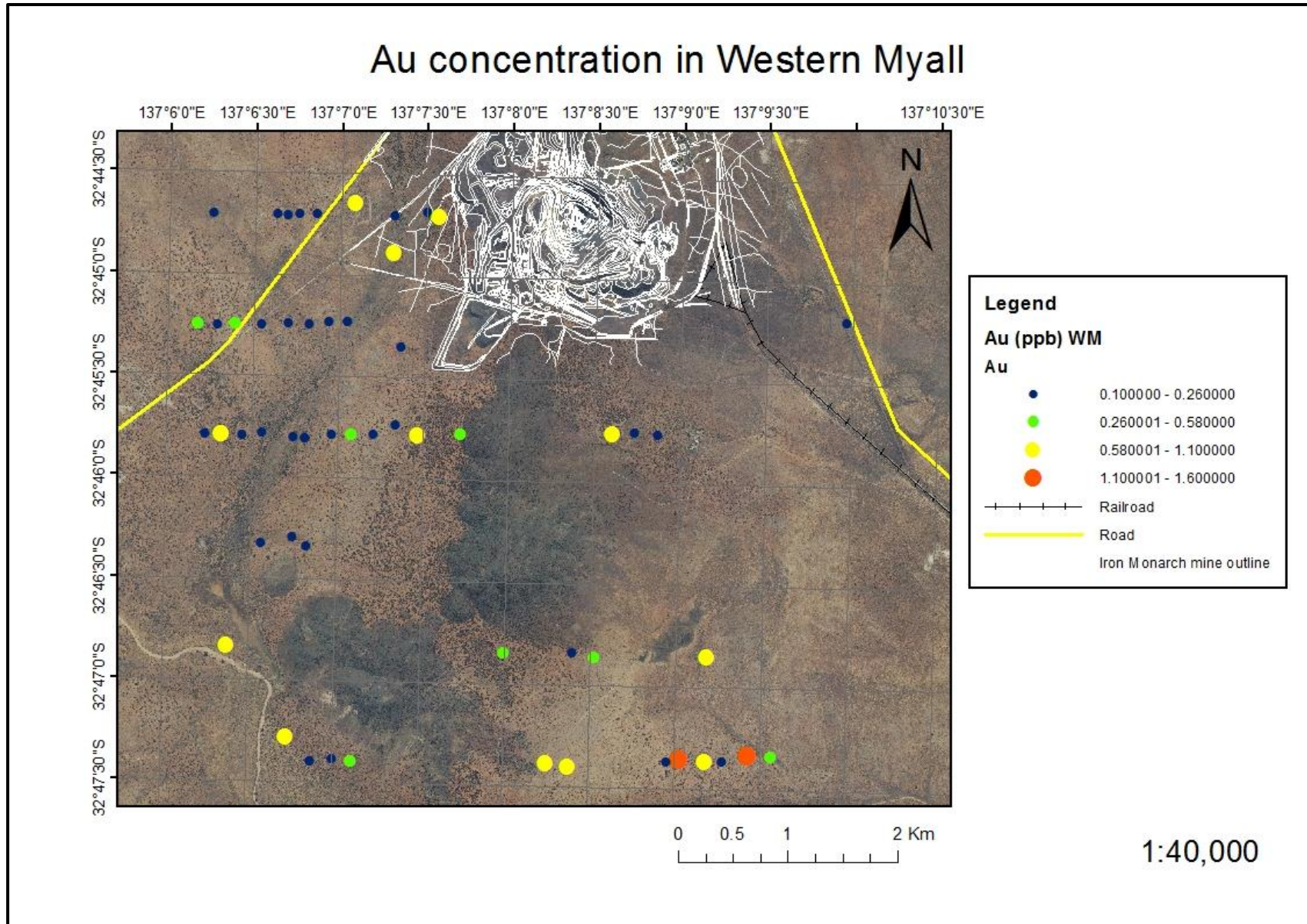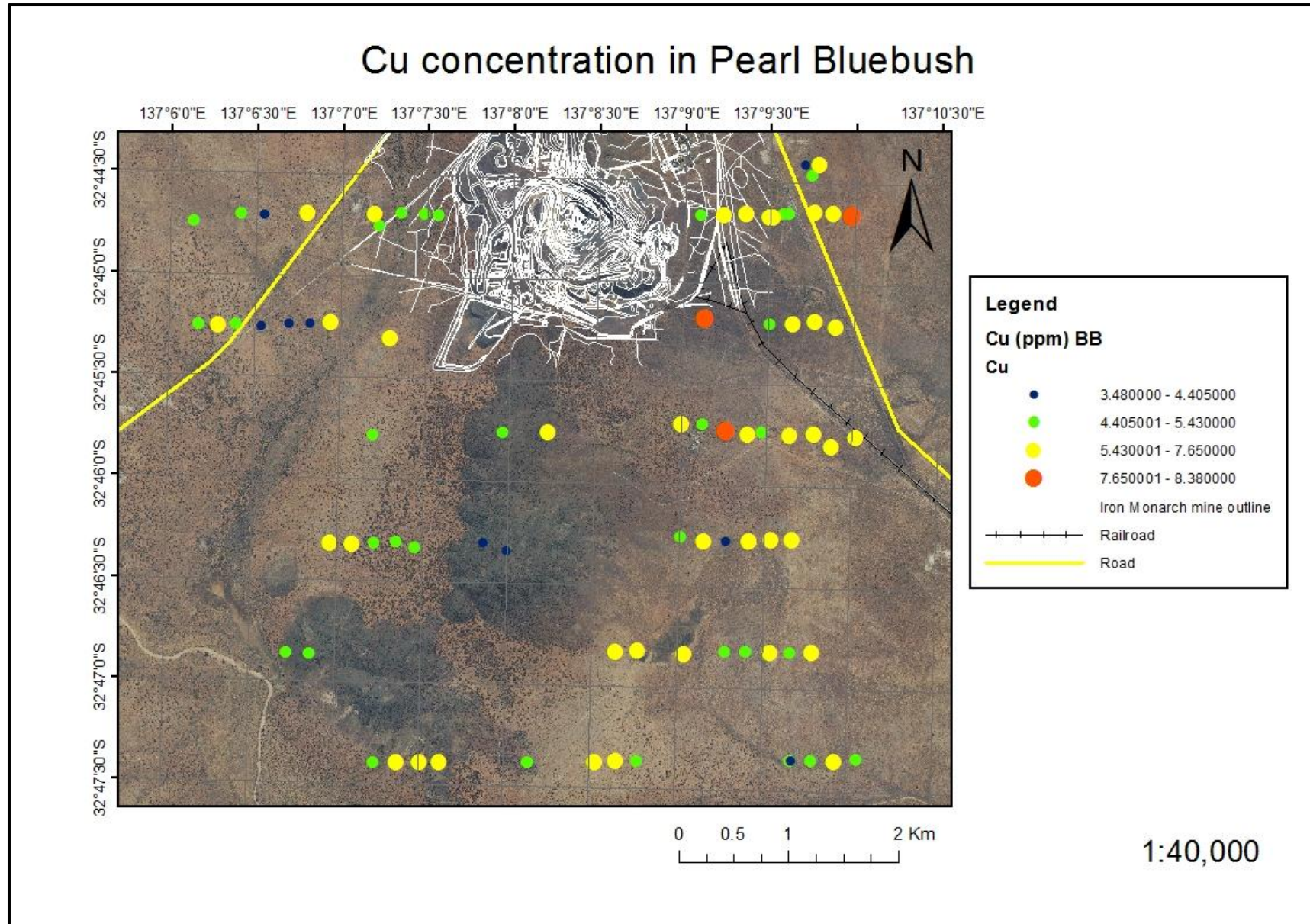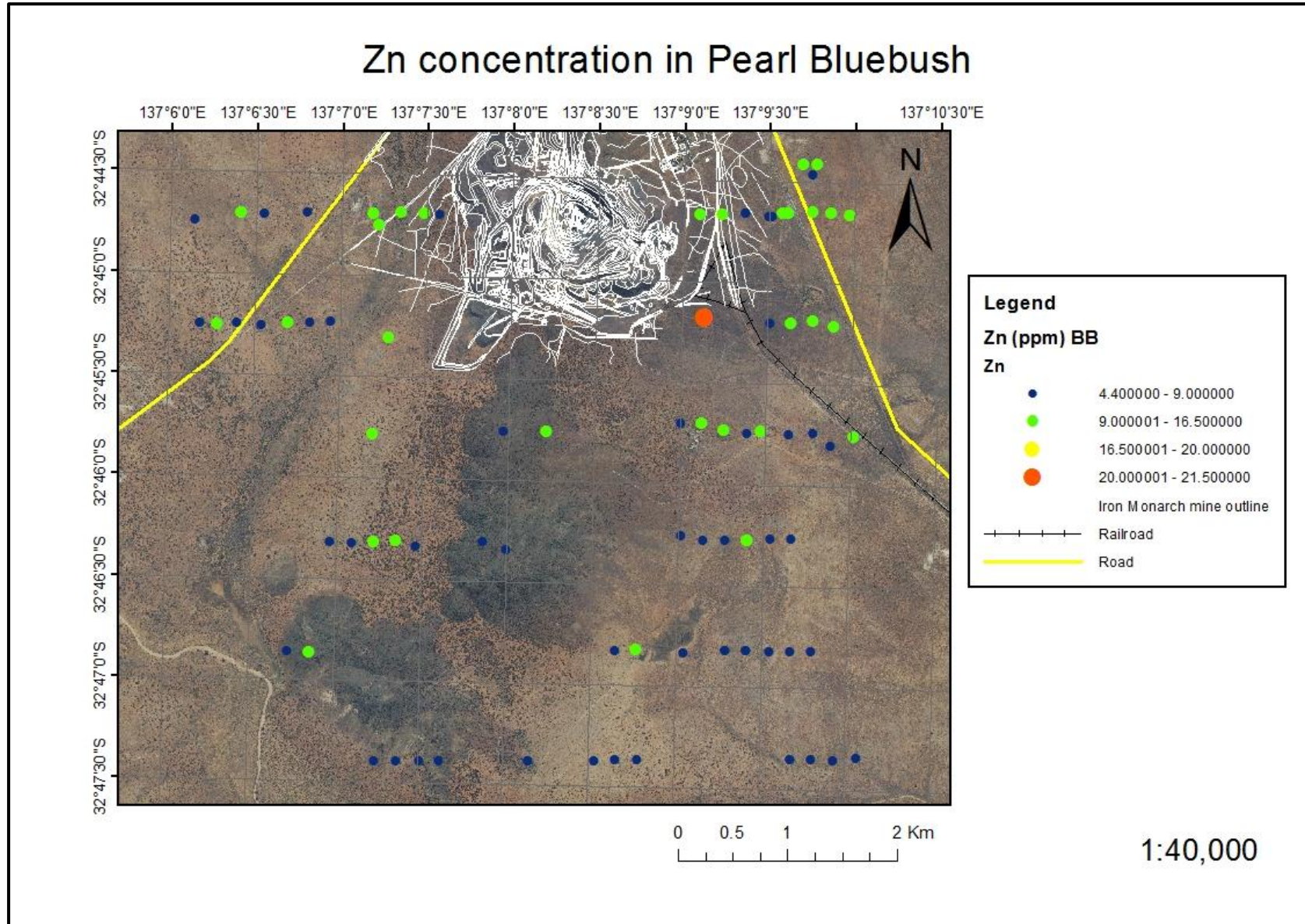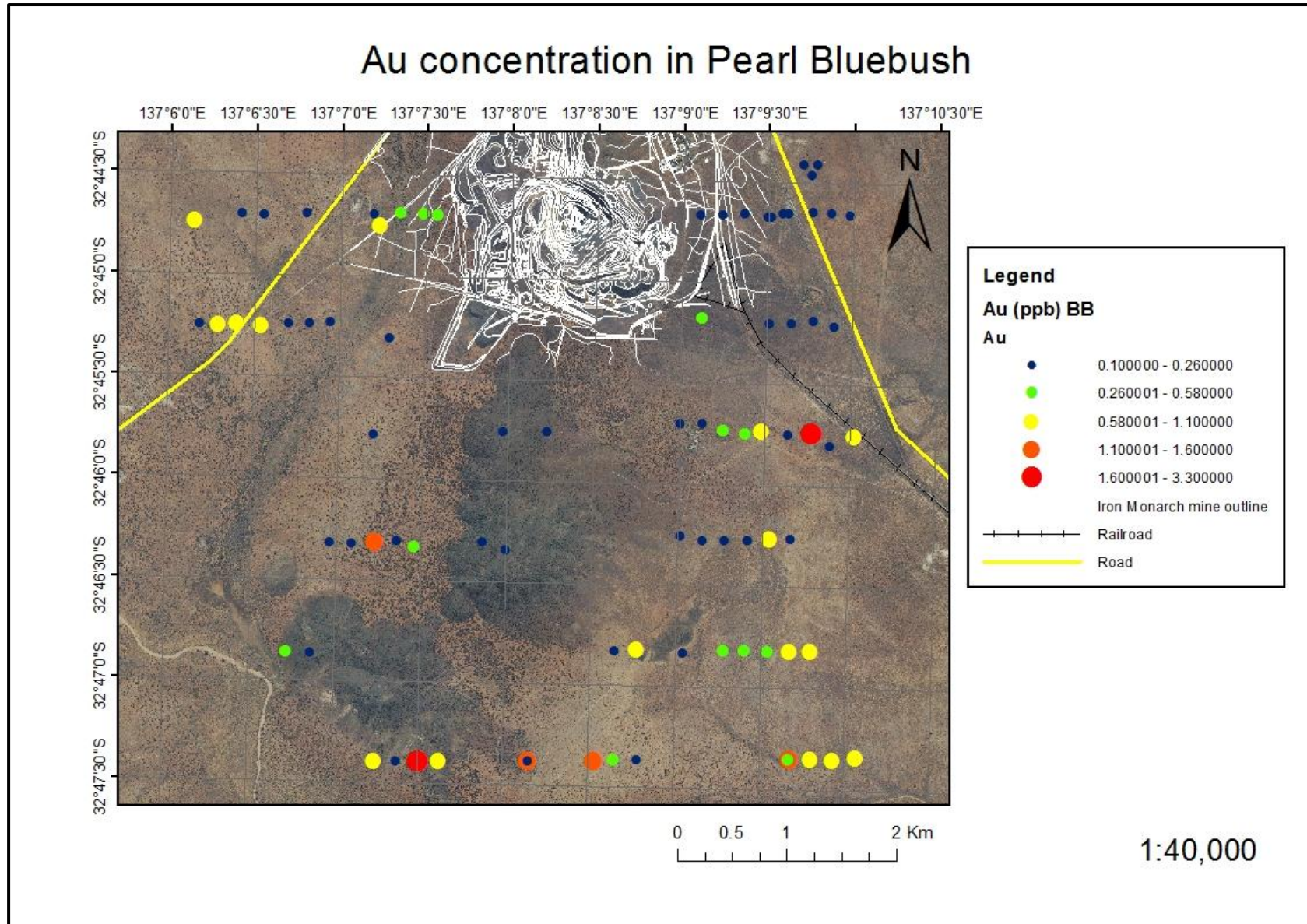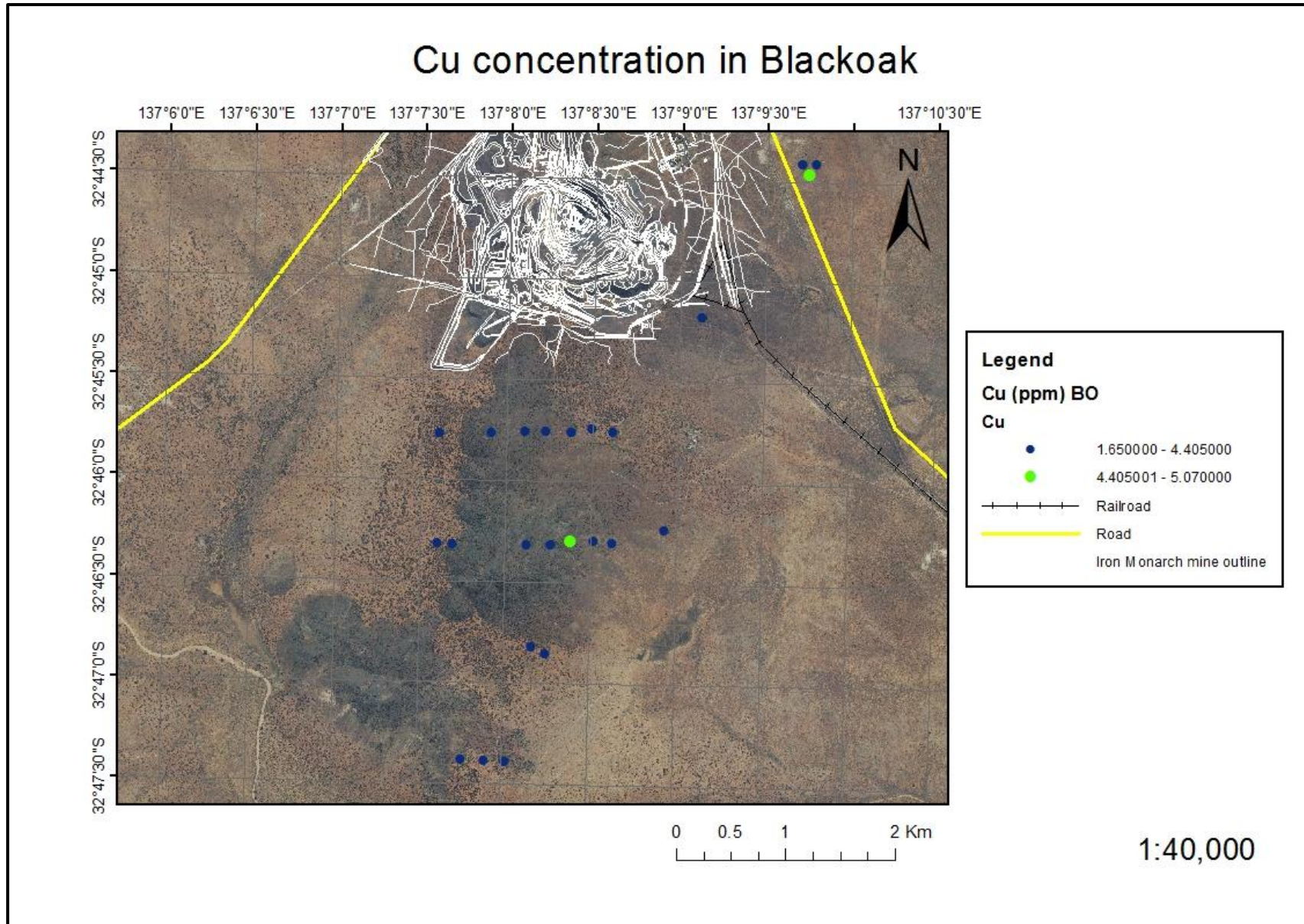
Figure 26

Figure 27

Figure 28
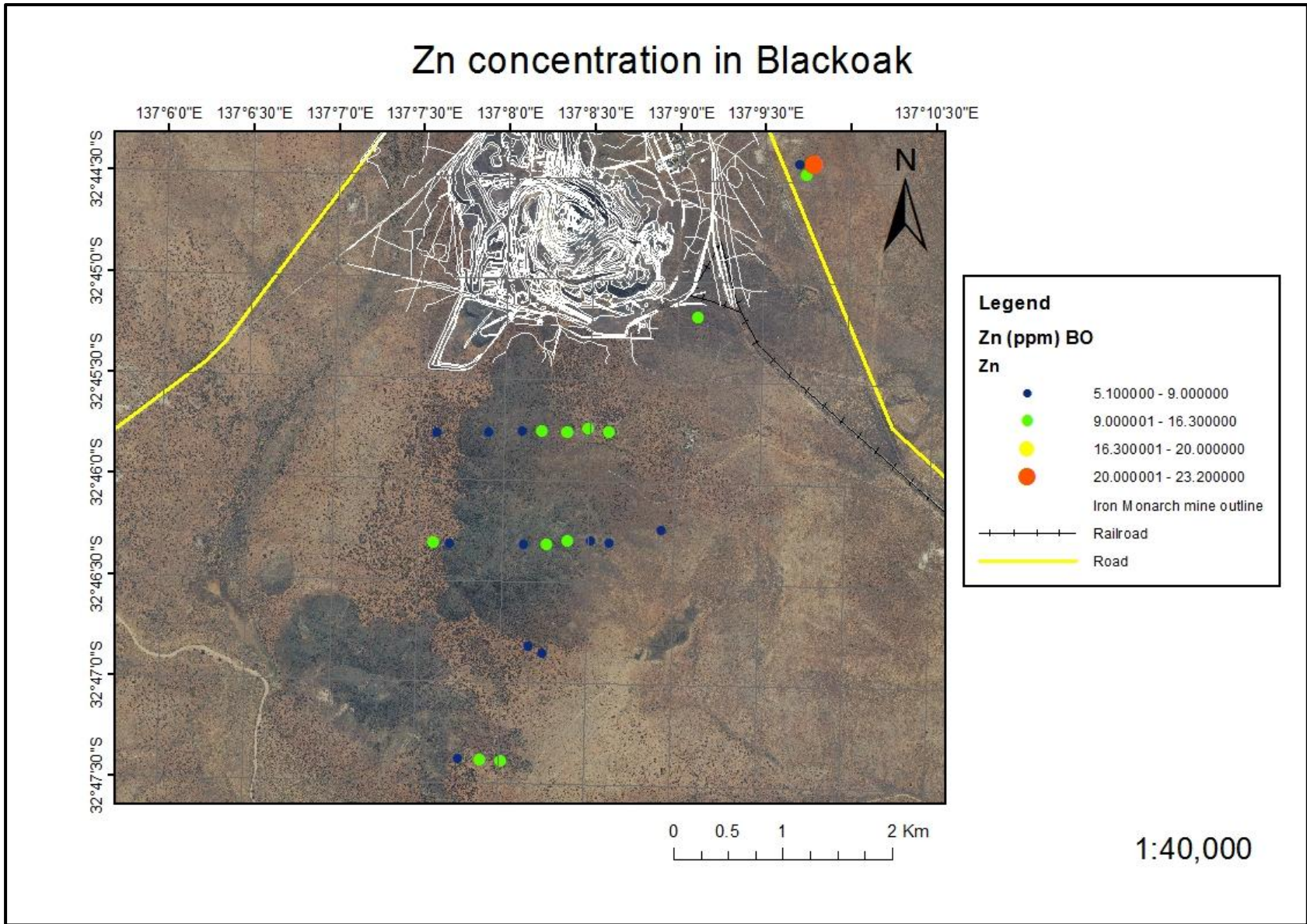
Figure 29
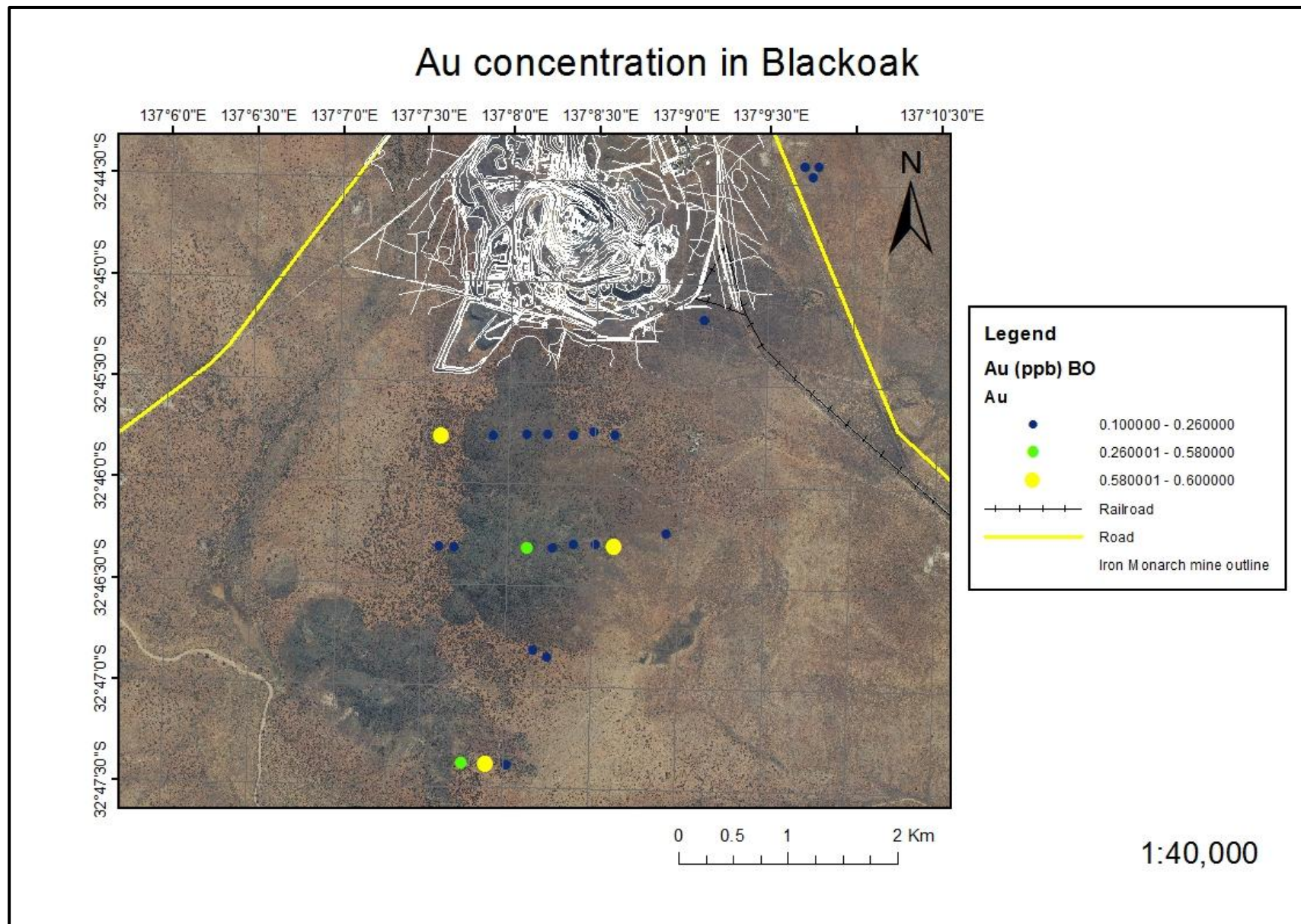
Figure 30

Figure 31
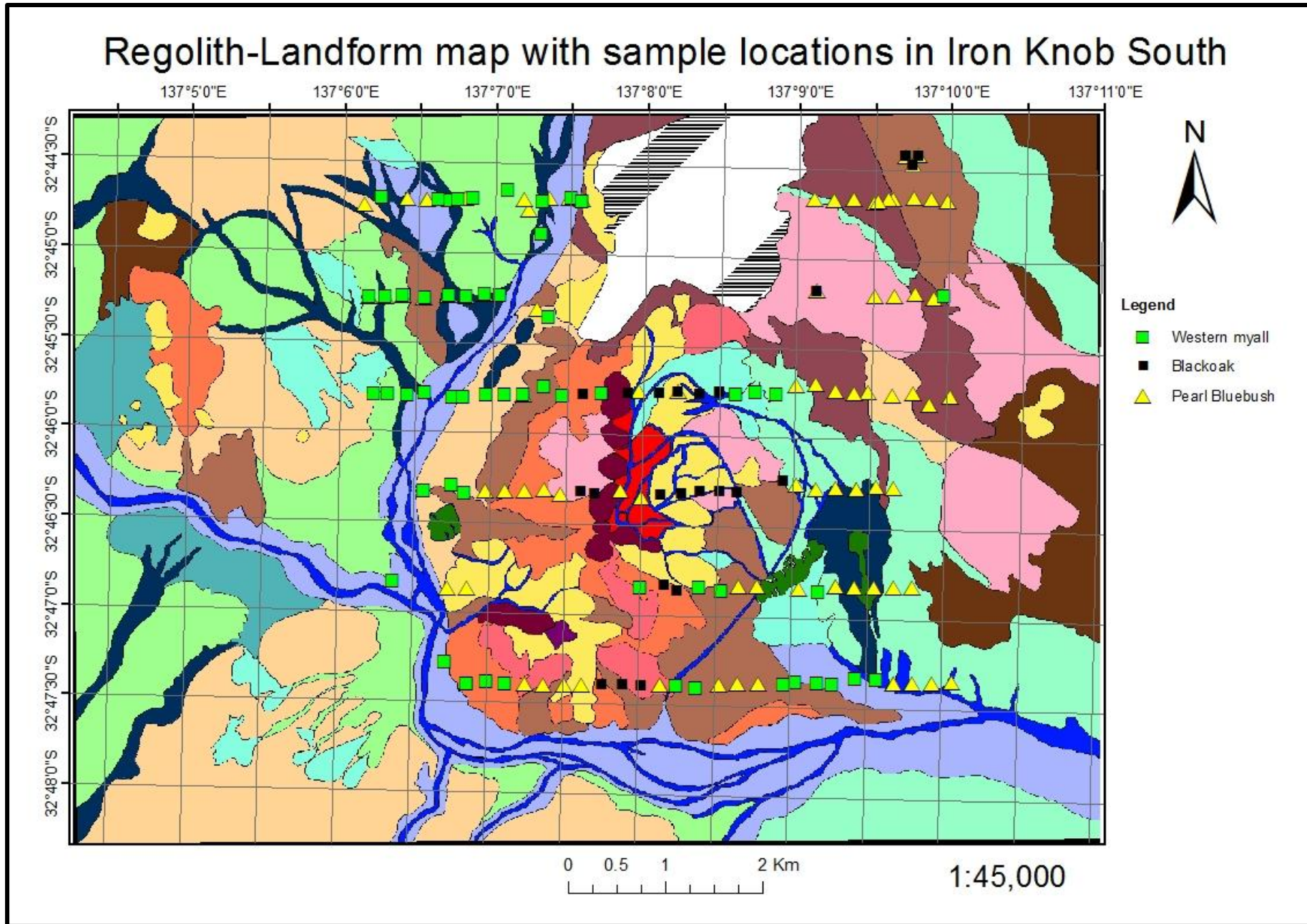
Figure 32

Figure 33

Figure 34

Figure 35

Figure 36

Figure 37

Figure 38

DATA AND IMAGES COLLECTED USING PHILIPS XL30 SEM

Acc.V Spot Magn Det WD Exp ⊢————————⊣ 500 µm
15.0 kV 4.0 150x SE 9.9 1
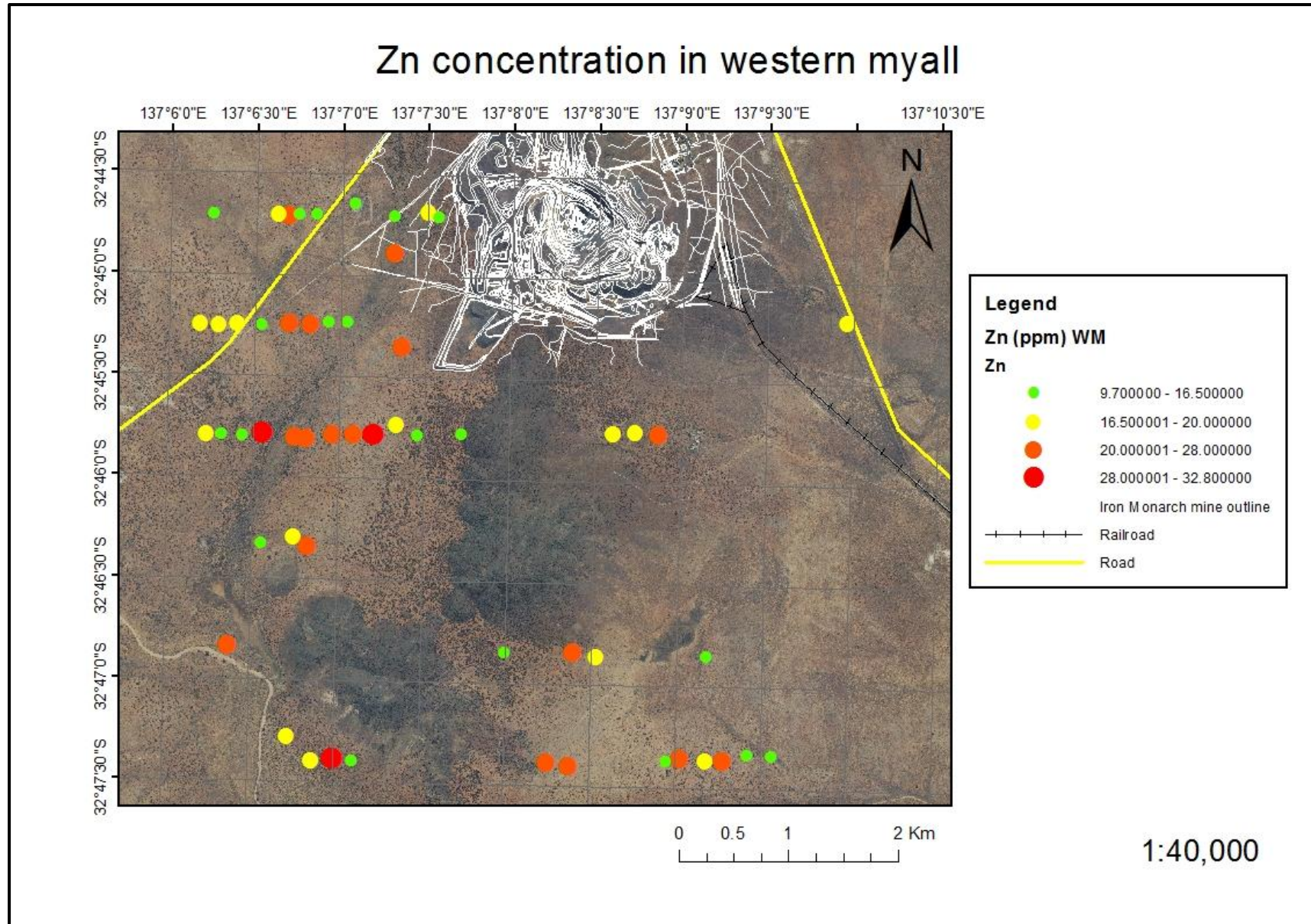
Figure 39

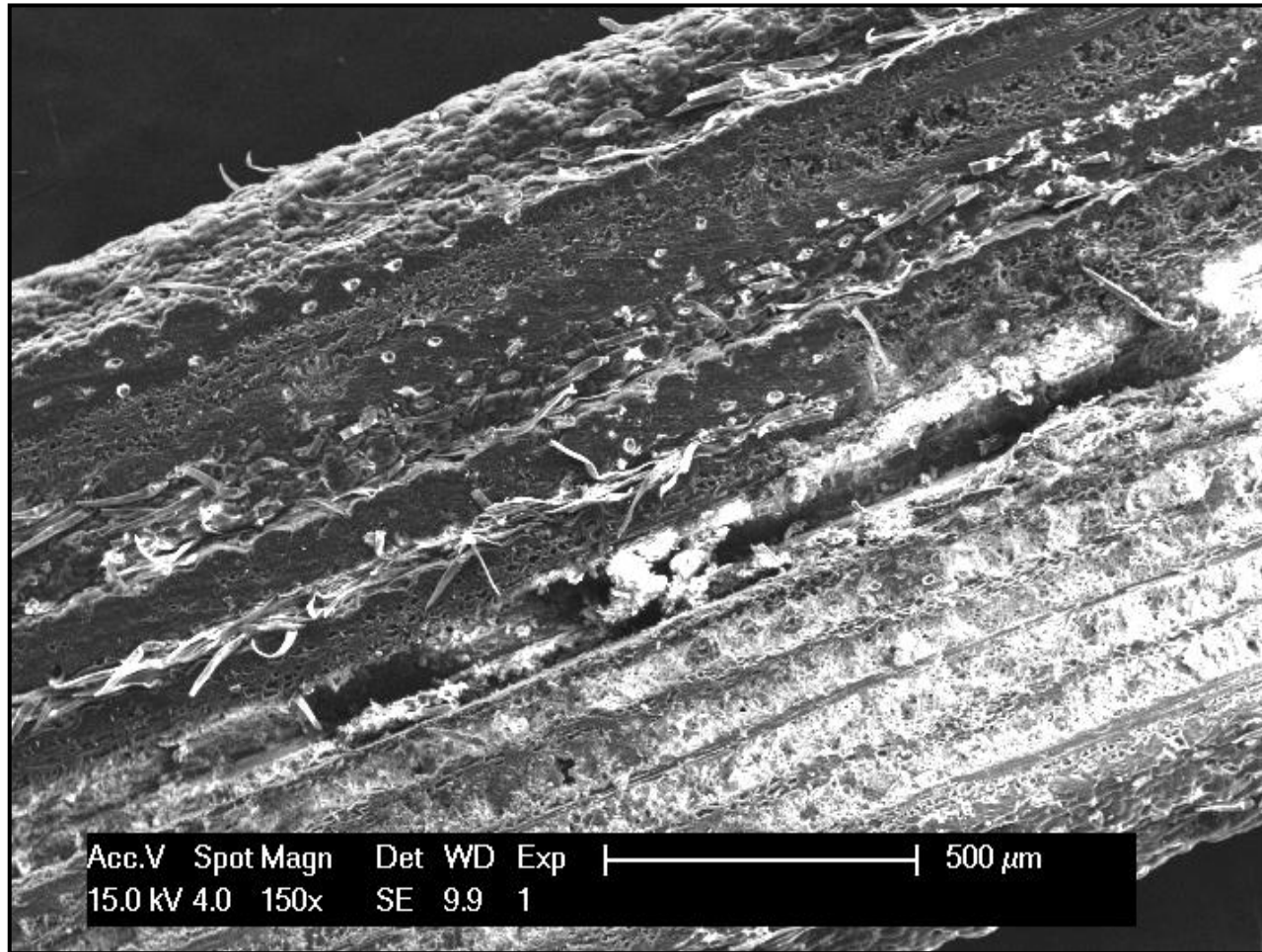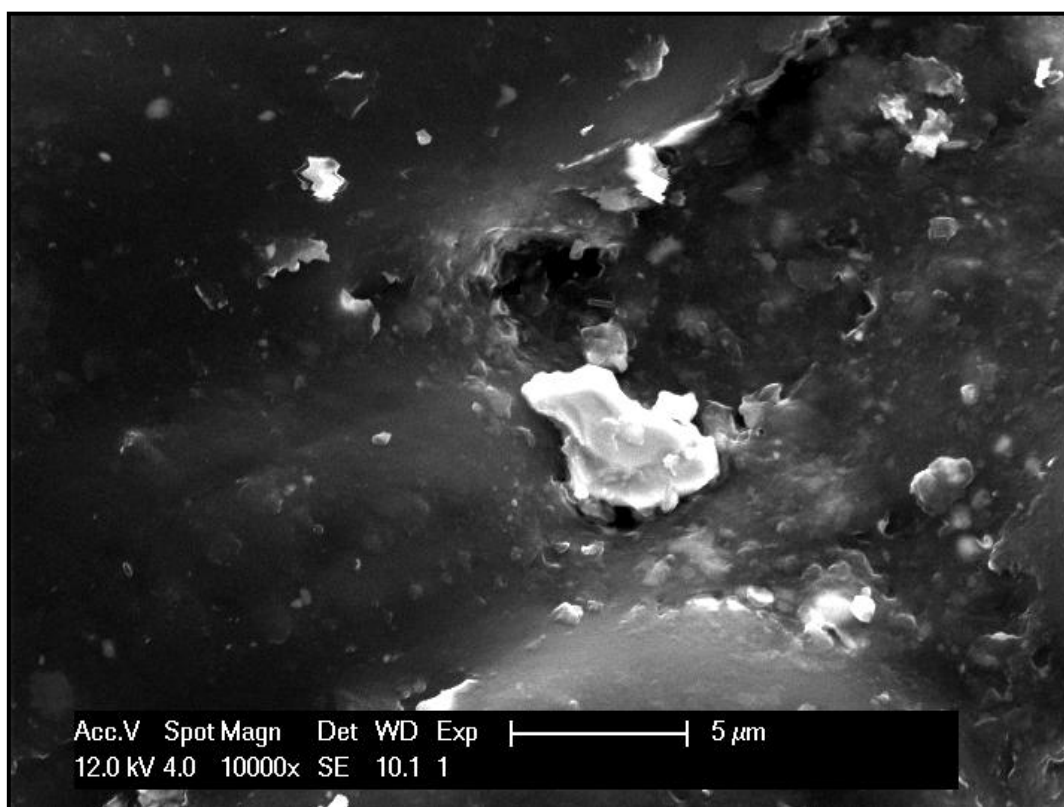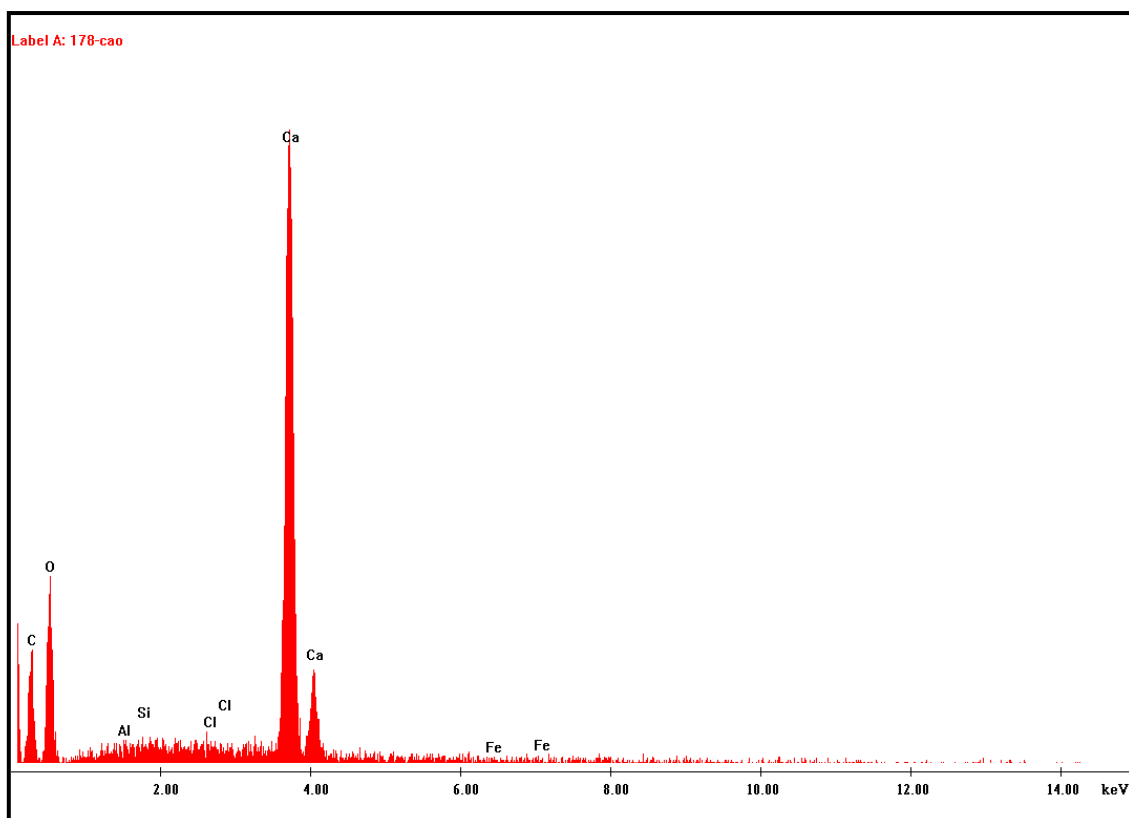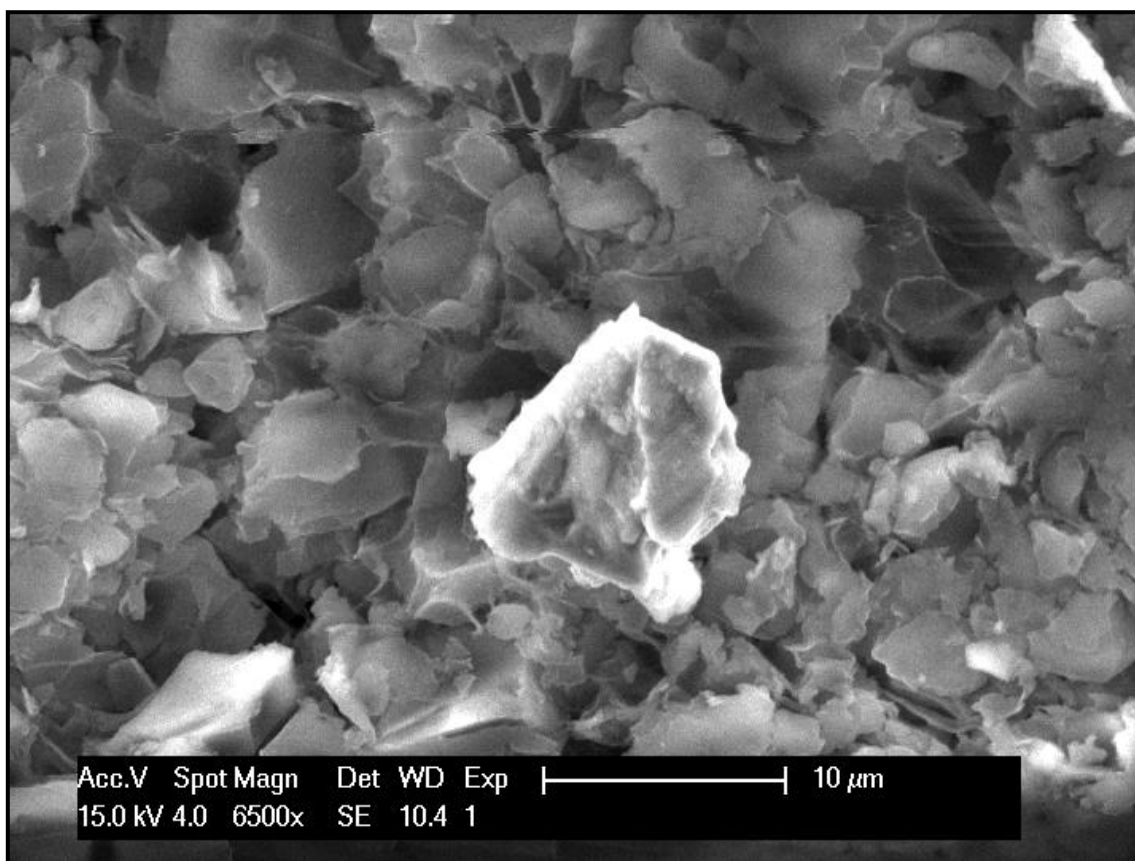**Figure 40**

Figure 41

Figure 42
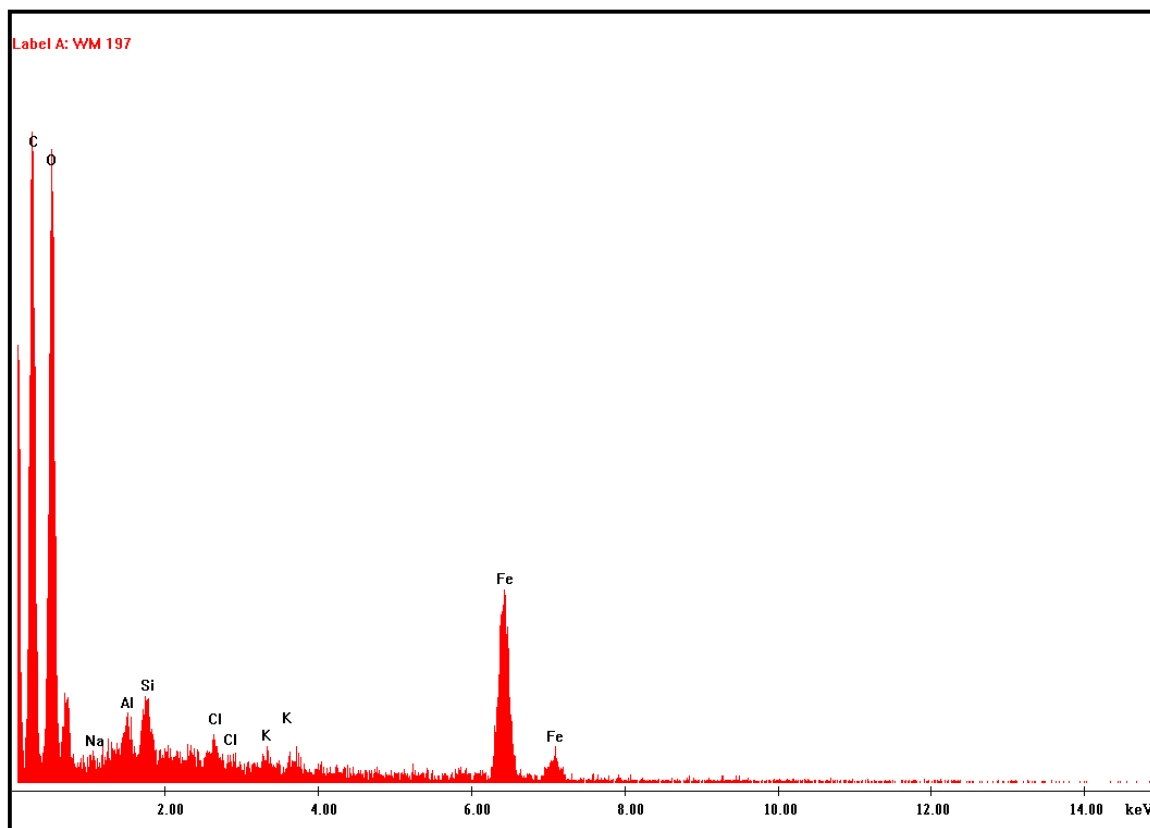
Figure 43
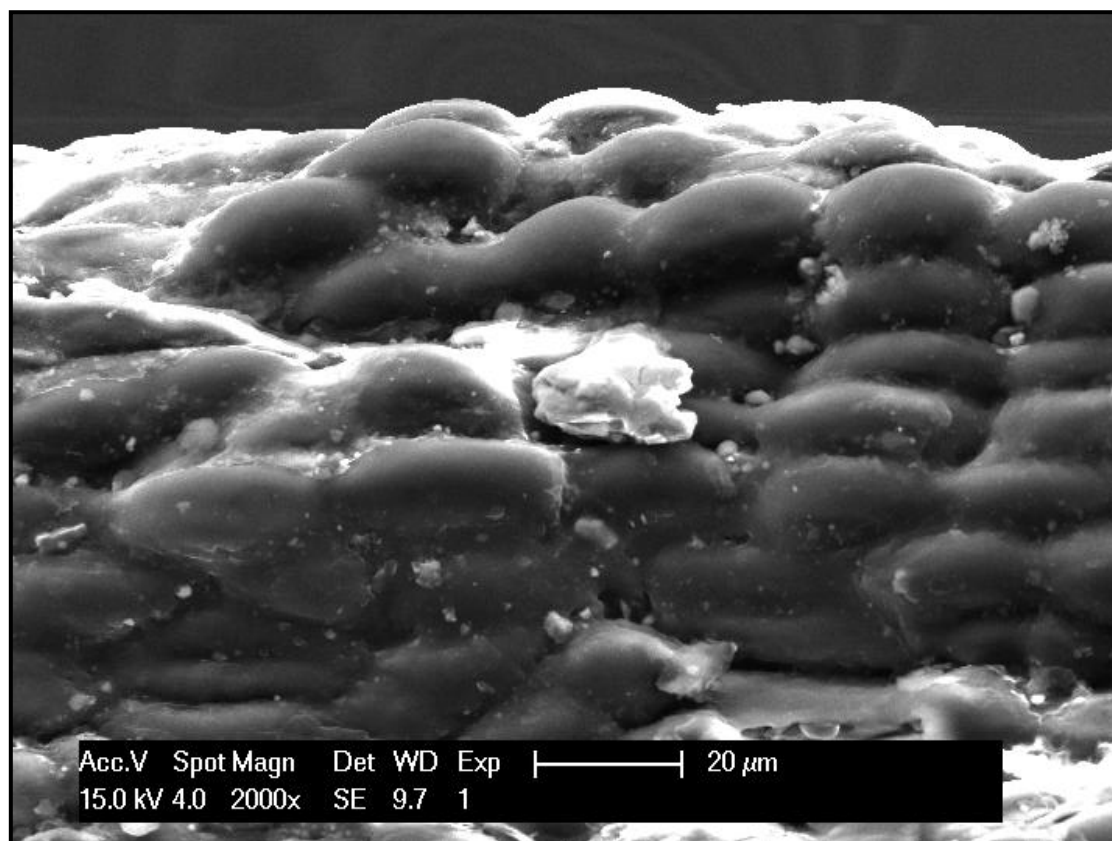
Figure 44

Figure 45

Figure 46

Location of new samples targeting high concentration areas
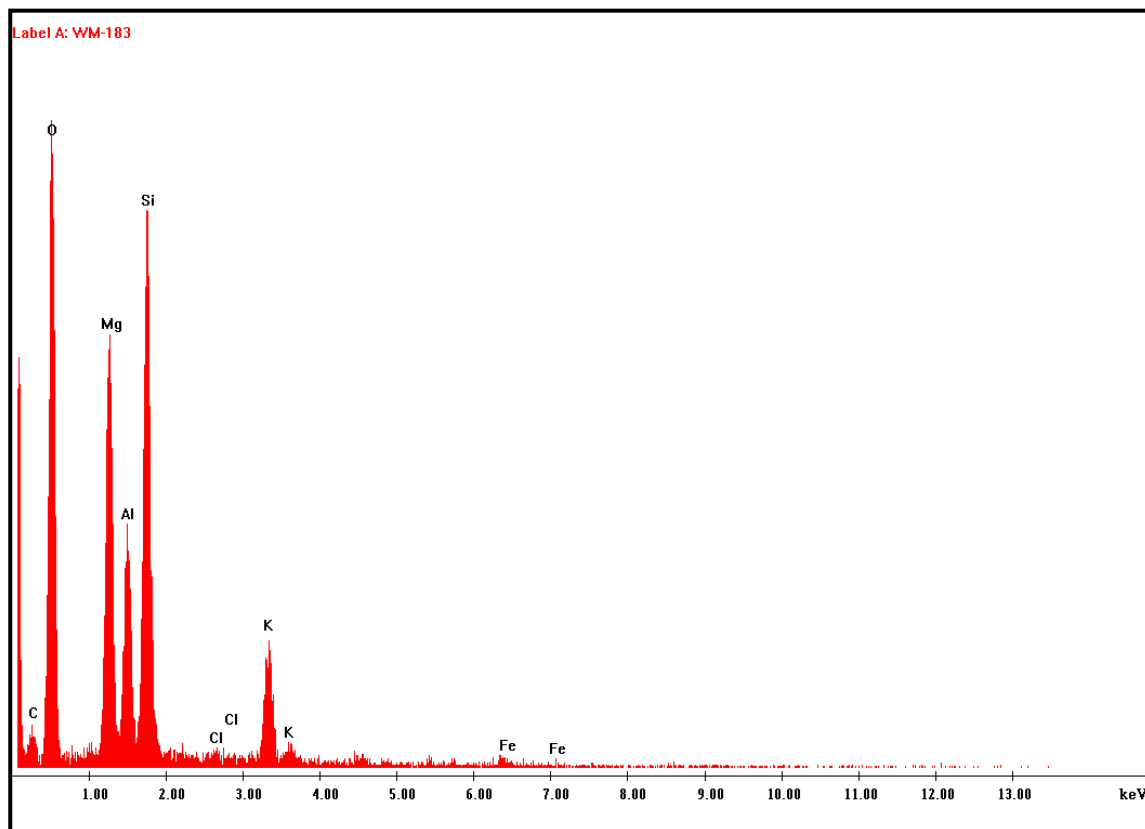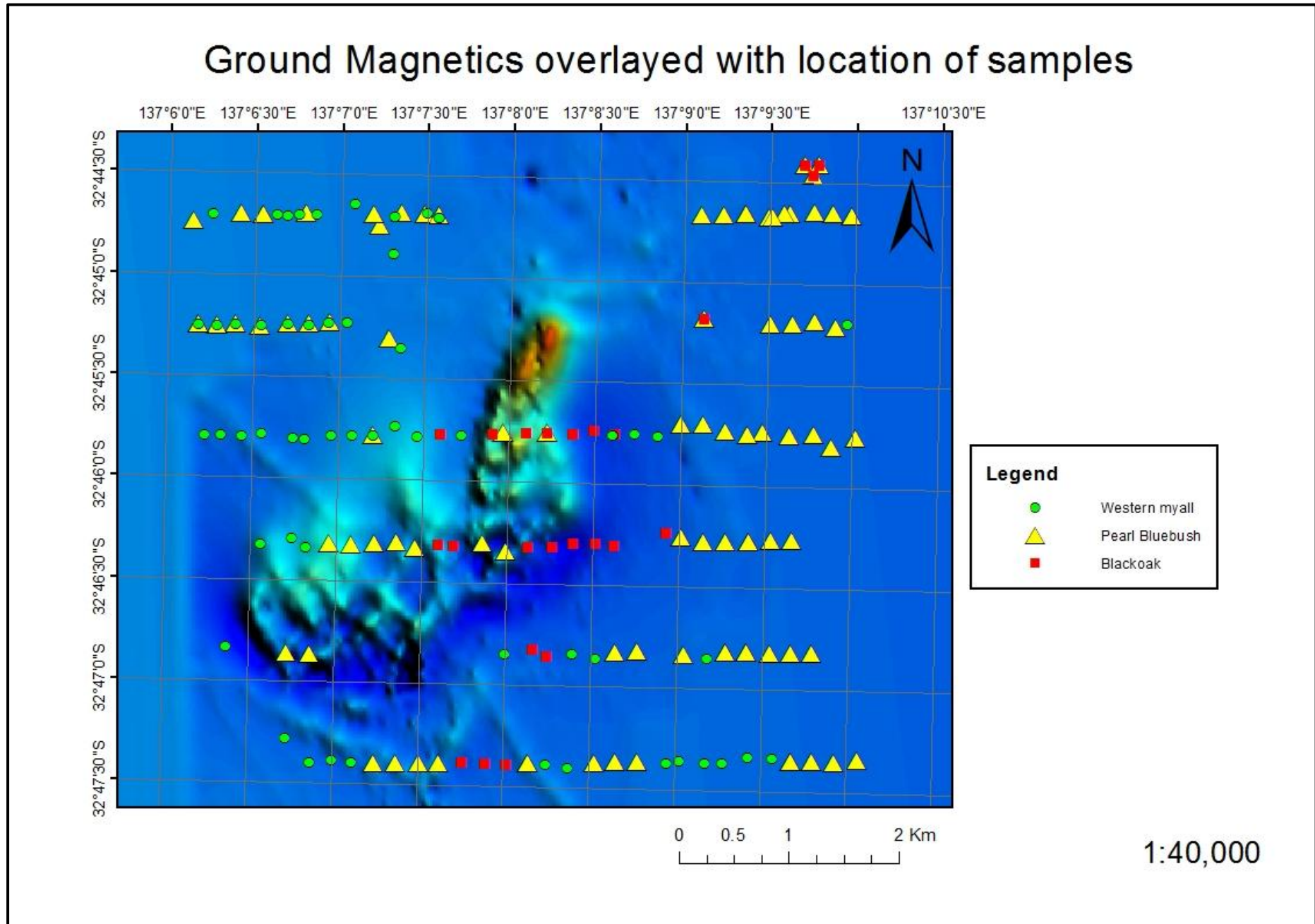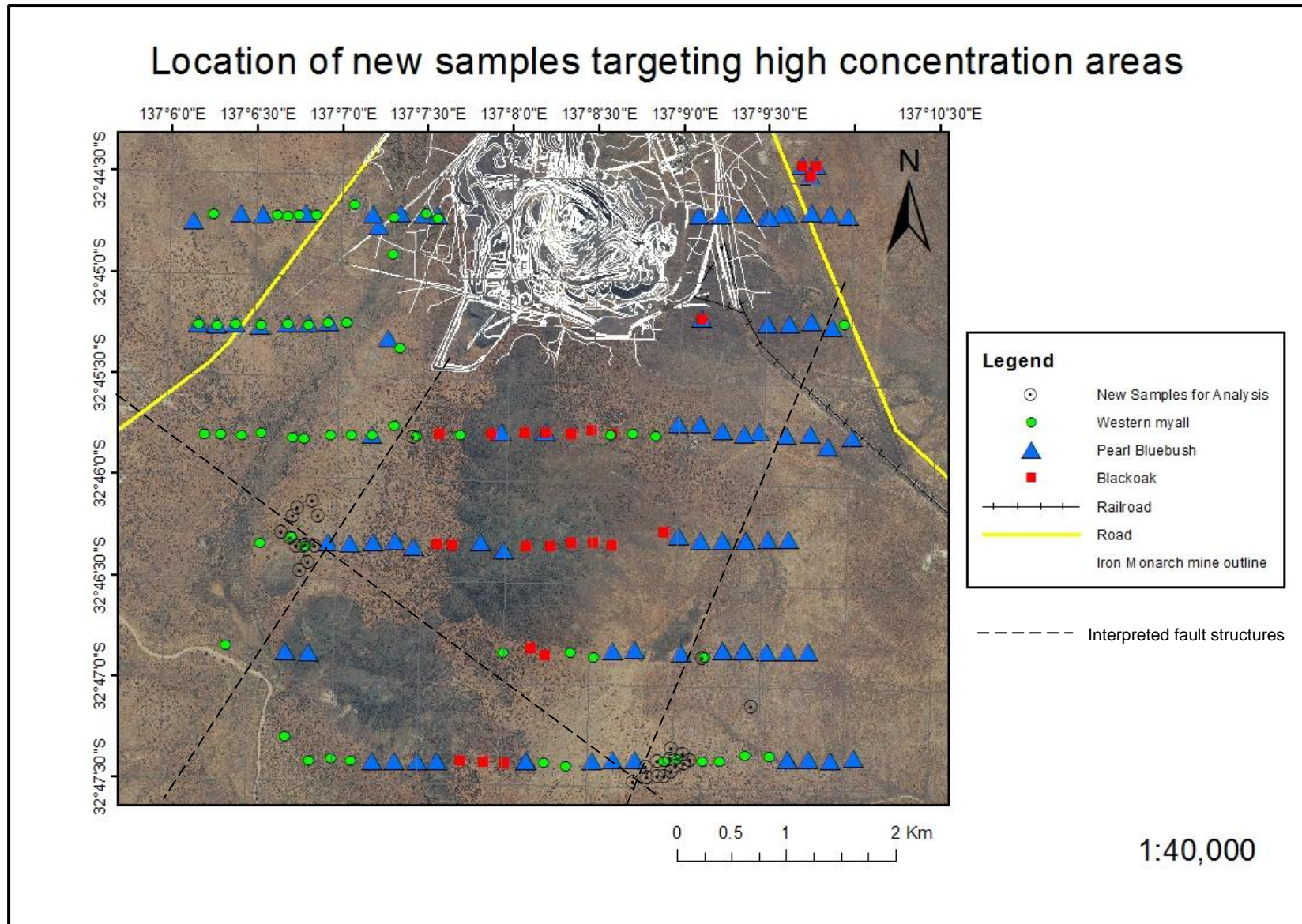
Figure 47

APPENDIX 1

Tables of raw data for target element suites including detection limits (modified to half of the laboratories original detection limit to allow use in map data)

SAMPLE	EASTING	NORTHING	SPECIES	Cu PPM	Zn PPM	Au PPB	Ag PPB	U PPM	Se PPM	Y PPM	Ce PPM	Re PPB	Li PPM	La PPM	Fe %	Pb PPM	Zr PPM	Al %
				0.005	0.05	0.1	1	0.005	0.05	0.0005	0.005	0.5	0.005	0.005	0.0005	0.005	0.005	0.005
KNOB-LT-001	698434	6375098	WM	3.59	15.6	0.6	3	0.02	0.5	0.056	0.22	0.5	1.01	0.09	0.030	0.48	0.09	0.01
KNOB-LT-002	698653	6374893	BB	4.61	9.9	0.9	4	0.01	0.3	0.119	0.41	0.5	0.25	0.18	0.065	0.45	0.22	0.03
KNOB-LT-003	698601	6374998	BB	6.60	10.3	0.1	5	0.03	0.4	0.170	0.53	0.5	0.27	0.24	0.120	0.60	0.26	0.03
KNOB-LT-004	698794	6374980	WM	3.50	13.6	0.1	1	0.01	0.5	0.029	0.08	0.5	1.01	0.03	0.015	0.16	0.04	0.005
KNOB-LT-005	698861	6375011	BB	4.93	9.1	0.4	6	0.02	0.3	0.102	0.38	0.5	0.18	0.15	0.074	0.38	0.18	0.03
KNOB-LT-006	699069	6375006	BB	4.50	11.9	0.3	4	0.02	0.4	0.128	0.38	0.5	0.20	0.17	0.091	0.36	0.21	0.03
KNOB-LT-007	699092	6375015	WM	4.78	16.7	0.1	1	0.005	0.8	0.035	0.10	0.5	0.48	0.06	0.019	0.22	0.05	0.005
KNOB-LT-008	699198	6374997	BB	4.72	8.4	0.5	4	0.03	0.4	0.191	0.58	0.5	0.31	0.24	0.142	0.58	0.27	0.04
KNOB-LT-009	699199	6374972	WM	3.96	15.3	0.1	10	0.005	0.6	0.033	0.11	0.5	0.49	0.05	0.016	0.27	0.05	0.005
KNOB-LT-010	698785	6374643	WM	5.25	21.0	1.0	2	0.005	0.5	0.024	0.08	1	1.16	0.03	0.013	0.79	0.04	0.005
KNOB-LT-011	697569	6373988	BB	3.85	5.7	0.7	3	0.005	0.3	0.112	0.36	0.5	0.22	0.16	0.041	0.32	0.16	0.02
KNOB-LT-012	697572	6373991	WM	2.77	11.4	0.1	1	0.04	0.5	0.030	0.20	1	0.87	0.06	0.019	0.20	0.05	0.005
KNOB-LT-013	697818	6374005	BB	3.48	10.4	0.1	4	0.005	0.4	0.047	0.16	0.5	0.08	0.08	0.019	0.23	0.06	0.005
KNOB-LT-014	697823	6374009	WM	6.96	21.4	0.1	3	0.005	0.6	0.032	0.15	0.5	0.72	0.04	0.013	0.15	0.04	0.005
KNOB-LT-015	698004	6374002	BB	4.38	6.2	0.1	7	0.005	0.4	0.068	0.27	0.5	0.13	0.11	0.027	0.25	0.09	0.01
KNOB-LT-016	698006	6373998	WM	6.62	27.9	0.1	4	0.005	0.6	0.032	0.22	3	0.53	0.04	0.015	0.17	0.03	0.005
KNOB-LT-017	698199	6374022	BB	6.23	8.0	0.1	4	0.005	0.5	0.033	0.11	2	0.09	0.05	0.016	0.16	0.06	0.005
KNOB-LT-018	698193	6374017	WM	5.33	14.6	0.1	1	0.01	0.5	0.018	0.06	3	0.32	0.03	0.012	0.12	0.03	0.005
KNOB-LT-019	698357	6374014	WM	6.26	15.2	0.1	1	0.005	0.3	0.008	0.02	0.5	0.30	0.005	0.005	0.08	0.01	0.005
KNOB-LT-020	698851	6373785	WM	8.71	24.7	0.1	3	0.005	0.6	0.048	0.19	3	1.33	0.07	0.025	0.29	0.06	0.005

SAMPLE	EASTING	NORTHING	SPECIES	Cu PPM 0.005	Zn PPM 0.05	Au PPB 0.1	Ag PPB 1	U PPM 0.005	Se PPM 0.05	Y PPM 0.0005	Ce PPM 0.005	Re PPB 0.5	Li PPM 0.005	La PPM 0.005	Fe % 0.0005	Pb PPM 0.005	Zr PPM 0.005	Al % 0.005
KNOB-LT-021	698738	6373864	BB	6.55	11.7	0.1	6	0.02	0.5	0.165	0.56	2	0.27	0.25	0.107	0.53	0.32	0.04
KNOB-LT-022	702620	6375011	BB	5.48	11.4	0.1	6	0.005	0.5	0.077	0.25	0.5	0.14	0.10	0.036	0.31	0.14	0.02
KNOB-LT-023	702793	6374999	BB	7.35	16.1	0.1	6	0.005	0.5	0.102	0.34	0.5	0.21	0.13	0.044	0.34	0.19	0.03
KNOB-LT-024	702963	6374978	BB	8.25	14.1	0.1	7	0.005	0.9	0.049	0.22	2	0.16	0.09	0.026	0.23	0.13	0.02
KNOB-LT-025	702403	6375001	BB	4.41	11.0	0.1	6	0.01	0.3	0.103	0.34	1	0.12	0.14	0.057	0.43	0.19	0.03
KNOB-LT-026	702348	6375002	BB	5.13	9.3	0.1	4	0.01	0.4	0.108	0.37	0.5	0.17	0.14	0.055	0.36	0.20	0.03
KNOB-LT-027	702211	6374967	BB	5.51	7.8	0.1	6	0.01	0.3	0.242	0.83	0.5	0.39	0.34	0.106	0.67	0.46	0.06
KNOB-LT-028	702244	6374975	BB	7.09	8.3	0.1	5	0.01	0.6	0.197	0.60	2	0.40	0.26	0.090	0.48	0.33	0.05
KNOB-LT-029	701991	6375001	BB	5.77	5.3	0.1	3	0.005	0.3	0.068	0.27	0.5	0.20	0.11	0.042	0.26	0.13	0.02
KNOB-LT-030	701799	6374992	BB	6.48	9.6	0.1	7	0.04	0.5	0.348	1.00	1	0.37	0.40	0.176	1.01	0.51	0.07
KNOB-LT-031	701591	6374993	BB	4.65	11.3	0.1	4	0.005	0.6	0.034	0.16	0.5	0.09	0.05	0.027	0.17	0.09	0.005
KNOB-LT-032	702922	6374001	WM	10.56	17.7	0.1	1	0.005	0.8	0.013	0.04	0.5	0.48	0.01	0.006	0.06	0.01	0.005
KNOB-LT-033	702815	6373968	BB	6.15	9.3	0.1	5	0.005	0.4	0.049	0.16	0.5	0.21	0.06	0.023	0.20	0.10	0.01
KNOB-LT-034	702624	6374016	BB	6.65	10.5	0.1	3	0.005	0.5	0.039	0.14	0.5	0.12	0.06	0.021	0.15	0.10	0.01
KNOB-LT-035	702415	6373993	BB	6.70	10.1	0.1	8	0.005	0.4	0.069	0.22	5	0.18	0.10	0.043	0.23	0.13	0.02
KNOB-LT-036	702213	6373998	BB	4.55	7.1	0.1	3	0.005	0.6	0.032	0.10	0.5	0.12	0.05	0.019	0.15	0.05	0.005
KNOB-LT-037	701612	6374052	BB	8.18	21.5	0.4	31	0.20	0.5	1.016	2.87	0.5	0.88	1.27	1.425	3.91	1.46	0.18
KNOB-LT-038	701612	6374052	BO	4.16	15.7	0.1	3	0.005	0.5	0.048	0.14	0.5	0.29	0.06	0.043	0.21	0.08	0.005
KNOB-LT-039	702532	6375447	BO	2.48	8.5	0.1	1	0.005	0.4	0.039	0.22	0.5	0.44	0.06	0.011	0.15	0.03	0.005
KNOB-LT-040	702534	6375443	BB	3.74	11.3	0.1	4	0.005	0.4	0.114	0.38	0.5	0.17	0.16	0.052	0.39	0.24	0.03

SAMPLE	EASTING	NORTHING	SPECIES	Cu	Zn	Au	Ag	U	Se	Y	Ce	Re	Li	La	Fe	Pb	Zr	Al
				PPM	PPM	PPB	PPB	PPM	PPM	PPM	PPM	PPB	PPM	PPM	%	PPM	PPM	%
				0.005	0.05	0.1	1	0.005	0.05	0.0005	0.005	0.5	0.005	0.005	0.0005	0.005	0.005	0.005
KNOB-LT-041	702607	6375358	BO	5.07	13.0	0.1	3	0.005	0.2	0.014	0.05	0.5	0.22	0.02	0.010	0.11	0.02	0.005
KNOB-LT-042	702607	6375358	BB	4.67	6.6	0.1	3	0.005	0.3	0.036	0.16	3	0.15	0.06	0.022	0.22	0.08	0.01
KNOB-LT-043	702665	6375450	BO	3.71	23.2	0.1	1	0.005	0.4	0.049	0.16	2	0.32	0.06	0.022	0.25	0.06	0.005
KNOB-LT-044	702665	6375450	BB	6.95	12.7	0.1	8	0.02	0.6	0.260	0.90	1	0.40	0.39	0.116	0.82	0.50	0.07
KNOB-LT-045	698081	6375007	WM	4.85	16.1	0.1	1	0.07	0.4	0.089	0.41	3	1.23	0.10	0.009	0.13	0.03	0.005
KNOB-LT-046	697990	6375012	BB	5.75	8.3	0.1	4	0.02	0.4	0.208	0.88	1	0.29	0.38	0.060	0.50	0.35	0.04
KNOB-LT-047	697816	6374989	WM	7.59	26.3	0.1	2	0.01	0.6	0.019	0.24	0.5	0.45	0.05	0.008	0.11	0.02	0.005
KNOB-LT-048	697927	6374999	WM	5.07	13.0	0.1	4	0.01	0.5	0.033	0.20	1	0.57	0.06	0.014	0.17	0.05	0.005
KNOB-LT-049	697597	6374999	BB	4.16	5.3	0.1	4	0.01	0.4	0.124	0.58	0.5	0.18	0.23	0.045	0.45	0.23	0.02
KNOB-LT-050	697721	6375003	WM	7.01	20.0	0.1	2	0.05	0.7	0.098	1.36	2	0.82	0.23	0.018	0.17	0.06	0.005
KNOB-LT-051	697396	6375014	BB	5.04	11.8	0.1	5	0.01	0.4	0.130	0.49	0.5	0.12	0.20	0.044	0.36	0.22	0.03
KNOB-LT-052	697136	6375018	WM	3.63	12.1	0.1	1	0.005	0.7	0.012	0.06	1	0.41	0.04	0.007	0.10	0.03	0.005
KNOB-LT-053	696962	6374955	BB	5.36	7.3	0.8	6	0.005	0.3	0.100	0.30	0.5	0.16	0.14	0.037	0.30	0.18	0.03
KNOB-LT-054	697346	6374010	BB	5.04	7.0	1.1	6	0.02	0.2	0.228	0.84	2	0.45	0.38	0.081	0.90	0.42	0.06
KNOB-LT-055	697346	6374010	WM	6.95	18.6	0.3	1	0.03	0.5	0.035	0.17	2	1.78	0.06	0.009	0.11	0.03	0.005
KNOB-LT-056	697169	6373999	WM	8.36	19.2	0.1	3	0.03	0.3	0.104	1.03	0.5	0.96	0.25	0.012	0.28	0.07	0.005
KNOB-LT-057	697005	6374003	WM	6.34	17.4	0.4	2	0.005	0.5	0.037	0.20	2	0.47	0.08	0.006	0.07	0.03	0.005
KNOB-LT-058	697169	6373999	BB	5.96	11.3	0.8	5	0.005	0.05	0.056	0.20	0.5	0.10	0.08	0.019	0.15	0.09	0.01
KNOB-LT-059	697005	6374003	BB	5.22	8.5	0.1	4	0.005	0.3	0.085	0.31	0.5	0.15	0.12	0.029	0.25	0.16	0.02
KNOB-LT-060	702988	6372962	BB	6.71	9.5	0.6	2	0.005	0.3	0.050	0.17	0.5	0.09	0.08	0.018	0.13	0.08	0.01

SAMPLE	EASTING	NORTHING	SPECIES	Cu	Zn	Au	Ag	U	Se	Y	Ce	Re	Li	La	Fe	Pb	Zr	Al
				PPM	PPM	PPB	PPB	PPM	PPM	PPM	PPM	PPB	PPM	PPM	%	PPM	PPM	%
				0.005	0.05	0.1	1	0.005	0.05	0.0005	0.005	0.5	0.005	0.005	0.0005	0.005	0.005	0.005
KNOB-LT-061	702766	6372876	BB	6.83	6.3	0.2	3	0.01	0.4	0.210	0.72	1	0.27	0.30	0.067	0.47	0.37	0.05
KNOB-LT-062	702606	6372993	BB	6.70	8.7	3.3	6	0.005	0.2	0.098	0.34	0.5	0.24	0.14	0.041	0.30	0.18	0.02
KNOB-LT-063	702384	6372978	BB	6.62	8.9	0.1	8	0.03	0.4	0.516	1.71	0.5	0.55	0.67	0.208	1.01	0.88	0.11
KNOB-LT-064	702145	6373008	BB	4.72	11.6	0.6	5	0.03	0.2	0.316	0.95	0.5	0.36	0.40	0.177	0.72	0.50	0.07
KNOB-LT-065	701802	6373023	BB	8.38	9.8	0.5	6	0.005	0.3	0.047	0.16	0.5	0.11	0.06	0.023	0.16	0.11	0.01
KNOB-LT-066	701401	6373085	BB	6.16	6.3	0.1	6	0.005	0.4	0.080	0.23	0.5	0.19	0.11	0.037	0.24	0.12	0.02
KNOB-LT-067	700980	6373003	WM	6.87	17.0	0.1	1	0.005	0.6	0.102	0.34	7	1.17	0.15	0.021	0.21	0.05	0.005
KNOB-LT-068	700609	6373026	BO	4.00	10.5	0.1	1	0.005	0.4	0.039	0.13	0.5	0.85	0.06	0.014	0.46	0.05	0.005
KNOB-LT-069	700415	6373002	BO	4.38	13.2	0.1	3	0.005	0.3	0.043	0.14	0.5	0.36	0.06	0.021	0.15	0.04	0.005
KNOB-LT-070	700184	6373015	BB	5.57	12.9	0.1	9	0.05	0.3	0.341	1.00	2	0.35	0.41	0.248	1.11	0.50	0.06
KNOB-LT-071	699995	6373012	BO	1.93	7.6	0.1	1	0.005	0.2	0.064	0.22	0.5	0.64	0.09	0.031	0.32	0.10	0.01
KNOB-LT-072	699679	6373003	BO	2.78	8.7	0.1	1	0.005	0.3	0.166	0.48	0.5	0.37	0.19	0.044	0.27	0.11	0.02
KNOB-LT-073	700220	6371969	BO	4.33	16.3	0.1	1	0.005	0.3	0.065	0.20	0.5	0.23	0.09	0.008	0.18	0.06	0.005
KNOB-LT-074	700414	6371998	BO	4.88	12.7	0.1	1	0.005	0.3	0.119	0.40	0.5	0.31	0.15	0.020	0.24	0.07	0.01
KNOB-LT-075	700615	6372002	BO	3.37	8.0	0.1	2	0.01	0.3	0.057	0.17	0.5	0.76	0.07	0.024	0.29	0.09	0.01
KNOB-LT-076	700790	6371986	BO	3.38	7.9	0.6	1	0.005	0.3	0.035	0.12	2	0.26	0.05	0.012	0.14	0.05	0.005
KNOB-LT-077	701264	6372101	BO	3.78	7.7	0.1	1	0.005	0.4	0.122	0.35	0.5	0.33	0.12	0.019	0.15	0.06	0.005
KNOB-LT-078	701402	6372057	BB	5.07	6.7	0.1	1	0.02	0.3	0.206	0.64	0.5	0.34	0.27	0.085	0.50	0.36	0.05
KNOB-LT-079	701601	6372013	BB	5.75	6.6	0.1	4	0.02	0.3	0.299	0.91	0.5	0.33	0.39	0.129	0.74	0.42	0.06
KNOB-LT-080	702016	6372010	BB	6.49	9.1	0.1	1	0.005	0.5	0.040	0.17	0.5	0.13	0.06	0.017	0.12	0.09	0.01

SAMPLE	EASTING	NORTHING	SPECIES	Cu PPM 0.005	Zn PPM 0.05	Au PPB 0.1	Ag PPB 1	U PPM 0.005	Se PPM 0.05	Y PPM 0.0005	Ce PPM 0.005	Re PPB 0.5	Li PPM 0.005	La PPM 0.005	Fe % 0.0005	Pb PPM 0.005	Zr PPM 0.005	Al % 0.005
KNOB-LT-081	702404	6372025	BB	6.01	7.2	0.1	5	0.03	0.3	0.508	1.78	0.5	0.55	0.71	0.168	1.15	0.87	0.11
KNOB-LT-082	699191	6371991	BO	4.01	13.2	0.1	1	0.005	0.5	0.050	0.13	0.5	0.19	0.05	0.014	0.14	0.06	0.005
KNOB-LT-083	698977	6371962	BB	5.07	7.6	0.3	1	0.005	0.4	0.028	0.08	0.5	0.08	0.03	0.012	0.10	0.04	0.005
KNOB-LT-084	698396	6371994	BB	5.47	4.5	0.1	1	0.005	0.3	0.119	0.34	2	0.21	0.14	0.041	0.26	0.16	0.02
KNOB-LT-085	697981	6371975	WM	11.54	22.8	0.1	1	0.005	0.5	0.081	0.26	3	1.92	0.10	0.015	0.30	0.07	0.01
KNOB-LT-086	702001	6372993	BB	5.76	6.3	0.4	4	0.03	0.3	0.290	0.92	0.5	0.31	0.37	0.139	0.77	0.40	0.05
KNOB-LT-087	701604	6373087	BB	5.32	11.0	0.1	8	0.03	0.6	0.386	1.25	0.5	0.40	0.48	0.173	1.02	0.58	0.06
KNOB-LT-088	701194	6372982	WM	12.20	23.7	0.1	3	0.005	0.2	1.493	6.74	3	2.17	3.92	0.016	0.58	0.05	0.005
KNOB-LT-089	700781	6372989	WM	6.53	18.0	0.1	3	0.005	0.5	0.164	0.63	4	0.88	0.31	0.009	0.12	0.03	0.005
KNOB-LT-090	700795	6372998	BO	2.90	11.6	0.1	1	0.005	0.4	0.046	0.11	1	0.35	0.05	0.013	0.12	0.03	0.005
KNOB-LT-091	700184	6373015	BO	3.03	12.0	0.1	1	0.01	0.3	0.147	0.46	1	0.41	0.19	0.043	0.39	0.12	0.02
KNOB-LT-092	699782	6373015	BB	5.30	8.4	0.1	9	0.04	0.3	0.297	0.90	1	0.46	0.38	0.210	1.29	0.44	0.06
KNOB-LT-093	699586	6371998	BB	4.33	7.3	0.2	2	0.005	0.2	0.073	0.29	0.5	0.22	0.13	0.041	0.29	0.15	0.02
KNOB-LT-094	699803	6371928	BB	4.19	6.6	0.1	2	0.01	0.2	0.099	0.29	0.5	0.19	0.13	0.044	0.39	0.15	0.02
KNOB-LT-095	700006	6371966	BO	1.65	5.1	0.3	1	0.005	0.05	0.009	0.02	0.5	0.16	0.005	0.003	0.05	0.01	0.005
KNOB-LT-096	701803	6372017	BB	3.99	6.6	0.1	5	0.02	0.3	0.195	0.68	4	0.36	0.28	0.090	0.60	0.33	0.04
KNOB-LT-097	702221	6372029	BB	5.66	7.3	0.6	9	0.03	0.2	0.370	1.36	0.5	0.63	0.56	0.157	1.01	0.77	0.11
KNOB-LT-098	697569	6371999	WM	5.31	13.9	0.1	1	0.03	0.6	0.030	0.09	1	0.32	0.03	0.012	0.18	0.04	0.005
KNOB-LT-099	697199	6372997	WM	8.88	13.4	0.9	2	0.02	0.2	0.020	0.43	0.5	0.47	0.07	0.007	0.12	0.02	0.005
KNOB-LT-100	697865	6372966	WM	4.61	20.3	0.1	1	0.005	0.3	0.014	0.04	0.5	0.40	0.02	0.007	0.05	0.02	0.005

SAMPLE	EASTING	NORTHING	SPECIES	Cu	Zn	Au	Ag	U	Se	Y	Ce	Re	Li	La	Fe	Pb	Zr	Al
				PPM	PPM	PPB	PPB	PPM	PPM	PPM	PPM	PPB	PPM	PPM	%	PPM	PPM	%
				0.005	0.05	0.1	1	0.005	0.05	0.0005	0.005	0.5	0.005	0.005	0.0005	0.005	0.005	0.005
KNOB-LT-101	698397	6372985	WM	7.61	25.4	0.4	1	0.005	0.4	0.049	0.19	3	1.51	0.06	0.011	0.17	0.03	0.005
KNOB-LT-102	698799	6373069	WM	6.93	19.4	0.1	1	0.005	0.5	0.955	4.71	2	6.44	1.13	0.023	1.70	0.10	0.01
KNOB-LT-103	699209	6373000	BO	2.64	7.1	0.6	1	0.005	0.2	0.049	0.09	3	0.38	0.08	0.019	0.12	0.04	0.005
KNOB-LT-104	700040	6371034	BO	2.41	7.6	0.1	1	0.005	0.4	0.083	0.23	0.5	0.55	0.10	0.012	0.10	0.04	0.005
KNOB-LT-105	700177	6370977	BO	3.70	7.5	0.1	3	0.01	0.4	0.064	0.15	0.5	0.60	0.09	0.016	0.14	0.05	0.005
KNOB-LT-106	700403	6371000	WM	5.38	20.9	0.1	2	0.005	0.4	0.107	0.52	1	1.01	0.22	0.018	0.31	0.08	0.01
KNOB-LT-107	700801	6371011	BB	6.69	4.8	0.2	7	0.02	0.1	0.195	0.70	0.5	0.40	0.27	0.078	0.43	0.35	0.05
KNOB-LT-108	701420	6370982	BB	5.95	4.4	0.1	4	0.005	0.4	0.123	0.41	3	0.25	0.18	0.045	0.27	0.18	0.03
KNOB-LT-109	701800	6371007	BB	4.29	5.0	0.1	5	0.01	0.2	0.178	0.59	0.5	0.29	0.25	0.063	0.49	0.29	0.04
KNOB-LT-110	702203	6370999	BB	6.96	7.4	0.3	3	0.005	0.1	0.121	0.37	2	0.21	0.18	0.040	0.28	0.23	0.03
KNOB-LT-111	699324	6371978	BO	3.84	8.6	0.1	4	0.005	0.3	0.018	0.06	0.5	0.18	0.03	0.008	0.07	0.03	0.005
KNOB-LT-112	698800	6372012	BB	5.43	11.5	0.1	5	0.005	0.4	0.092	0.27	0.5	0.17	0.12	0.042	0.25	0.14	0.02
KNOB-LT-113	698600	6372000	BB	4.47	12.1	1.5	5	0.005	0.2	0.029	0.11	0.5	0.17	0.04	0.016	0.13	0.06	0.005
KNOB-LT-114	698194	6372000	BB	5.91	7.3	0.1	3	0.005	0.4	0.064	0.24	0.5	0.16	0.11	0.035	0.22	0.09	0.02
KNOB-LT-115	697853	6372054	WM	7.21	17.4	0.1	1	0.005	0.4	0.016	0.06	0.5	0.80	0.02	0.010	0.08	0.02	0.005
KNOB-LT-116	697055	6372995	WM	5.79	19.1	0.1	3	0.005	0.2	0.076	0.87	0.5	1.06	0.15	0.015	0.14	0.04	0.005
KNOB-LT-117	697396	6372990	WM	6.35	16.2	0.1	2	0.005	0.3	0.022	0.06	1	0.52	0.03	0.008	0.06	0.04	0.005
KNOB-LT-118	697574	6373008	WM	7.18	29.4	0.1	5	0.04	0.3	0.034	0.15	0.5	0.74	0.04	0.007	0.07	0.02	0.005
KNOB-LT-119	697972	6372956	WM	6.59	26.6	0.1	1	0.005	0.4	0.022	0.06	4	0.50	0.03	0.011	0.11	0.04	0.005
KNOB-LT-120	698209	6372990	WM	6.70	23.1	0.1	2	0.01	0.4	0.054	0.19	3	1.49	0.07	0.013	0.30	0.05	0.005

SAMPLE	EASTING	NORTHING	SPECIES	Cu PPM 0.005	Zn PPM 0.05	Au PPB 0.1	Ag PPB 1	U PPM 0.005	Se PPM 0.05	Y PPM 0.0005	Ce PPM 0.005	Re PPB 0.5	Li PPM 0.005	La PPM 0.005	Fe % 0.0005	Pb PPM 0.005	Zr PPM 0.005	Al % 0.005
KNOB-LT-121	698595	6372986	WM	13.65	32.8	0.1	3	0.005	0.5	0.474	2.44	0.5	3.48	0.75	0.024	1.10	0.09	0.01
KNOB-LT-122	698595	6372986	BB	4.52	9.5	0.2	3	0.005	0.2	0.057	0.21	0.5	0.23	0.10	0.029	0.26	0.09	0.01
KNOB-LT-123	698996	6372976	WM	1.96	9.7	0.9	1	0.02	0.2	0.115	0.34	1	0.50	0.16	0.051	0.43	0.13	0.02
KNOB-LT-124	699402	6372992	WM	3.42	9.8	0.5	1	0.005	0.2	0.050	0.16	0.5	0.34	0.06	0.026	0.19	0.06	0.005
KNOB-LT-125	699791	6370993	WM	11.09	15.6	0.4	5	0.005	1.0	0.045	0.13	2	0.46	0.06	0.013	0.11	0.04	0.005
KNOB-LT-126	700621	6370958	WM	7.63	16.6	0.5	2	0.005	0.4	0.150	0.43	2	1.54	0.40	0.024	0.26	0.08	0.01
KNOB-LT-127	700997	6371013	BB	7.59	13.4	0.9	6	0.005	0.2	0.122	0.40	0.5	0.25	0.16	0.035	0.23	0.19	0.03
KNOB-LT-128	701632	6370949	WM	4.14	10.7	0.8	1	0.005	0.3	0.025	0.09	0.5	0.60	0.05	0.007	0.06	0.02	0.005
KNOB-LT-129	701999	6371001	BB	4.91	6.3	0.3	3	0.01	0.2	0.144	0.54	0.5	0.20	0.23	0.063	0.44	0.29	0.04
KNOB-LT-130	702400	6370999	BB	4.43	8.1	0.6	5	0.01	0.05	0.129	0.51	0.5	0.19	0.19	0.048	0.32	0.24	0.03
KNOB-LT-131	703002	6370016	BB	5.43	7.1	0.7	3	0.005	0.05	0.162	0.54	0.5	0.21	0.21	0.043	0.37	0.25	0.04
KNOB-LT-132	702588	6370009	BB	5.11	6.7	1.0	2	0.005	0.3	0.113	0.39	0.5	0.18	0.16	0.037	0.28	0.19	0.03
KNOB-LT-133	702228	6370039	WM	7.89	11.9	0.5	2	0.005	0.3	0.027	0.10	1	0.64	0.05	0.011	0.09	0.05	0.005
KNOB-LT-134	701770	6369995	WM	8.93	25.2	0.1	3	0.005	0.3	0.255	0.83	2	1.47	0.20	0.016	0.18	0.06	0.01
KNOB-LT-135	701384	6370022	WM	11.45	22.6	1.6	1	0.005	0.5	0.320	0.86	4	2.34	0.28	0.026	0.32	0.39	0.02
KNOB-LT-136	701003	6370008	BB	4.98	5.3	0.1	2	0.01	0.2	0.181	0.68	0.5	0.24	0.28	0.059	0.45	0.29	0.04
KNOB-LT-137	700605	6369998	BB	5.65	7.7	1.4	6	0.01	0.2	0.221	0.76	0.5	0.29	0.32	0.069	0.55	0.37	0.05
KNOB-LT-138	700166	6369984	WM	8.96	23.7	0.7	4	0.005	0.3	0.196	0.88	2	2.65	0.36	0.033	0.63	0.16	0.02
KNOB-LT-139	700001	6370001	BB	5.04	5.4	1.3	4	0.005	0.3	0.089	0.35	0.5	0.20	0.14	0.039	0.26	0.17	0.02
KNOB-LT-140	699802	6369992	BO	3.89	13.3	0.1	1	0.005	0.2	0.052	0.13	0.5	0.64	0.08	0.010	0.13	0.03	0.005

SAMPLE	EASTING	NORTHING	SPECIES	Cu PPM 0.005	Zn PPM 0.05	Au PPB 0.1	Ag PPB 1	U PPM 0.005	Se PPM 0.05	Y PPM 0.0005	Ce PPM 0.005	Re PPB 0.5	Li PPM 0.005	La PPM 0.005	Fe % 0.0005	Pb PPM 0.005	Zr PPM 0.005	Al % 0.005
KNOB-LT-141	699609	6370004	BO	3.20	11.7	0.6	2	0.01	0.2	0.051	0.15	0.5	0.33	0.07	0.014	0.18	0.06	0.005
KNOB-LT-142	699401	6370007	BO	1.91	5.3	0.5	1	0.01	0.2	0.050	0.19	2	0.96	0.07	0.019	0.18	0.06	0.01
KNOB-LT-143	699191	6370000	BB	6.45	7.9	0.6	5	0.005	0.05	0.104	0.37	0.5	0.16	0.17	0.044	0.36	0.21	0.03
KNOB-LT-144	699001	6369999	BB	6.05	8.2	2.4	7	0.02	0.4	0.175	0.62	0.5	0.22	0.26	0.071	0.57	0.24	0.04
KNOB-LT-145	697785	6370233	WM	6.63	19.6	1.0	1	0.02	0.4	0.032	0.10	0.5	0.67	0.04	0.013	0.10	0.04	0.005
KNOB-LT-146	697246	6371072	WM	8.76	22.9	1.1	1	0.01	0.5	0.060	0.17	0.5	0.80	0.08	0.023	0.20	0.07	0.01
KNOB-LT-147	702589	6370999	BB	6.52	7.2	0.9	6	0.005	0.4	0.155	0.55	0.5	0.21	0.23	0.056	0.42	0.31	0.04
KNOB-LT-148	702795	6370002	BB	6.05	8.9	0.9	4	0.01	0.4	0.211	0.77	0.5	0.34	0.33	0.068	0.47	0.43	0.06
KNOB-LT-149	702400	6370009	BB	4.66	6.0	1.3	3	0.005	0.3	0.169	0.62	1	0.30	0.29	0.061	0.40	0.35	0.05
KNOB-LT-150	702011	6370056	WM	6.57	14.5	1.2	3	0.005	0.3	0.122	0.61	3	0.75	0.18	0.025	0.33	0.14	0.02
KNOB-LT-151	701615	6370003	WM	11.55	17.6	0.6	3	0.005	0.3	0.074	0.30	0.5	1.65	0.12	0.015	0.19	0.07	0.01
KNOB-LT-152	701265	6369996	WM	6.25	16.1	0.1	1	0.005	0.5	0.070	0.30	2	1.62	0.15	0.018	0.33	0.08	0.01
KNOB-LT-153	700797	6370010	BB	5.65	8.0	0.3	2	0.005	0.05	0.045	0.15	0.5	0.14	0.06	0.016	0.13	0.07	0.01
KNOB-LT-154	700365	6369961	WM	6.74	20.7	0.6	1	0.005	0.3	0.041	0.11	5	1.08	0.06	0.005	0.08	0.01	0.005
KNOB-LT-155	698795	6370000	BB	5.95	5.8	0.1	2	0.005	0.2	0.067	0.18	0.5	0.15	0.08	0.027	0.19	0.09	0.01
KNOB-LT-156	698597	6370002	BB	4.51	7.8	0.9	3	0.005	0.4	0.094	0.29	0.5	0.12	0.14	0.038	0.24	0.15	0.02
KNOB-LT-157	698396	6370013	WM	4.75	12.8	0.3	2	0.005	0.9	0.037	0.12	3	0.85	0.05	0.015	0.14	0.03	0.005
KNOB-LT-158	698206	6370026	WM	7.82	30.5	0.1	6	0.005	0.4	0.036	0.09	0.5	0.70	0.04	0.010	0.12	0.03	0.005
KNOB-LT-159	698005	6370012	WM	6.14	17.8	0.1	3	0.005	0.2	0.022	0.08	0.5	0.63	0.03	0.011	0.12	0.05	0.005
KNOB-LT-160	699199	6374972	WM	4.16	16.4	0.6	1	0.005	0.4	0.037	0.10	1	0.47	0.05	0.018	0.19	0.04	0.005

SAMPLE	EASTING	NORTHING	SPECIES	Cu PPM	Zn PPM	Au PPB	Ag PPB	U PPM	Se PPM	Y PPM	Ce PPM	Re PPB	Li PPM	La PPM	Fe %	Pb PPM	Zr PPM	Al %
				0.005	0.05	0.1	1	0.005	0.05	0.0005	0.005	0.5	0.005	0.005	0.0005	0.005	0.005	0.005
KNOB-LT-161	698357	6374014	WM	6.47	12.7	0.2	2	0.005	0.3	0.008	0.02	0.5	0.36	0.01	0.005	0.08	0.01	0.005
KNOB-LT-162	701991	6375001	BB	5.70	5.6	0.1	4	0.01	0.2	0.113	0.35	0.5	0.24	0.17	0.062	0.43	0.19	0.03
KNOB-LT-163	697798	6371001	BB	4.88	5.2	0.5	2	0.005	0.2	0.097	0.31	0.5	0.10	0.12	0.036	0.27	0.17	0.02
KNOB-LT-164	698010	6370991	BB	4.61	9.1	0.1	5	0.005	0.2	0.050	0.16	0.5	0.07	0.08	0.022	0.19	0.09	0.01
KNOB-LT-165	697597	6374999	BB	4.40	5.6	0.1	4	0.01	0.3	0.180	0.72	4	0.18	0.34	0.057	0.56	0.30	0.04
KNOB-LT-166	702532	6375447	BO	2.37	8.3	0.1	1	0.005	0.2	0.036	0.18	0.5	0.31	0.04	0.009	0.11	0.02	0.005
KNOB-LT-167	697005	6374003	BB	4.44	8.1	0.1	6	0.005	0.2	0.116	0.40	0.5	0.16	0.17	0.037	0.28	0.19	0.03
KNOB-LT-168	700415	6373002	BO	3.35	11.9	0.1	1	0.005	0.2	0.026	0.11	0.5	0.29	0.05	0.016	0.13	0.04	0.005
KNOB-LT-169	702016	6372010	BB	6.34	11.2	0.1	4	0.005	0.3	0.040	0.13	0.5	0.11	0.06	0.016	0.16	0.08	0.01
KNOB-LT-170	700781	6372989	WM	6.63	18.5	0.8	2	0.005	0.7	0.176	0.65	1	0.98	0.33	0.008	0.13	0.03	0.005
KNOB-LT-171	697199	6372997	WM	9.37	14.0	0.7	4	0.02	0.1	0.020	0.45	2	0.53	0.06	0.006	0.11	0.03	0.005
KNOB-LT-172	701800	6371007	BB	4.71	6.7	0.5	5	0.01	0.2	0.161	0.54	0.5	0.26	0.23	0.066	0.50	0.28	0.04
KNOB-LT-173	697972	6372956	WM	6.75	26.5	0.1	1	0.005	0.4	0.025	0.06	1	0.56	0.03	0.011	0.14	0.05	0.005
KNOB-LT-174	701999	6371001	BB	4.85	5.8	0.4	4	0.01	0.2	0.144	0.51	2	0.27	0.21	0.059	0.44	0.27	0.04
KNOB-LT-175	700001	6370001	BB	5.01	6.2	0.1	5	0.005	0.2	0.091	0.34	0.5	0.24	0.14	0.040	0.28	0.17	0.02
KNOB-LT-176	702400	6370009	BB	4.37	6.1	0.5	5	0.005	0.2	0.187	0.64	1	0.28	0.24	0.059	0.42	0.35	0.05
KNOB-LT-177	698005	6370012	WM	6.37	17.4	0.1	1	0.005	0.4	0.021	0.06	1	0.74	0.03	0.010	0.10	0.04	0.005

Regolith-landform Unit (RLU) mapping codes from Pain *et al.* (2007)*.

REGOLITH TYPES		LANDFORMS	
TRANSPORTED REGOLITH		a	alluvial landforms
		ap	alluvial plain
A	Alluvial sediments	ah	alluvial channel
AC	Channel deposits	af	flood plain
AO	Overbank deposits	aa	anastomatic plain
		ab	bar plain
I	Aeolian sediments	ac	covered plain
IS	Aeolian sand	am	meander plain
IL	Loess	ao	floodout
IP	Parna	at	alluvial terrace
		as	stagnant alluvial plain
C	Colluvial sediments	al	terraced land
CM	Mass movement	aw	alluvial swamp
CH	Sheet flow deposit		
CF	Fanglomerate	u	dunefield
		ul	longitudinal dunefield
E	Evaporite		
EH	Halite	f	fan
EG	Gypsum	fa	alluvial fan
		fc	colluvial fan
L	Lacustrine sediments	fs	sheet-flood fan
G	Glacial sediments	p	plain
		pd	depositional plain
V	Volcanic sediments	pl	lacustrine plain
VT	Tephra	pp	playa plain
		ps	sandplain
F	Fill		
		g	glacial landforms
O	Coastal sediments	gd	depositional glacial landforms
OB	Beach sediments	ge	erosional glacial landforms
OE	Estuarine sediments		
OC	Coral	d	delta
OM	Marine sediments		
		c	coastal lands
IN-SITU **REGOLITH**		cb	beach ridge plain
		cc	chenier plain
W	Weathered bedrock	cr	coral reef
		cm	marine plain
R	Residual material	ct	tidal flat
		cd	coastal dunes
S	Saprolite	cp	coastal plain
SC	Completely weathered bedrock	cc	beach
SV	Very highly weathered bedrock		
SH	Highly weathered bedrock	e	erosional landforms
SM	Moderately weathered bedrock	ep	erosional plain
SS	Slightly weathered bedrock	ei	pediment
		ea	pediplain
		en	peneplain
		ec	etchplain
		er	rise
		eu	residual rise
		el	low hill
		eh	hill
		em	mountain
		ee	escarpment
		eb	badlands
		ed	drainage depression
		k	karst
		l	plateau
		v	volcanic landform
		vc	caldera
		vv	cone
		vl	lava plain
		va	ash plain
		vf	lava flow
		vp	lava plateau
		m	made land
		t	meteor crater

Regolith - Landform Map of Iron Knob South
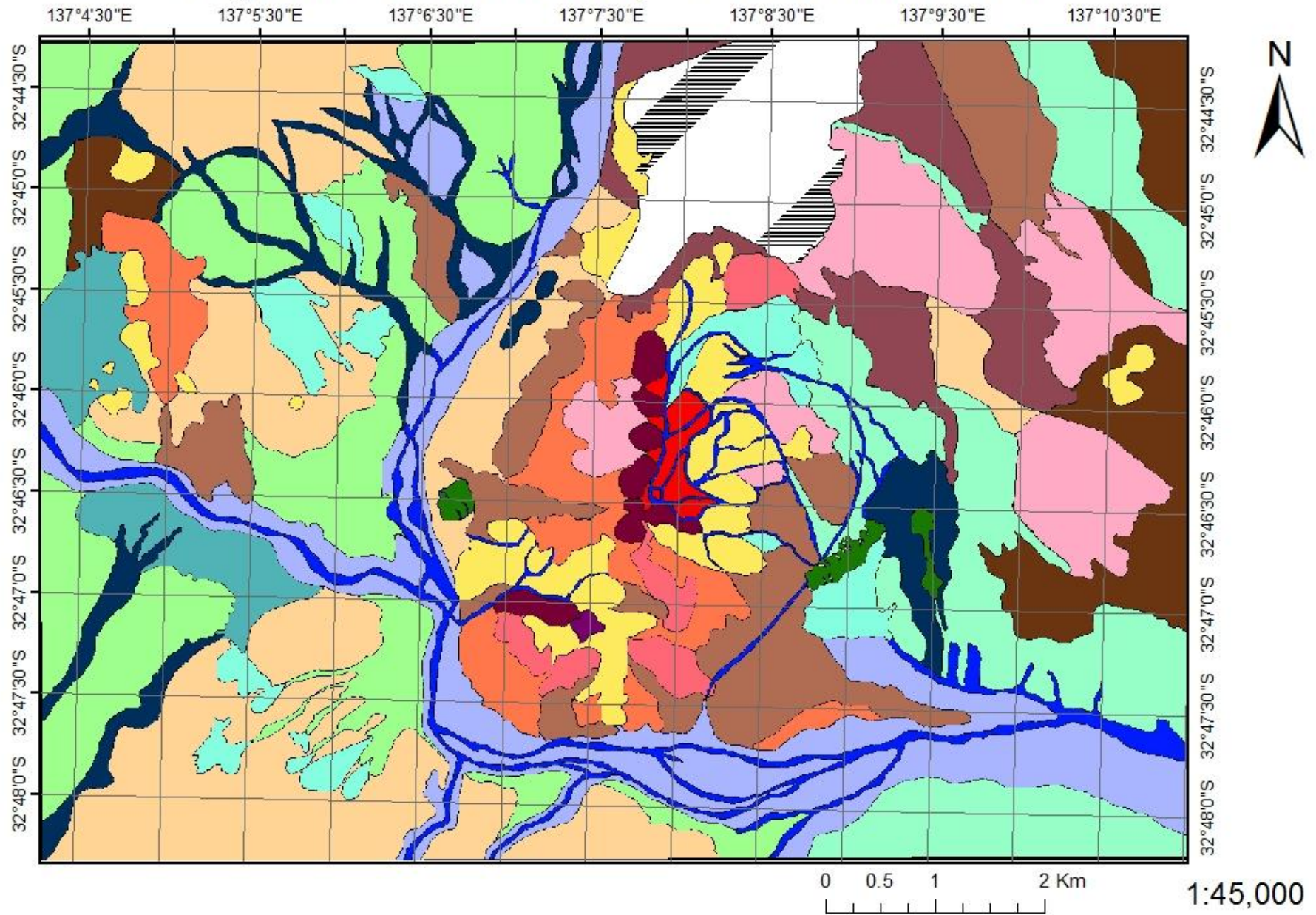
| Map Symbol	RLU code	Regolith-Landform Unit Descriptions
	Aaf	Alluvial flood plain: Alluvial plain characterised by erosion from channelled stream flow and aggradation by over-bank stream flow. Fine light grey/brown clays and fine sand. Lag composed of ± sub-angular to sub-rounded gravel – cobble, ironstone, silcrete, calcrete, BIF lag and vein quartz. Chenopod shrubland, mainly made up of *Maireana sedifolia*, *Atriplex vesicaria* and local grasses.
	Aap	Alluvial Plain: A level land surface produced by deposition of alluvial material, adjacent to alluvial drainage depression. Iron rich sands and clays, lag composed of ± sub-rounded to rounded gravel, calcrete, silcrete, ironstone, conglomerate, volcanic lag and vein quartz. Western myall, black oak pockets and understoreys of chenopod shrubland make up the vegetation in this unit.
	Aaw	Alluvial Swamp: An almost level depression with a seasonal or permanent water table at the surface. Dark brown medium grained loamy clay soils with an association with long reed grasses, western myall, red mallee and sugarwood trees.
	Aed_1	Alluvial Drainage Depression: Large incised channel over plain of low topographic relief created by alluvial processes with evidence of seasonal water. Fine red-brown silts and clays, lag composed of sub-rounded - rounded iron stone and quartz lag ± granite, conglomerate and volcanic clasts. Native reed grasses are most common within channels.
	Aed2	Alluvial Drainage Depression: Dried up, no signs of water except for the vegetation picking out the channels, Fine red-brown silts and clays ± sub-rounded - rounded ironstone, quartz lag, volcanic clasts, granite and conglomerate lag. Western myalls, sugarwood trees and native grasses are all associated.
	Afa	Alluvial Fan: Red-brown, fine sandy clay located within outwash fans and channels. The fans grade from larger angular clasts at the origin to smaller rounder clasts at the terminus lobe, this is most evident with the fans on the east side of 'Katunga' ridge. Bluebush favours the depositional setting of the alluvial fans.
	Apd1	Alluvial Deposition Plain: East side of the ridge, less Aeolian red sands, some Iron stone lag, channels cutting through surface with iron stone and calcrete lag. Bluebush and saltbush are abundant.

	Apd$_2$	Alluvial Deposition Plain: West side of the ridge, composed of fine well rounded, well sorted Aeolian red sands, Apd channels throughout the area featuring bluebush and western myalls
	CHep	Sheet-wash erosional plain: An area of very low relief (<9 m) eroded by sheet-wash activity off a smaller rise close by. The area consists of fine red/brown alluvial sands and clays with lag composed of quartz vein ± ironstone, silcrete and conglomerate lag. Spaced out chenopod shrubland is the main vegetation group on this landform.
	CHel	Sheet-wash low hill: A landform of moderate relief composed almost entirely of angular iron stone lag eroding off and carried by sheet-wash from the in-situ regolith above. Beneath the lag is fine red sand and clays. Spinifex, small pearl bluebush shrubs and the occasional red mallee tree habitate this landform.
	CHer	Sheet-wash erosional rise: most commonly occurring just before the base of the Katunga ridge at low-moderate relief. The rises are composed of angular iron stone lag that is eroding off the in-situ regolith above and being transported by sheet-wash. Other rises around the field area are composed of ferricrete and silcrete lag. At lower relief the vegetation consists of chenopod shrubland with larger pearl bluebush shrubs and blackoak groves.
	CHfs$_1$	Sheet-flood fan: Large sub-angular – sub-rounded iron stone lag moving into rounder finer lag the further away from ridge. Fine grained orangey red alluvial sediment. There is not a lot of vegetation situated on these fans, dry grasses, salt bush and bluebush however are the most common.
	CHfs$_2$	Sheet-flood fan: As for CHfs$_1$ with a decrease in iron stone lag.
	CHfs$_3$	Sheet-flood fan: Large sub-angular – sub-rounded iron stone lag moving into rounder finer lag the further away from ridge. Fine grained red/brown aeolian sands lay under the lag. The vegetation is abundant and includes blackoak, pearl bluebush and western myall.
	CHpd$_1$	Sheet-wash depositional plain: A level landform with low relief, sub-angular to sub-rounded gravel-cobble stone surface lag consisting of ironstone, quartz lag, conglomerate lag and silcrete. Chenopod shrubland makes up majority of the vegetation on this unit.
	CHpd$_2$	Sheet-wash depositional plain: Sub-angular to sub-rounded gravel-cobble stone surface lag consisting of ironstone, quartz lag, conglomerate lag and silcrete. Chenopod shrubland makes up majority of the vegetation on this unit.

	ISps	Aeolian sand plain: Consisting of well rounded and well sorted, fine orange/red quartz grains. The unit has been forming on the east side of the 'Katunga' ridge after being transported from dune fields to the west. Dense vegetation with a diverse range of species including western myall, blackoak, sugarwood, and understories of chenopod shrubs including pearl bluebush and saltbush has made the sand plains habitat.
	Man Made	Iron Monarch mine and town of Iron Knob
	SSeh	Hill: Slightly weathered dark grey iron stone weathering a deep purple/maroon colour, with silica enriched veins throughout. Beds are massive with joint fractures every 30-60 cm, quartz veins up to 10-15 cm thick present. Evidence of fluid movement through the system with botryoidal hematite commonly found close to the outcrops. Beds are dipping 30-45° towards the E.
	SSel	Low Hill: Slightly weathered dark grey iron stone weathering a deep purple/maroon colour, with silica enriched veins throughout. Beds are massive with joint fractures every 30-60 cm, quartz veins up to 10-15 cm thick present. Evidence of fluid movement through the system with botryoidal hematite commonly found close to the outcrops. Beds are dipping 30-45° towards the E.

Element Probability Plots (created in ioGAS) - Bluebush (Blue), Black Oak (Red), Western Myall (Green)
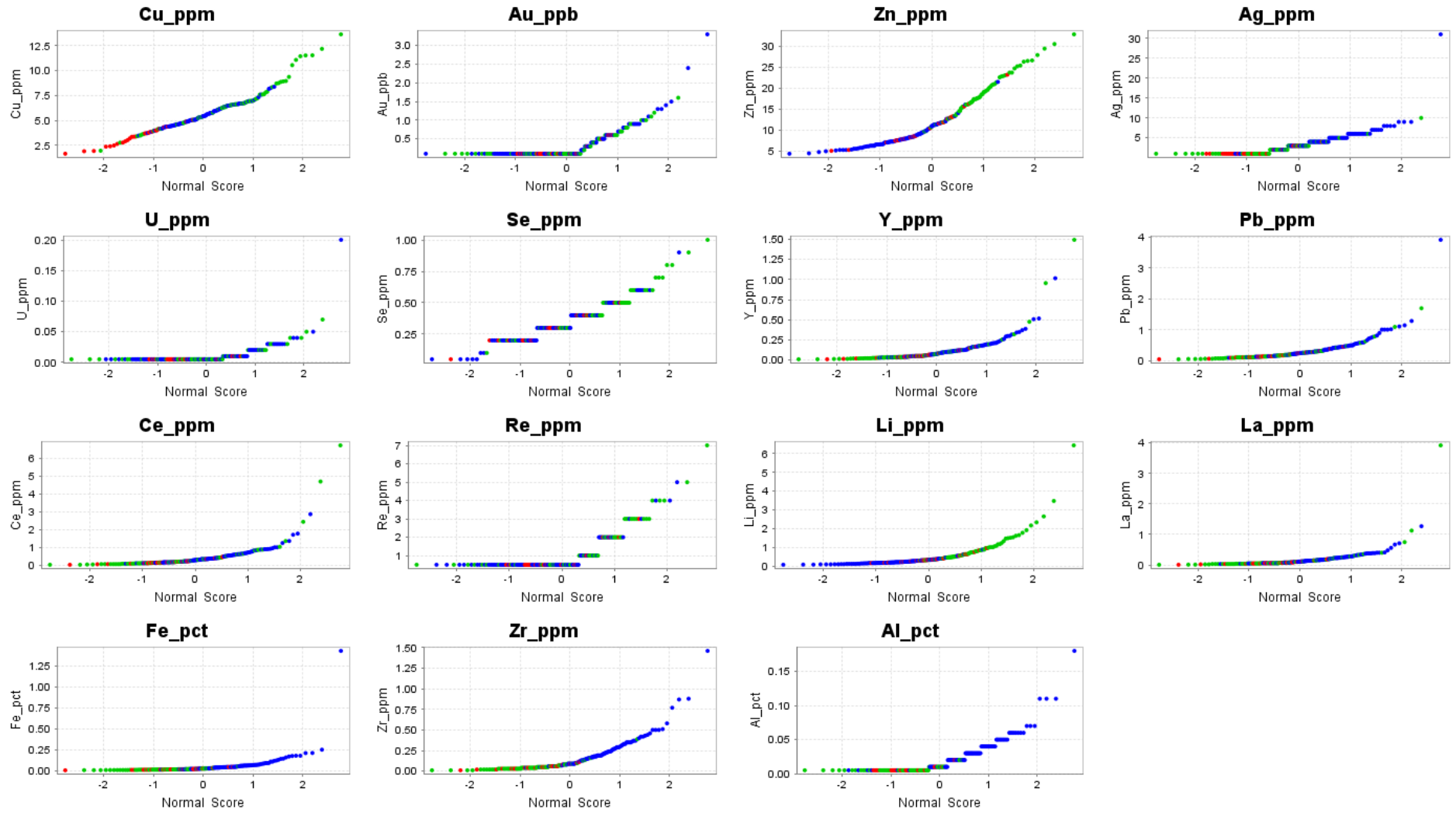
Target Element Histogram Plots (created in ioGAS)- Bluebush (Blue), Black Oak (Red), Western Myall (Green)
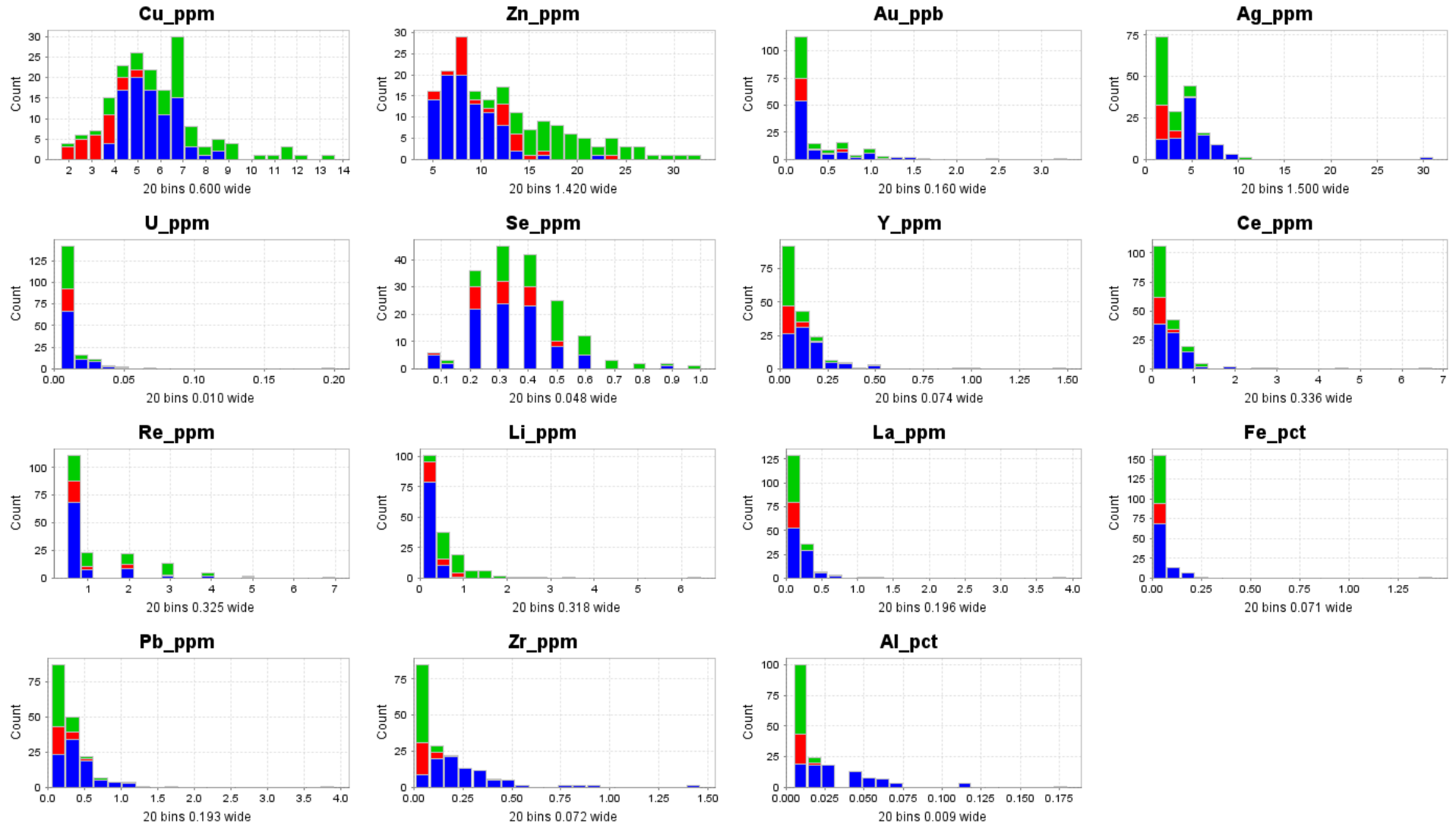
ERROR CALCULATION WITH CORRESPONDING GRAPHS BELOW

% difference error = ((assay1 - assay2) / maximum (assay1 or assay2)) x 100

Half relative difference = ((assay1 - assay2) / (assay1 + assay2)) x 100

$$95\%\,confidence = \pm1.96\left(\frac{\sigma}{\sqrt{n}}\right)$$

Note: where σ is the standard deviation of all assay 1-assay 2 values, and n is the number of duplicates (not all duplicates are displayed in the tables below, however they were used in calculation). The 95% confidence error was applied to the differences.

Western myall error calculations for QAQC

SAMPLE	SPECIES	Cu	Zn	Au	Ag	U	Se	Y	Ce	Re	Li	La	Pb	Fe	Zr	Al
		PPM	PPM	PPB	PPB	PPM	PPM	PPM	PPM	PPB	PPM	PPM	PPM	%	PPM	%
KNOB-LT-157	Veg Pulp	4.75	12.8	0.3	2	0.005	0.9	0.037	0.12	3.00	0.85	0.050	0.14	0.015	0.03	0.005
KNOB-LT-157	REP	4.78	12.0	0.3	1	0.005	1.1	0.029	0.10	2.00	1.01	0.060	0.12	0.016	0.03	0.005
	A1-A2	-0.03	0.80	0.00	1.00	0.00	-0.20	0.01	0.02	1.00	-0.16	-0.01	0.02	0.00	0.00	0.00
ERROR Calc	STD-DEV	0.1377	1.0608	0.286	3.464	0.0033	0.142	0.0067	0.015	1.9221	0.0692	0.014	0.0367	0.001	0.007	0
	% difference error	-0.632														
	1/2 relative error	-0.315														
n=18	± 95% confidence	0.0636	0.4901	0.132	1.6	0.0015	0.066	0.0031	0.007	0.888	0.032	0.007	0.0169	5E-04	0.003	0
		-0.064	-0.49	-0.132	-1.6	-0.002	-0.07	-0.003	-0.007	-0.888	-0.032	-0.007	-0.017	-0	-0	0

Pearl bluebush error calculations for QAQC

SAMPLE	SPECIES	Cu	Zn	Au	Ag	U	Se	Y	Ce	Re	Li	La	Pb	Fe	Zr	Al
		PPM	PPM	PPB	PPB	PPM	PPM	PPM	PPM	PPB	PPM	PPM	PPM	%	PPM	%
KNOB-LT-164	Veg Pulp	4.61	9.1	0.1	5	0.005	0.2	0.050	0.16	1	0.07	0.080	0.19	0.022	0.09	0.010
KNOB-LT-164	REP	4.59	9.3	0.1	4	0.005	0.3	0.054	0.18	2	0.05	0.080	0.19	0.021	0.10	0.010
	A1-A2	0.02	-0.20	0.00	1.00	0.00	-0.10	0.00	-0.02	-1.50	0.02	0.00	0.00	0.00	-0.01	0.00
ERROR Calc	STD-DEV	0.34544	0.9158	0.472	1.317	0.0034	0.0972	0.027	0.0625	1.18	0.037	0.048	0.061	0.008	0.0306	0.007
	% difference error	0.43573														
	1/2 relative confidence	0.21739														
n=20	95% confidence	-0.1514	-0.4014	-0.207	-0.58	-0.001	-0.043	-0.012	-0.027	-0.517	-0.02	-0.02	-0.03	-0	-0.013	-0
		0.1514	0.4014	0.207	0.577	0.0015	0.0426	0.012	0.0274	0.517	0.016	0.021	0.027	0.003	0.0134	0.003

Blackoak Error Calculations for QAQC

SAMPLE	SPECIES	Cu	Zn	Au	Ag	U	Se	Y	Ce	Re	Li	La	Pb	Fe	Zr	Al
		PPM	PPM	PPB	PPB	PPM	PPM	PPM	PPM	PPB	PPM	PPM	PPM	%	PPM	%
KNOB-LT-039	BO	2.48	8.5	0.1	1	0.005	0.4	0.039	0.22	0.50	0.44	0.060	0.15	0.011	0.03	0.005
KNOB-LT-166	REP	2.37	8.3	0.1	1	0.005	0.2	0.036	0.18	0.50	0.31	0.040	0.11	0.009	0.02	0.005
	A1-A2	0.11	0.20	0.00	0.00	0.00	0.20	0.00	0.04	0.00	0.13	0.02	0.04	0.00	0.01	0.00
ERROR Calc	STD-DEV	0.65054	0.7778	0	1.4142		0.0707	0.0099	0.0071	0	0.042	0.0071	0.014	0.002	0.01	0
	% difference error	4.44														
	1/2 relative difference	2.26804														
n=4	95% confidence	-0.6375	-0.762	0	-1.386	0	-0.069	-0.01	-0.007	0	-0.042	-0.007	-0.01	-0	-0.01	0
		0.63753	0.7623	0	1.3859	0	0.0693	0.0097	0.0069	0	0.042	0.0069	0.014	0.002	0.01	0

V14 Standard Error Calculation for QAQC

STANDARDS		Cu	Zn	Au	Ag	U	Se	Y	Ce	Re	Li	La	Fe	Pb	Zr	Al
STD V14	STD	4.98	14.4	7.3	19	0.01	0.1	0.025	0.07	1	0.11	0.03	0.016	0.90	0.05	0.14
STD V14	STD	4.86	15.6	8.1	19	0.01	0.1	0.016	0.08	1	0.05	0.03	0.016	0.91	0.04	0.16
	A1-A2	0.12	-1.20	-0.80	0.00	0.00	0.05	0.01	-0.01	0.50	0.06	0.00	0.00	-0.01	0.01	-0.02
	STD-DEV	0.2686	0.8505	1.3454	3.7859	0	0.1607	0.009	0.0058	0.2887	0.029	0.0058	0.0012	0.1155	0.021	0.0058
	% DIFFERENCE ERROR	2.4691														
	1/2 RELATIVE DIFFERENCE	1.2195														
N=6	± 95% CONFIDENCE	-0.2149	-0.681	-1.077	-3.029	0	-0.129	0.007	-0.0046	-0.231	0.023	-0.005	-9E-04	-0.092	0.017	-0.005
		0.2149	0.6805	1.0765	3.0294	0	0.1286	0.007	0.0046	0.231	0.023	0.0046	0.0009	0.0924	0.017	0.0046

Western Myall Error Calc
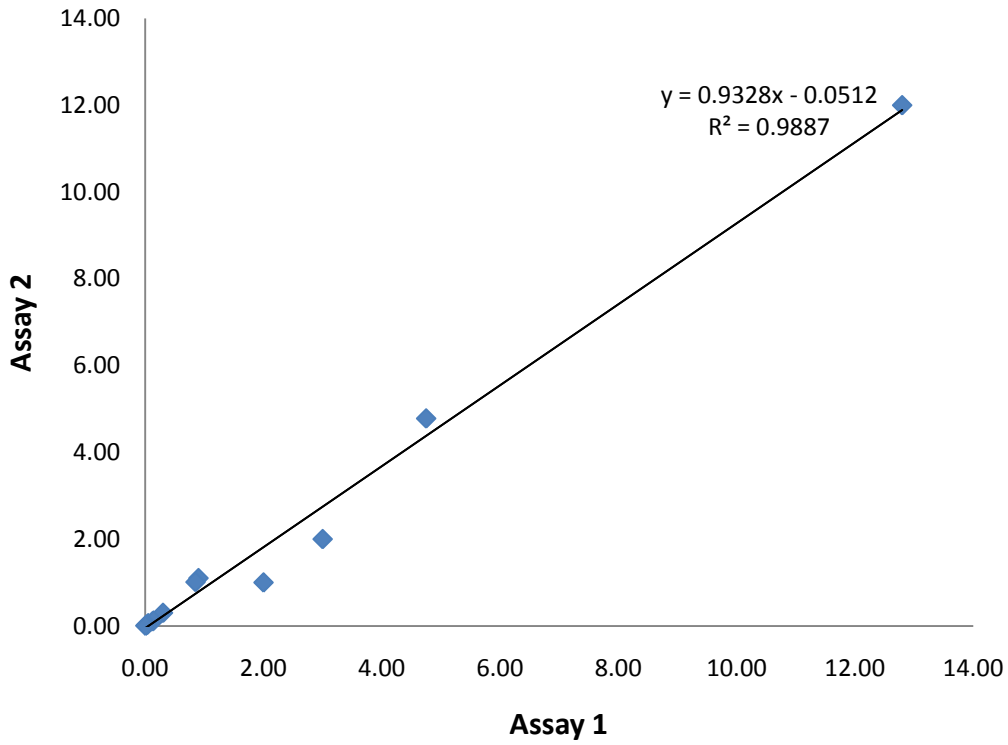
Assay 2 (y-axis) vs Assay 1 (x-axis)

y = 0.9328x - 0.0512
R² = 0.9887

Bluebush Error Calc

Assay 2 (y-axis) vs Assay 1 (x-axis)

y = 0.9651x + 0.0998
R² = 0.9681

Blackoak Error Calc

y = 0.9788x - 0.0306
R² = 0.9993

Assay 2 (vertical axis)
Assay 1 (horizontal axis)

V14 Standard Error Calc

y = 1.0362x - 0.0301
R² = 0.997

Assay 2 (vertical axis)
Assay 1 (horizontal axis)
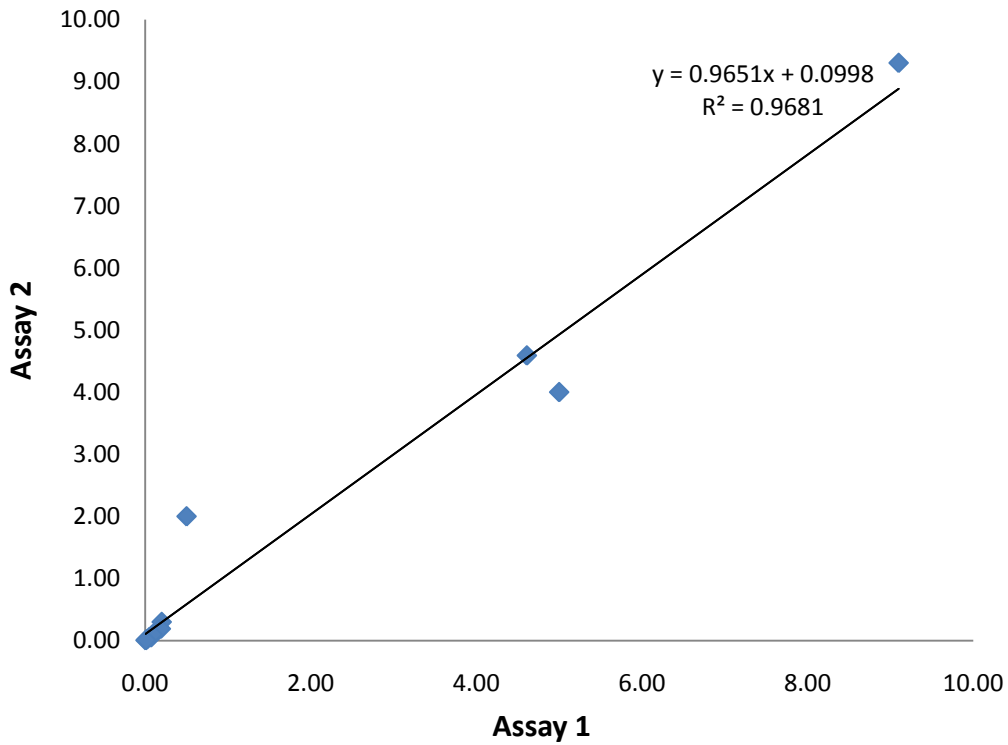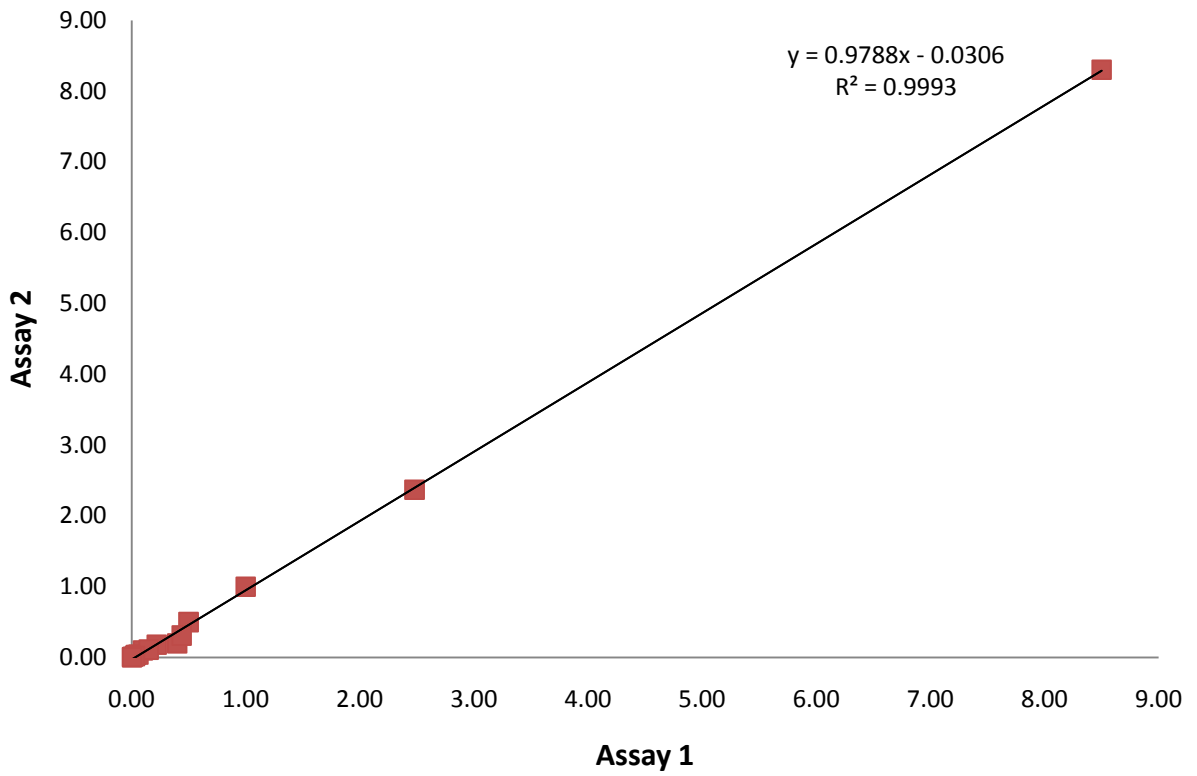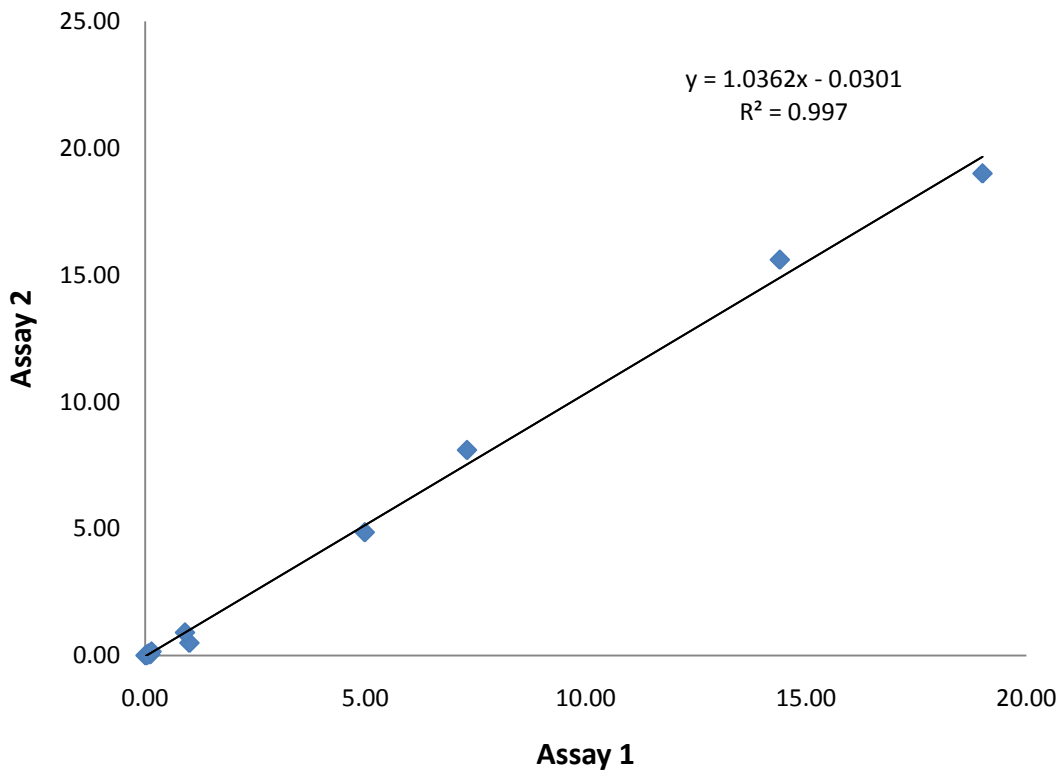
Western myall element association
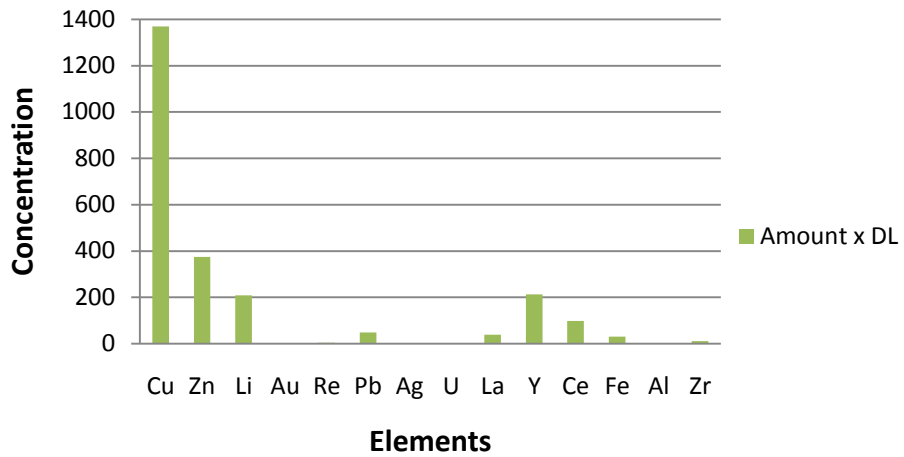
Pearl bluebush element association
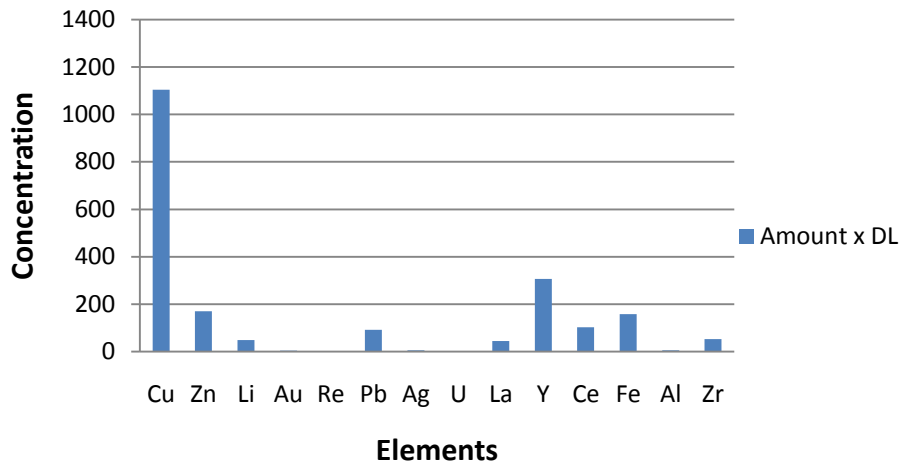
Blackoak element association
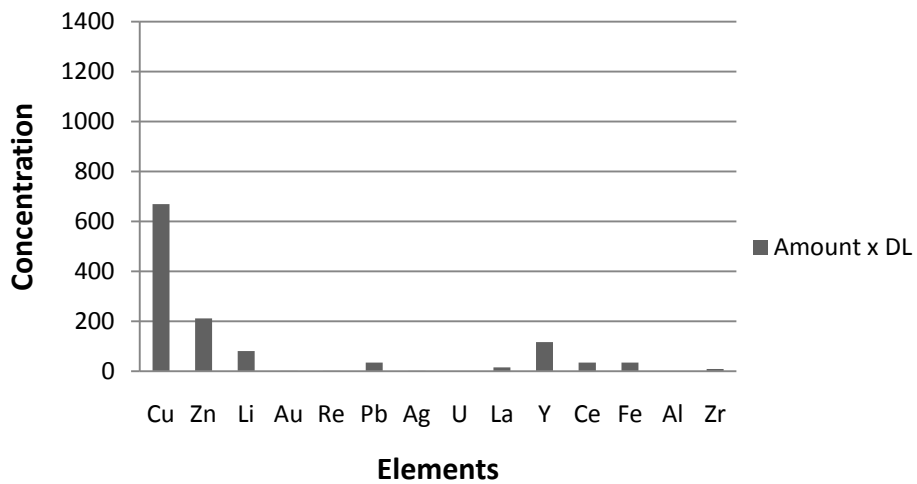
Cu concentration (ppm)
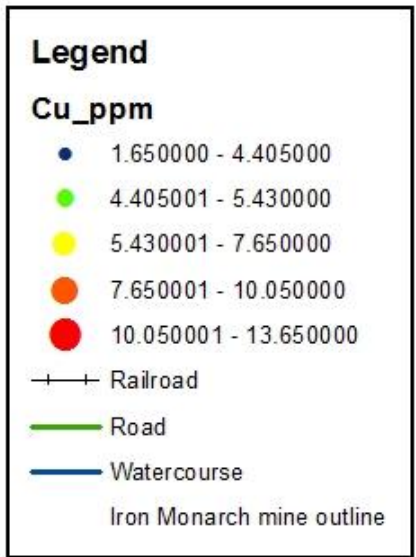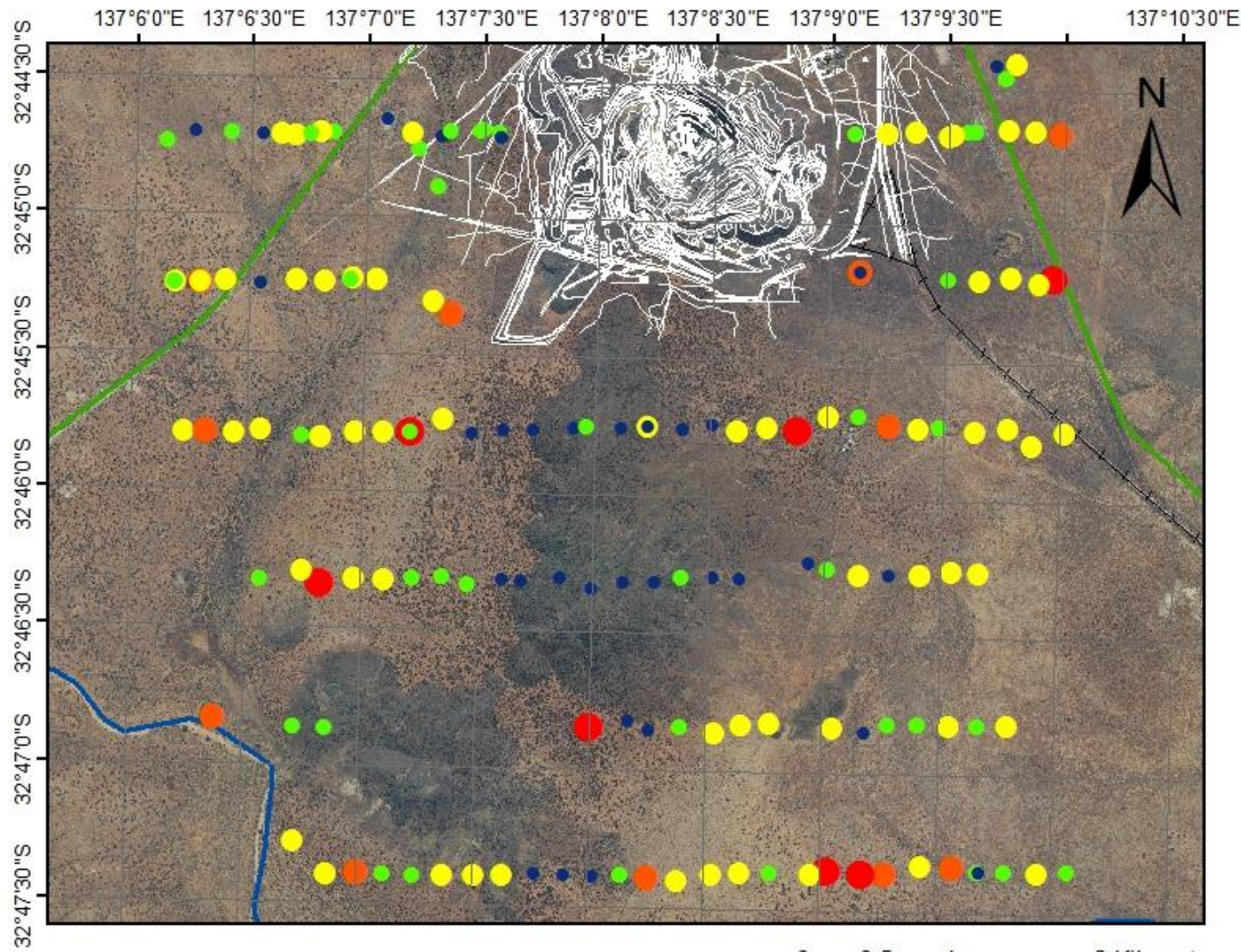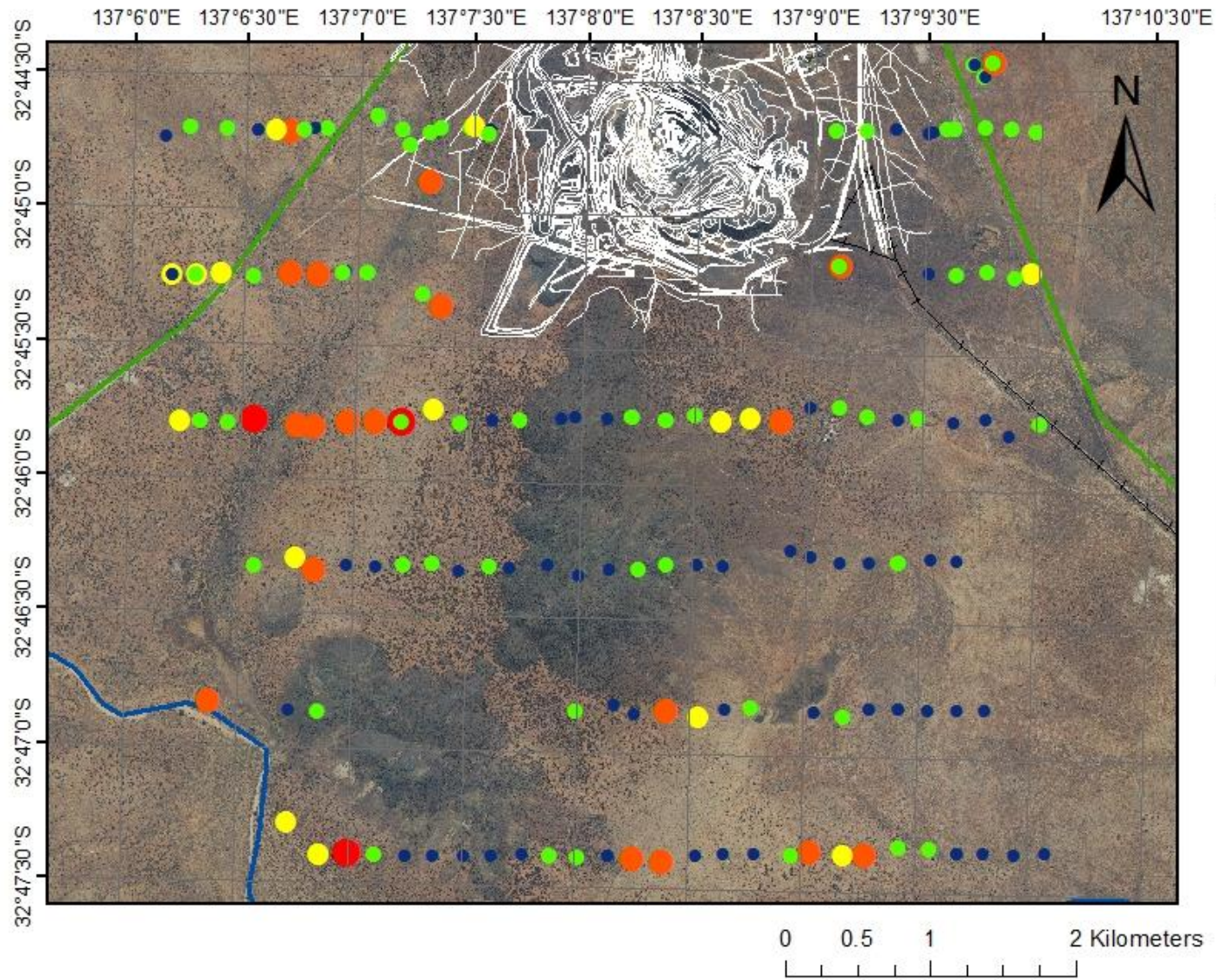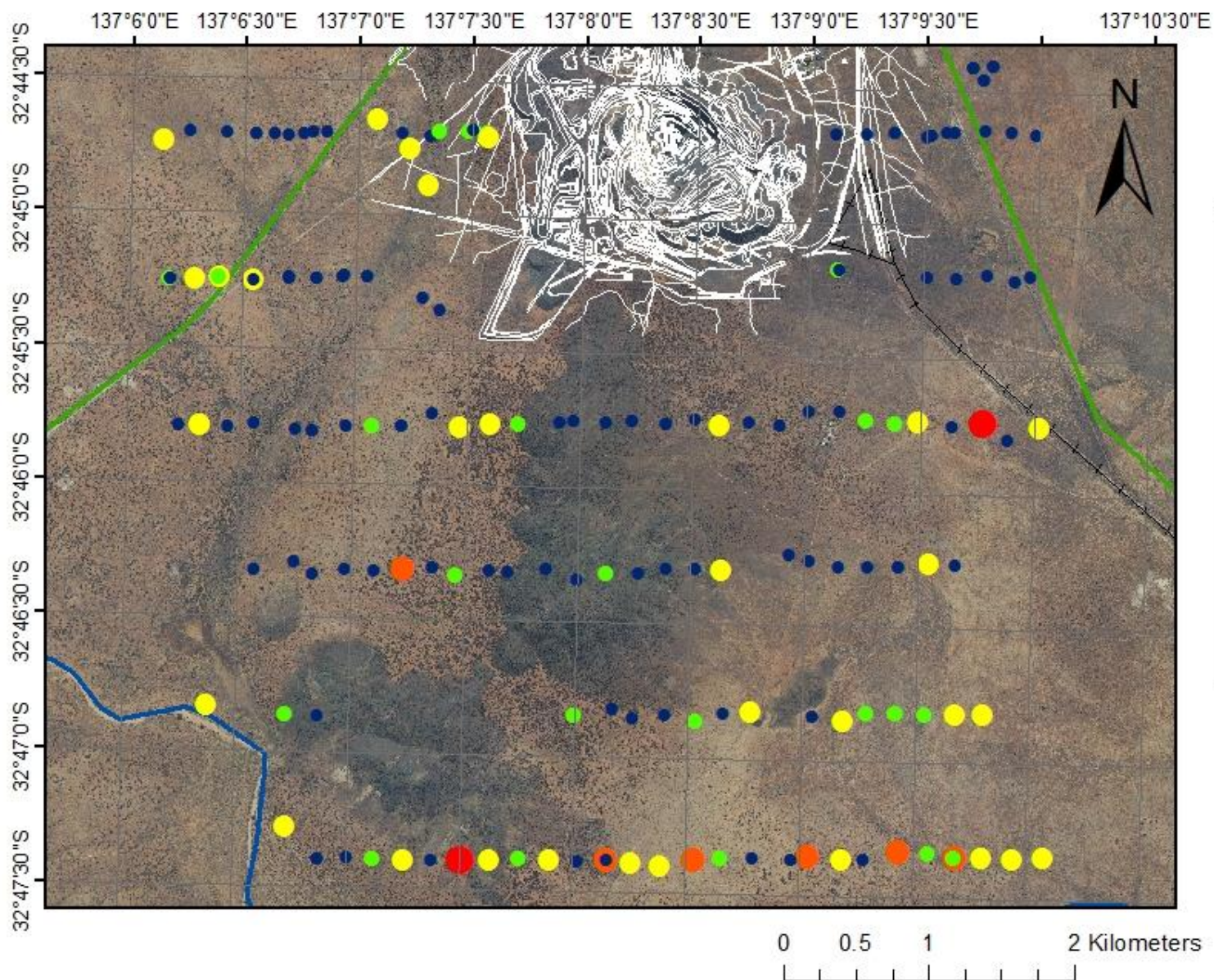
1:40,000

Legend

Cu_ppm

- 1.650000 - 4.405000
- 4.405001 - 5.430000
- 5.430001 - 7.650000
- 7.650001 - 10.050000
- 10.050001 - 13.650000

+—+ Railroad

—— Road

—— Watercourse

Iron Monarch mine outline

Zn concentration (ppm)

1:40,000

Legend

Zn_ppm
- 4.400000 - 9.000000
- 9.000001 - 16.500000
- 16.500001 - 20.000000
- 20.000001 - 28.000000
- 28.000001 - 32.800000
- Railroad
- Road
- Watercourse
- Iron Monarch mine outline

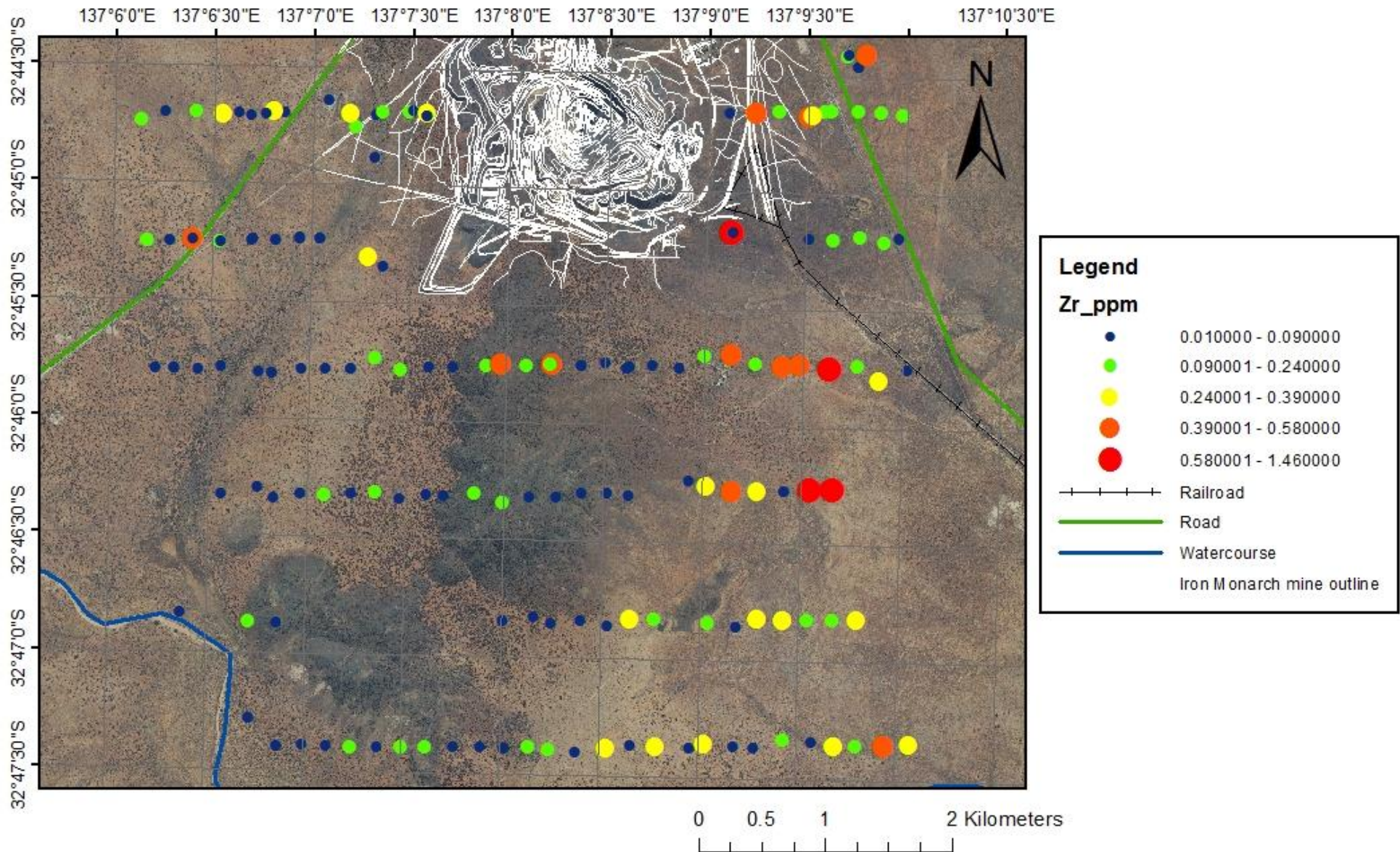Ce concentration (ppm)

Re concentration (ppm)

1:40,000

Legend

Re_ppm
- 0.500000 - 1.150000
- 1.150001 - 2.125000
- 2.125001 - 3.100000
- 3.100001 - 4.000000
- 4.000001 - 7.000000

Railroad
Road
Watercourse
Iron Monarch mine outline
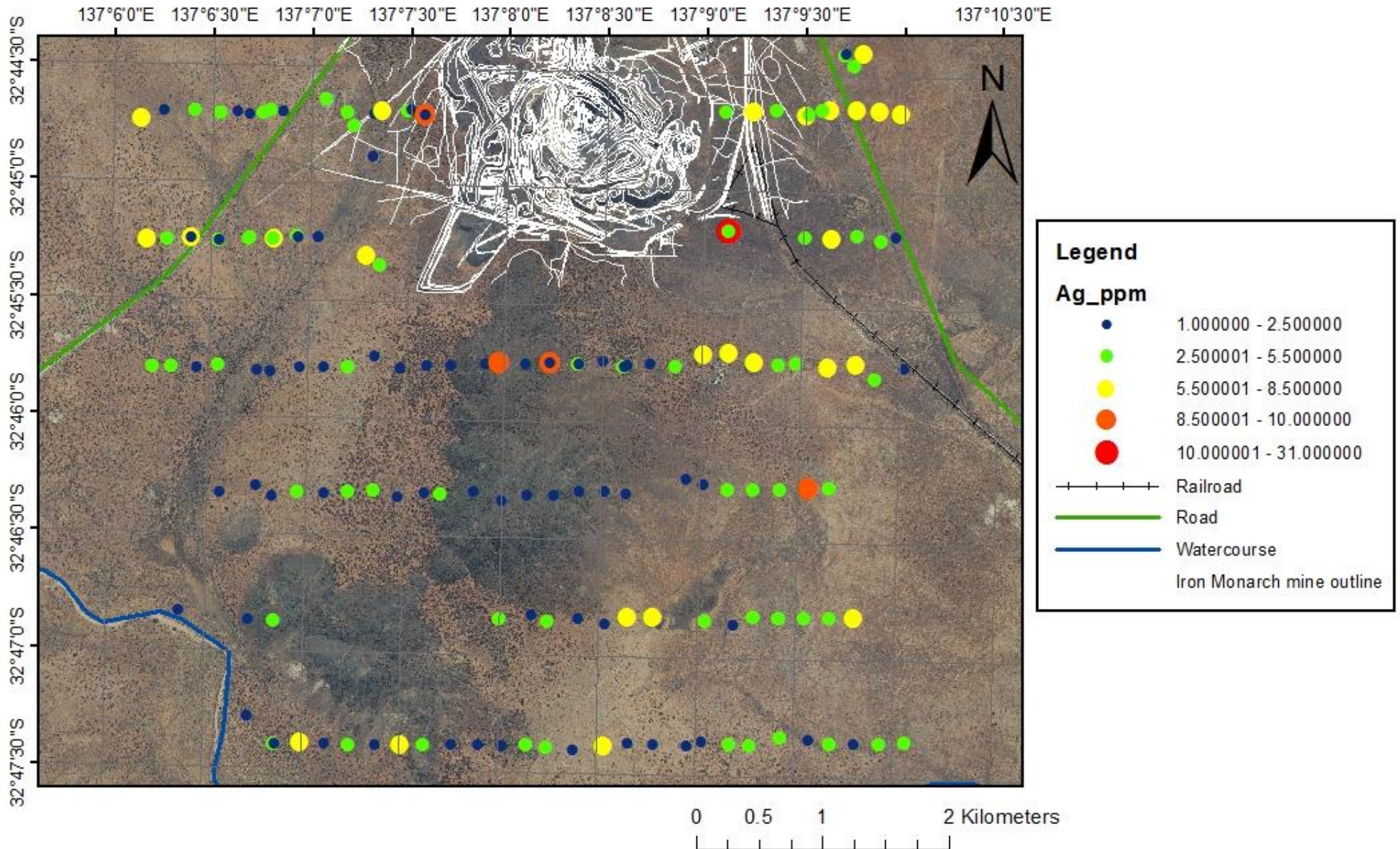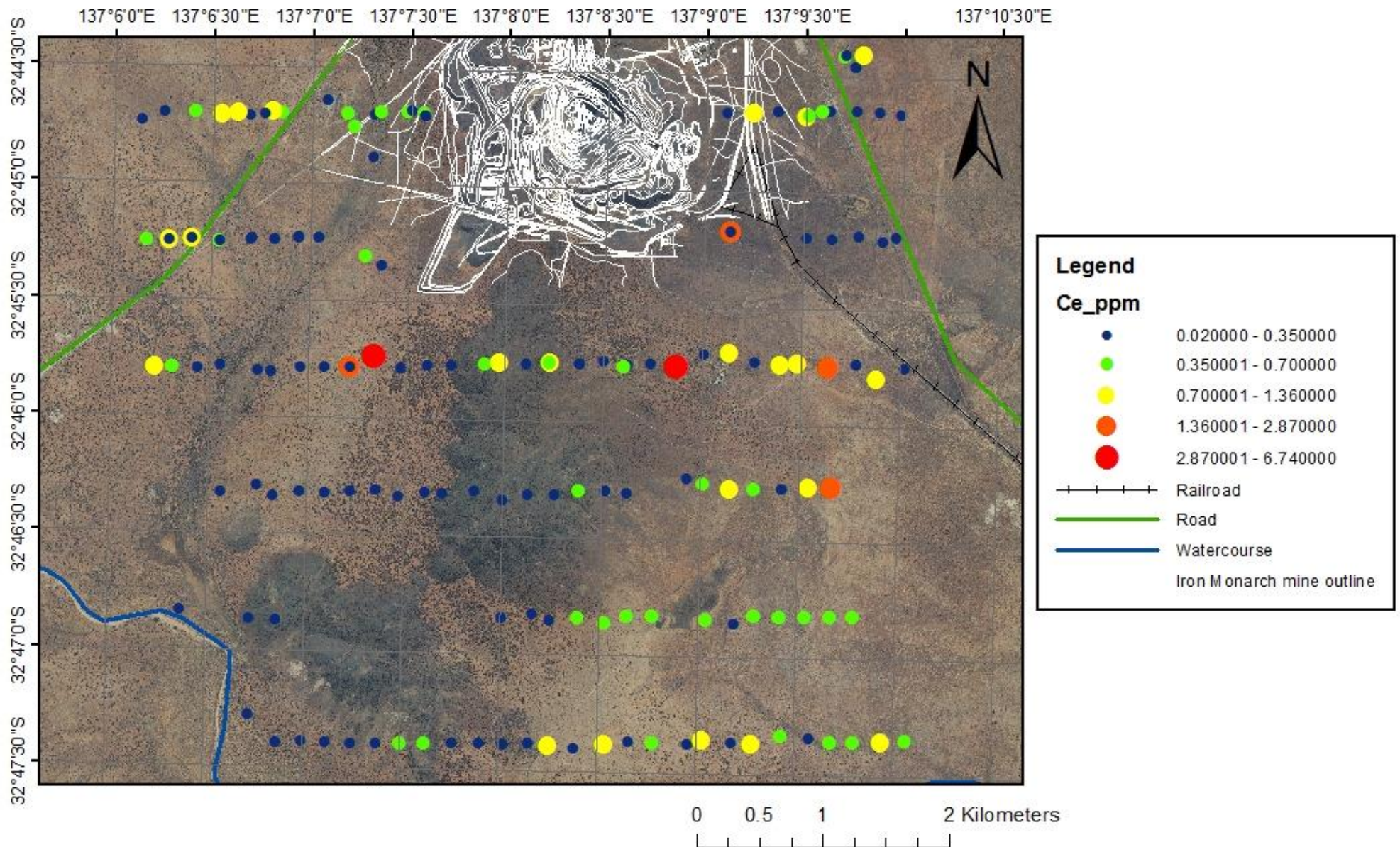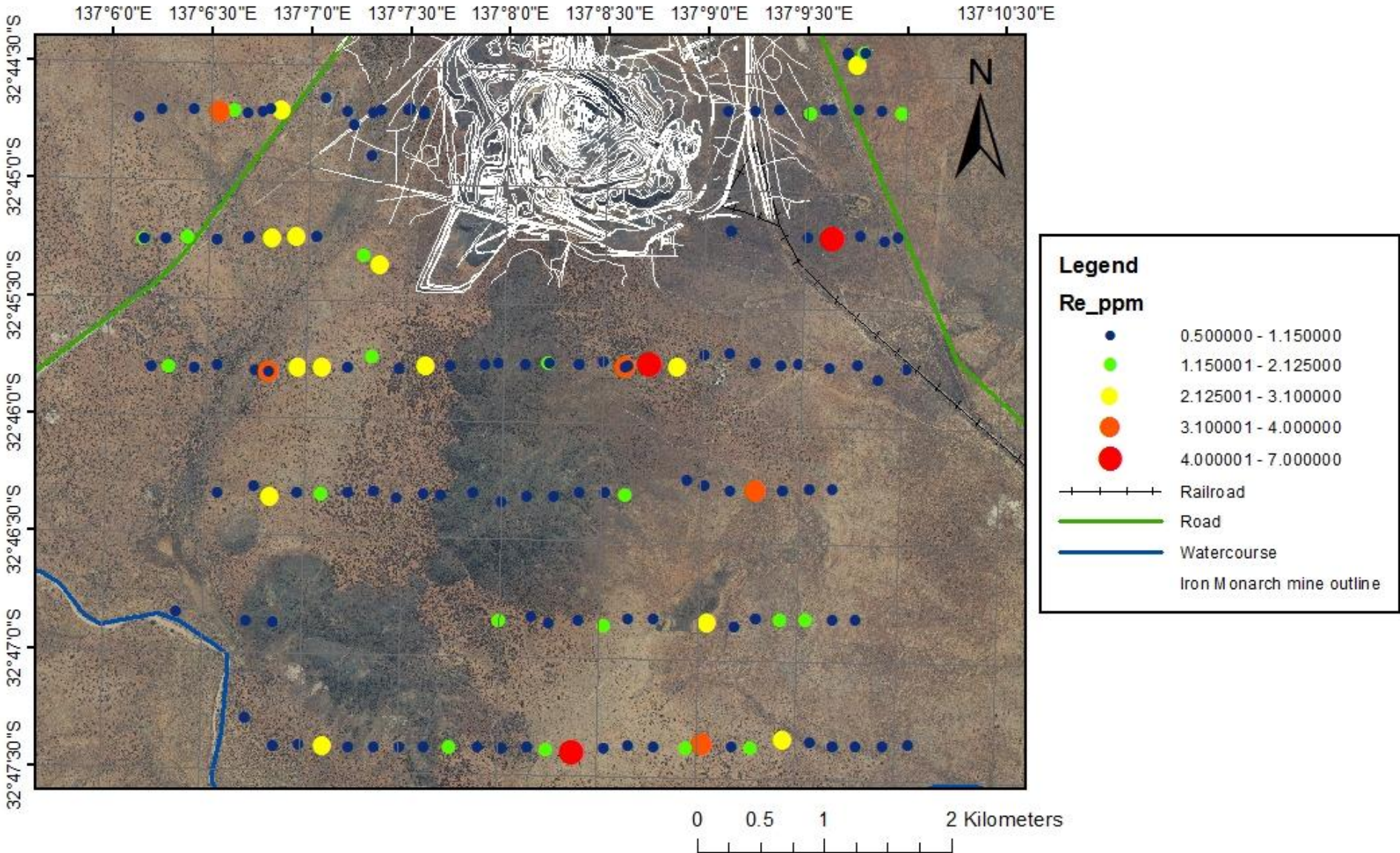
Se concentration (ppm)

1:40,000

Legend

Se_ppm

- 0.050000 - 0.240000
- 0.240001 - 0.430000
- 0.430001 - 0.525000
- 0.525001 - 0.715000
- 0.715001 - 1.000000
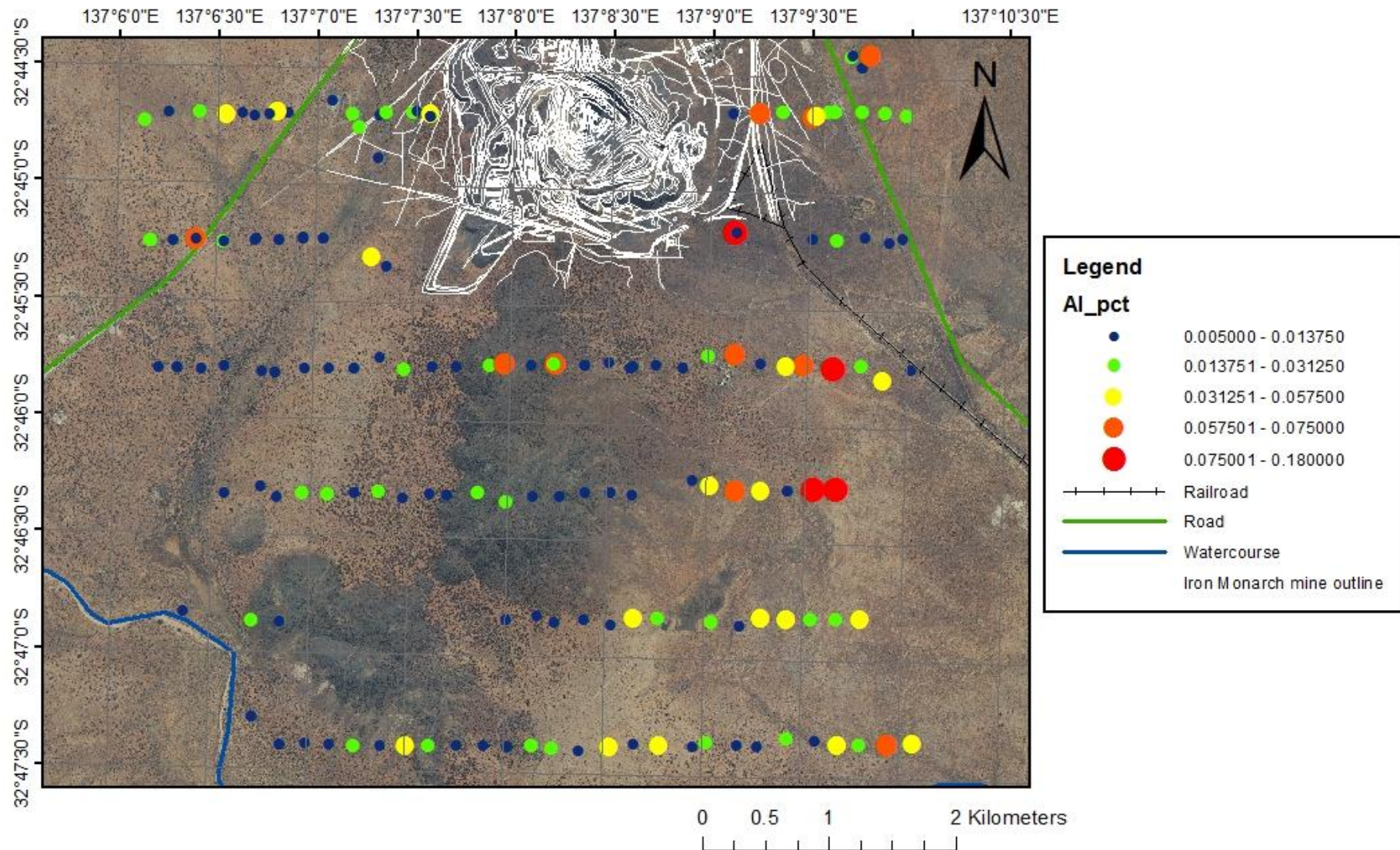
Railroad
Road
Watercourse
Iron Monarch mine outline
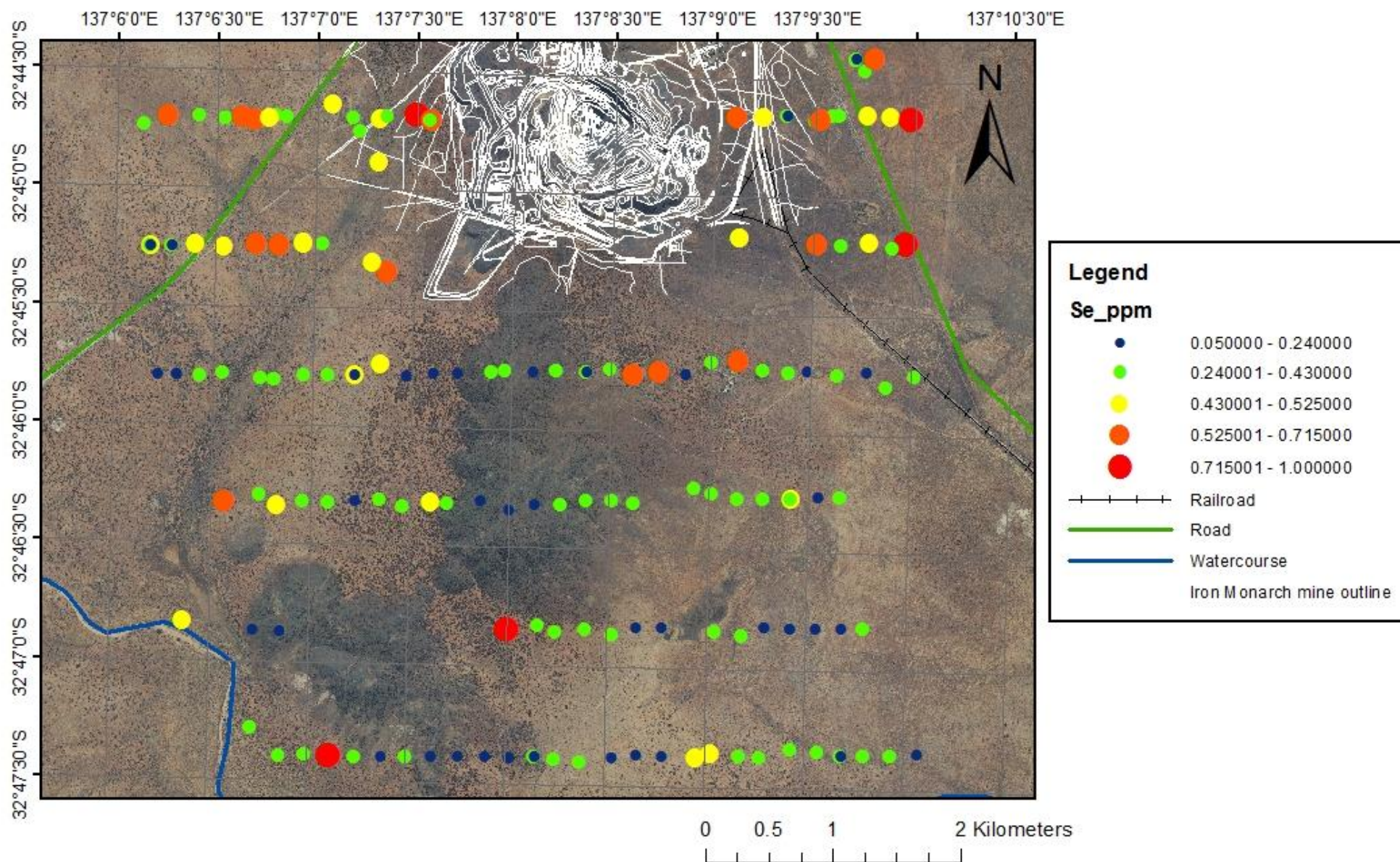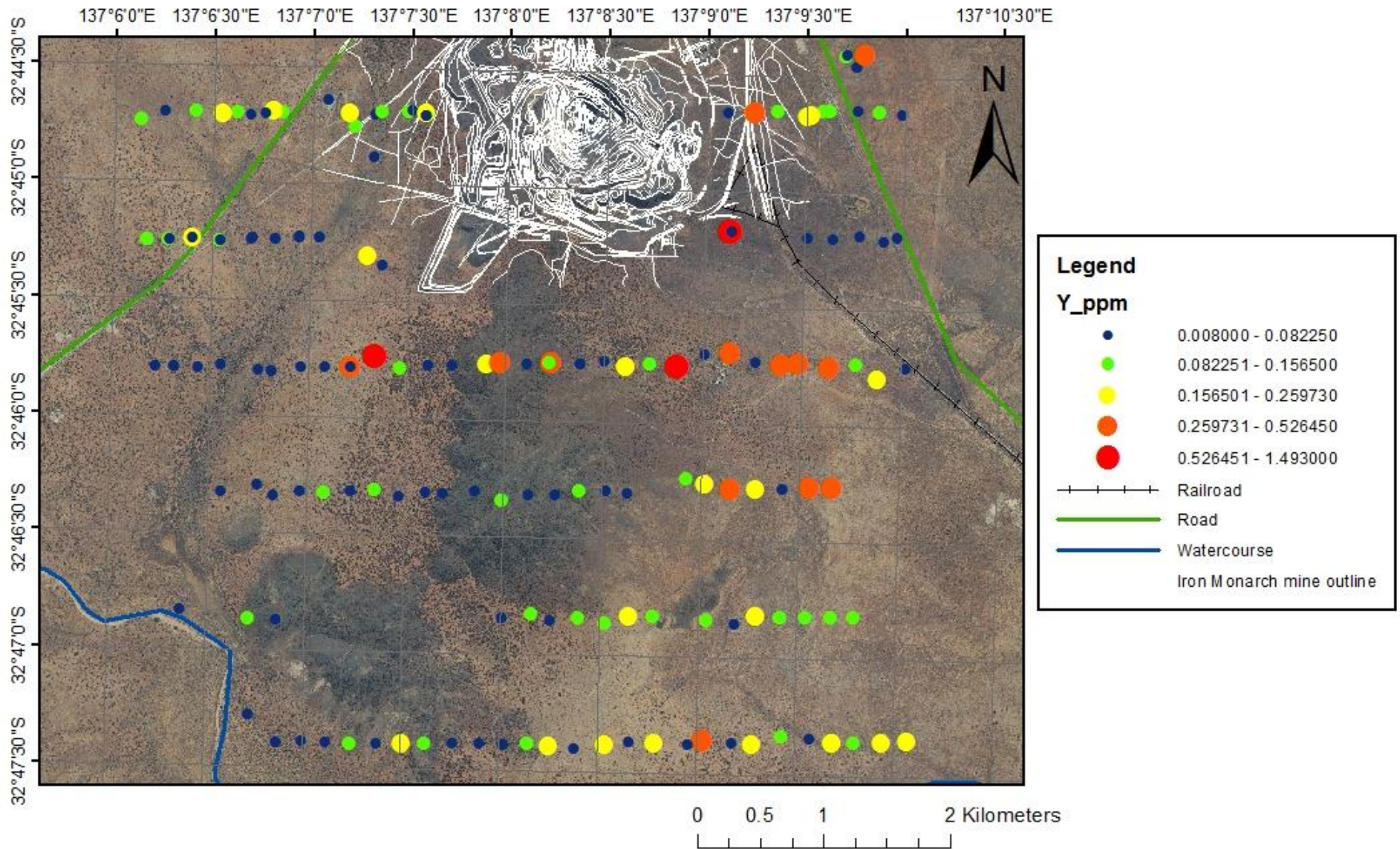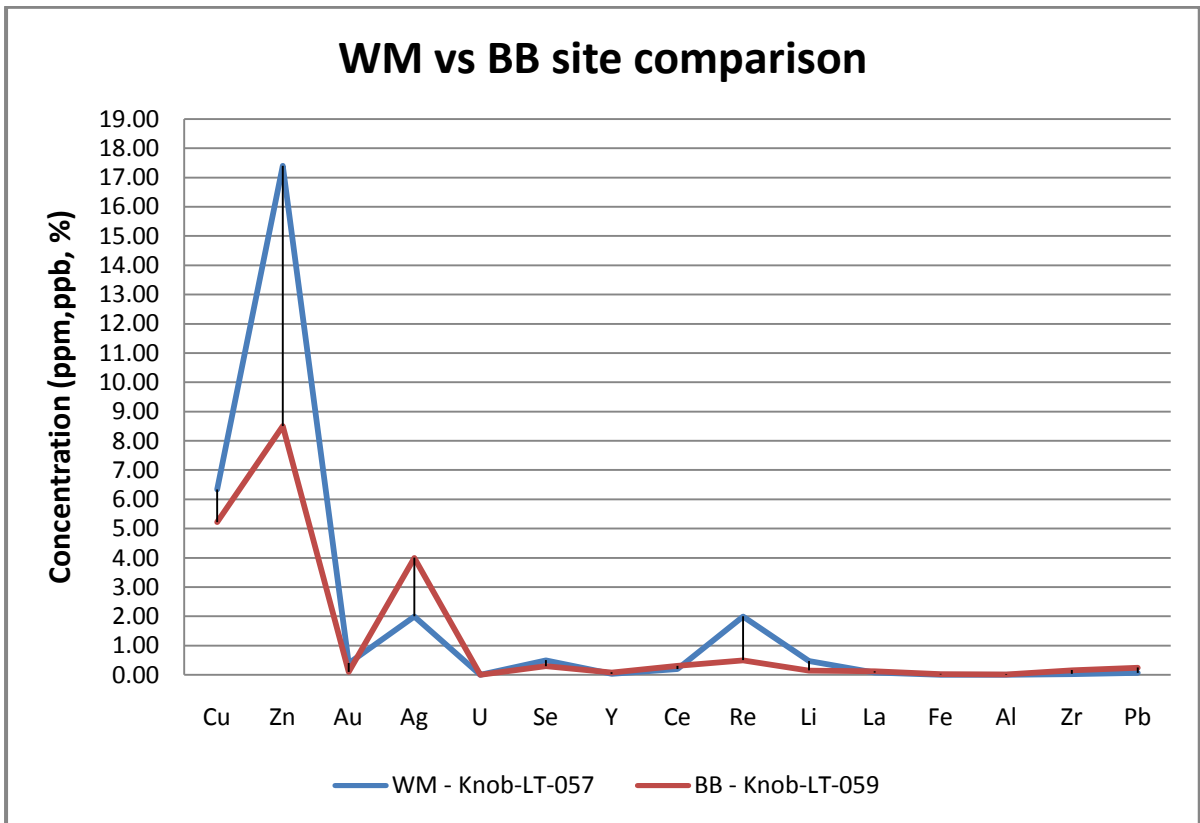
Li concentration (ppm)
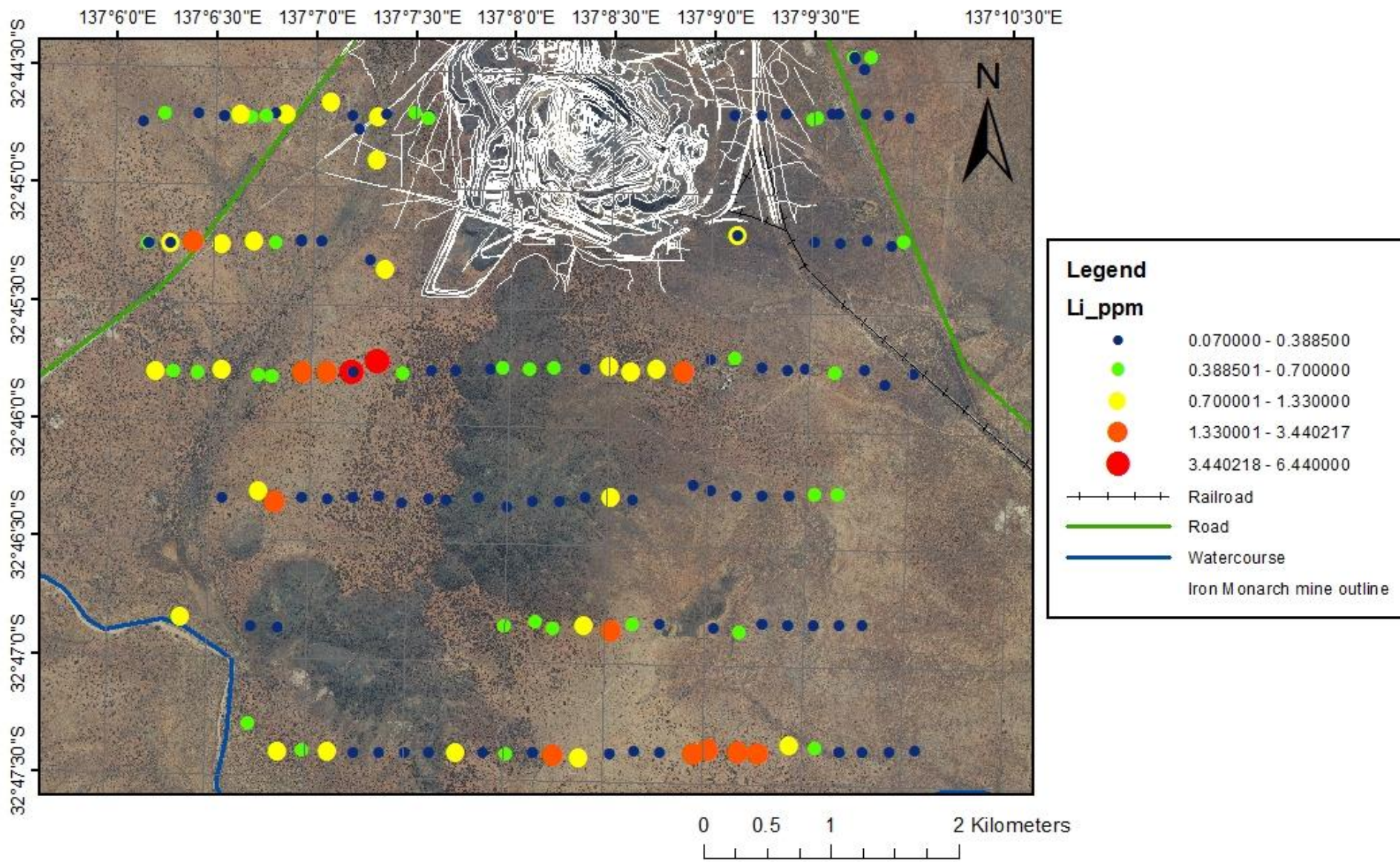
1:40,000

La concentration (ppm)
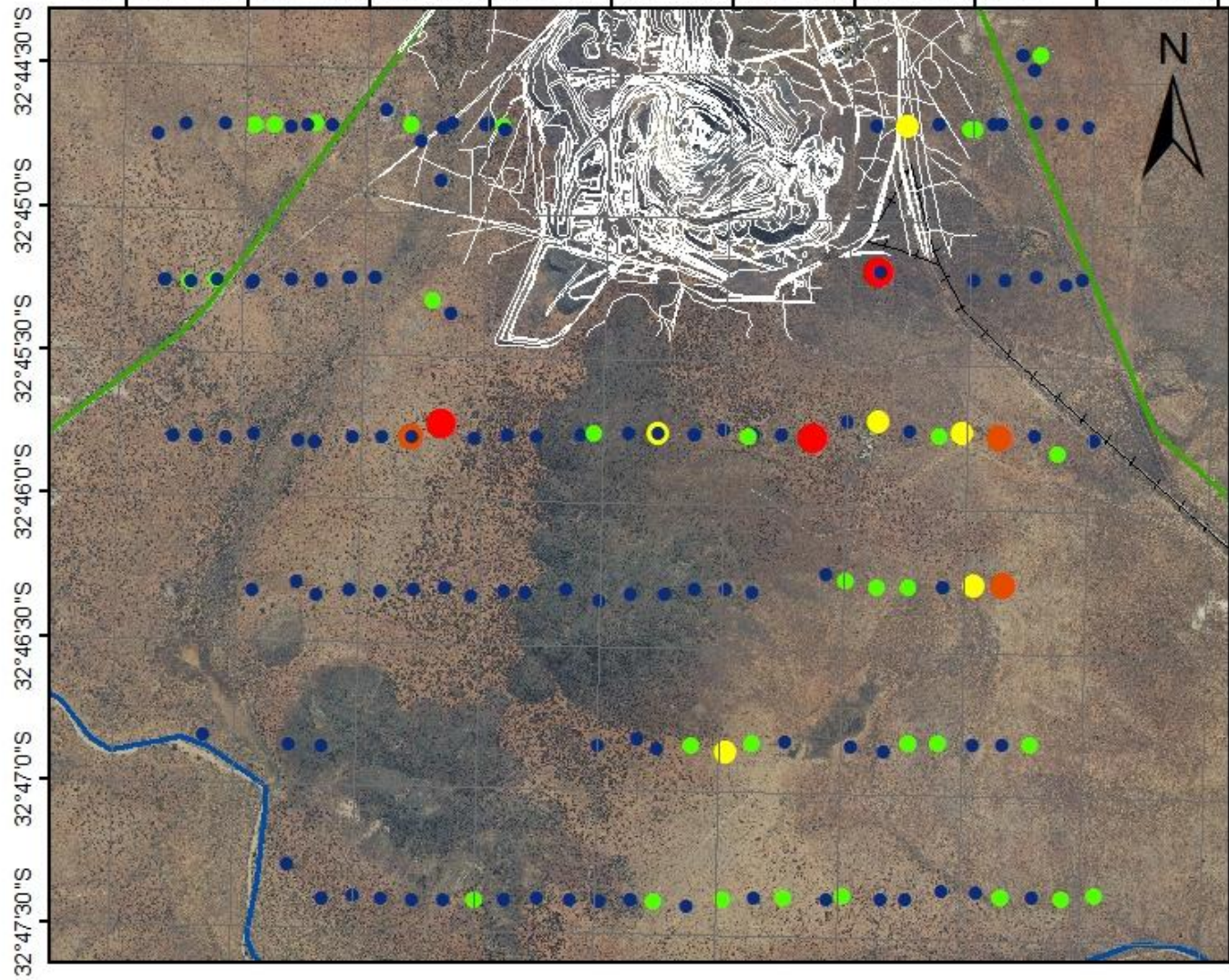
1:40,000

Legend

La_ppm
- 0.005000 - 0.200750
- 0.200751 - 0.396500
- 0.396501 - 0.592250
- 0.592251 - 0.788000
- 0.788001 - 3.920000

+—+—+ Railroad

——— Road
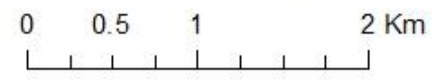
——— Watercourse

Iron Monarch mine outline

Pb concentration (ppm)
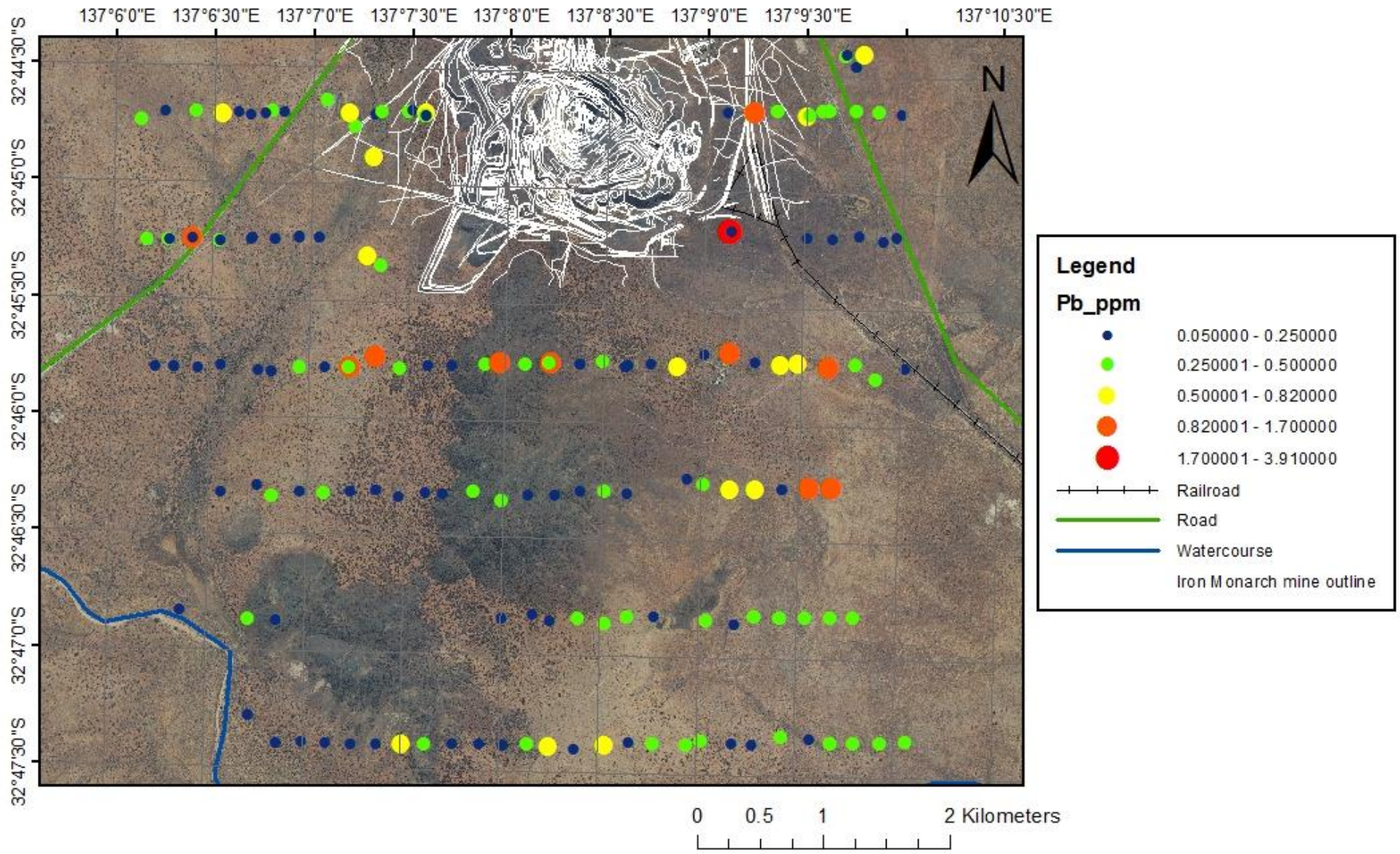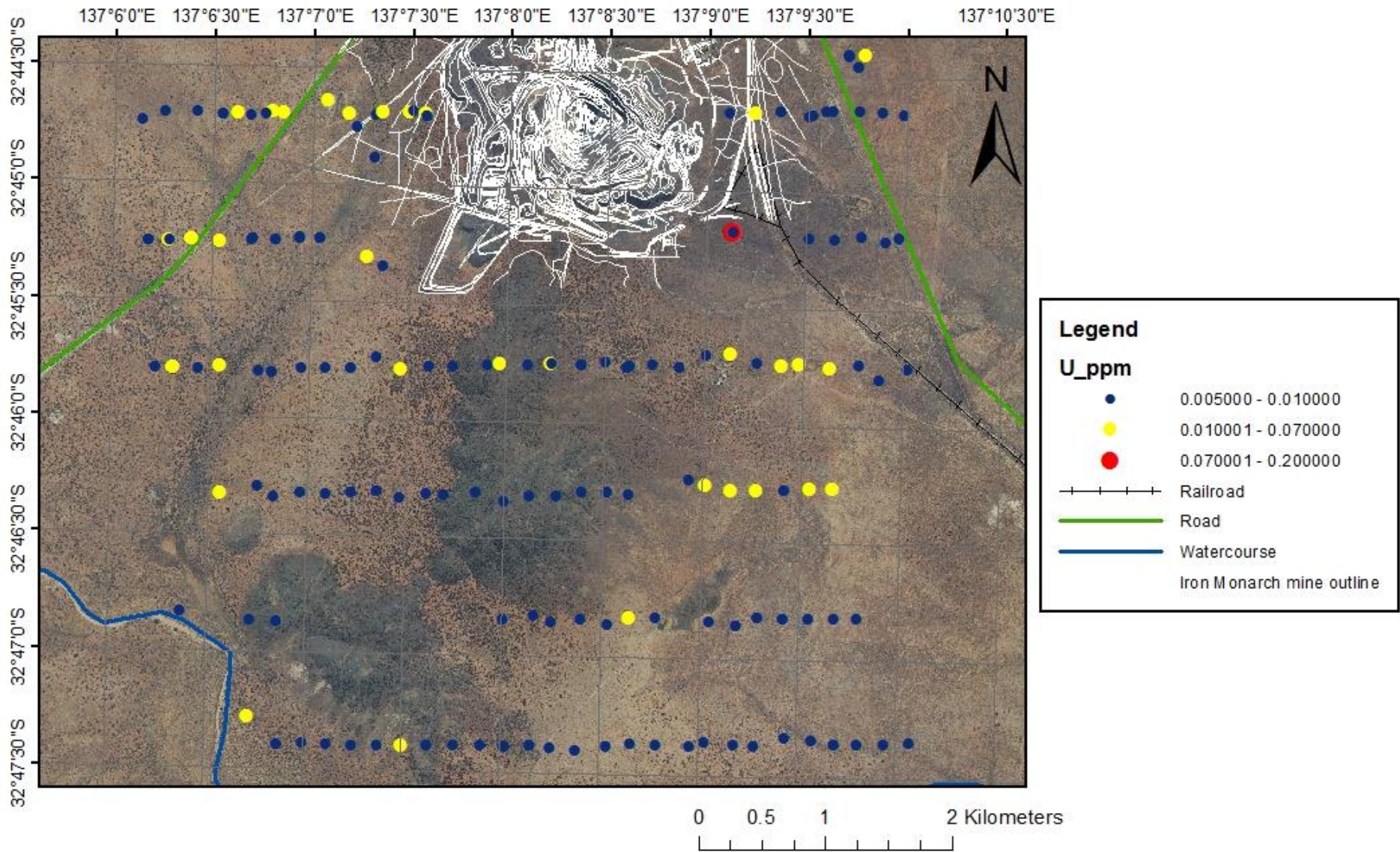
1:40,000

Zr concentration (ppm)

1:40,000

Legend

Zr_ppm
- 0.010000 - 0.090000
- 0.090001 - 0.240000
- 0.240001 - 0.390000
- 0.390001 - 0.580000
- 0.580001 - 1.460000

---+---+--- Railroad
——— Road
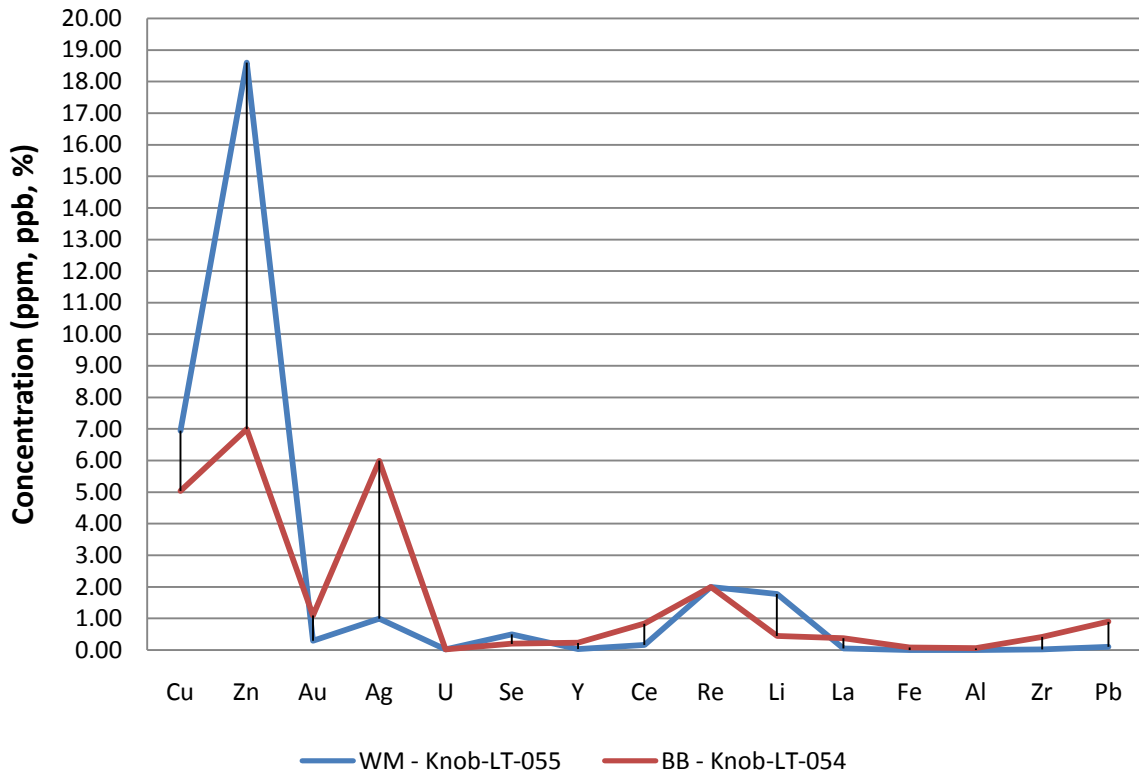——— Watercourse
Iron Monarch mine outline
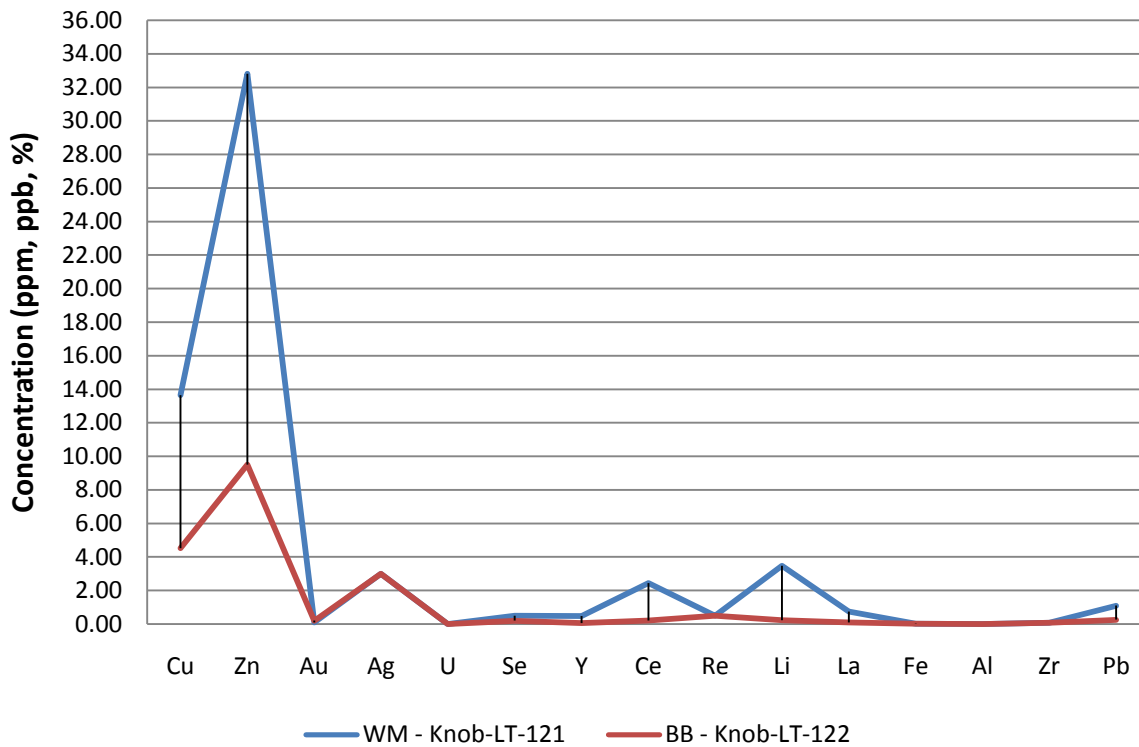
0   0.5   1   2 Kilometers
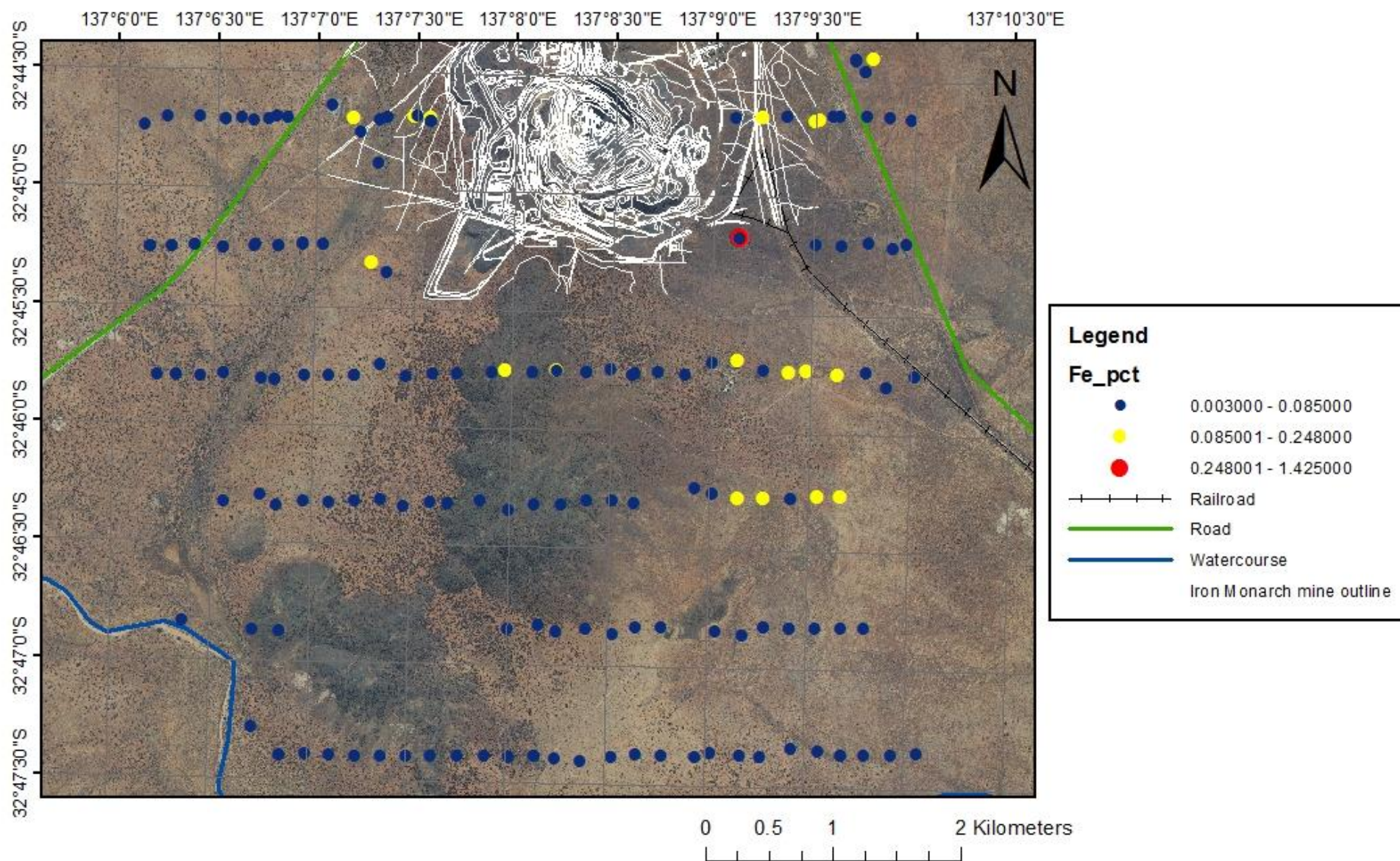
Western Myall vs. Bluebush site comparisons (BB = red), (WM = Blue)

WM vs BB site comparison

Y-axis: Concentration (ppm,ppb, %)
X-axis: Cu, Zn, Au, Ag, U, Se, Y, Ce, Re, Li, La, Fe, Al, Zr, Pb

— WM - Knob-LT-057   — BB - Knob-LT-059

WM vs BB site comparison

Y-axis: Concentration (ppm, ppb, %)
X-axis: Cu, Zn, Au, Ag, U, Se, Y, Ce, Re, Li, La, Fe, Al, Zr, Pb

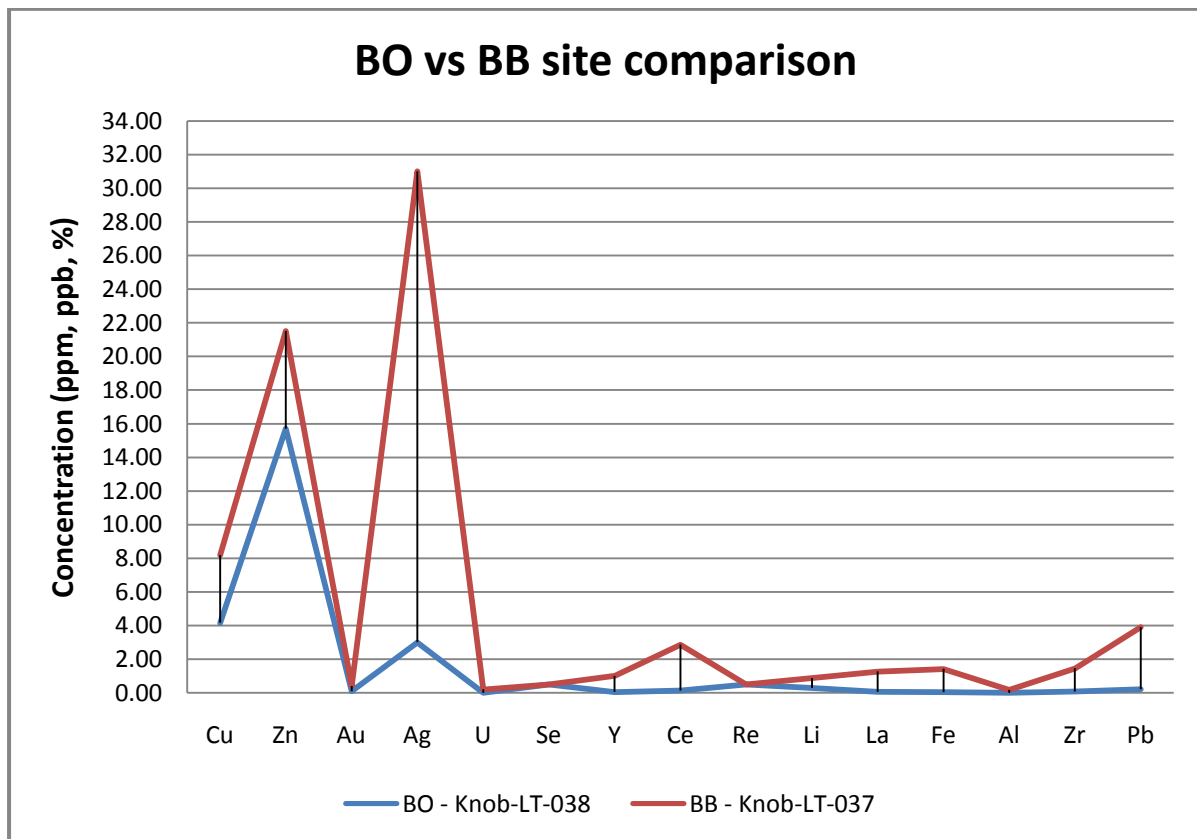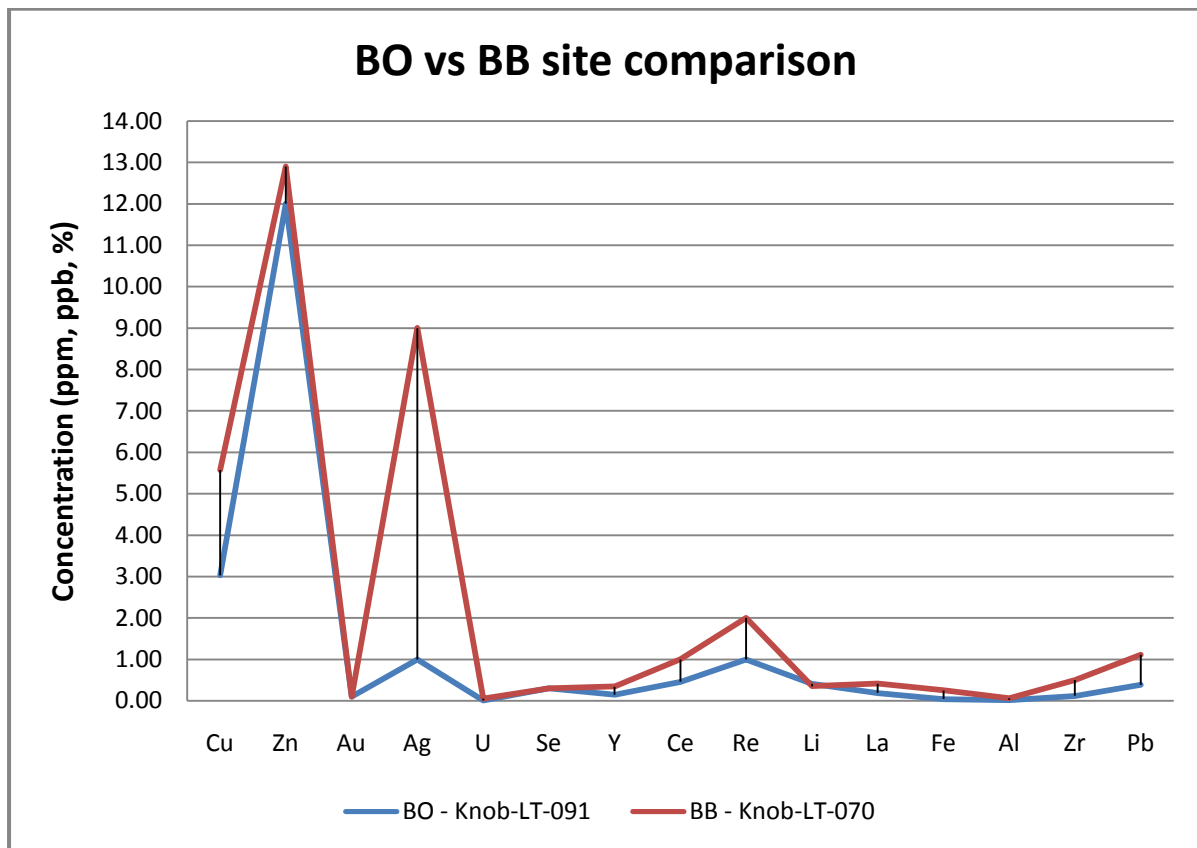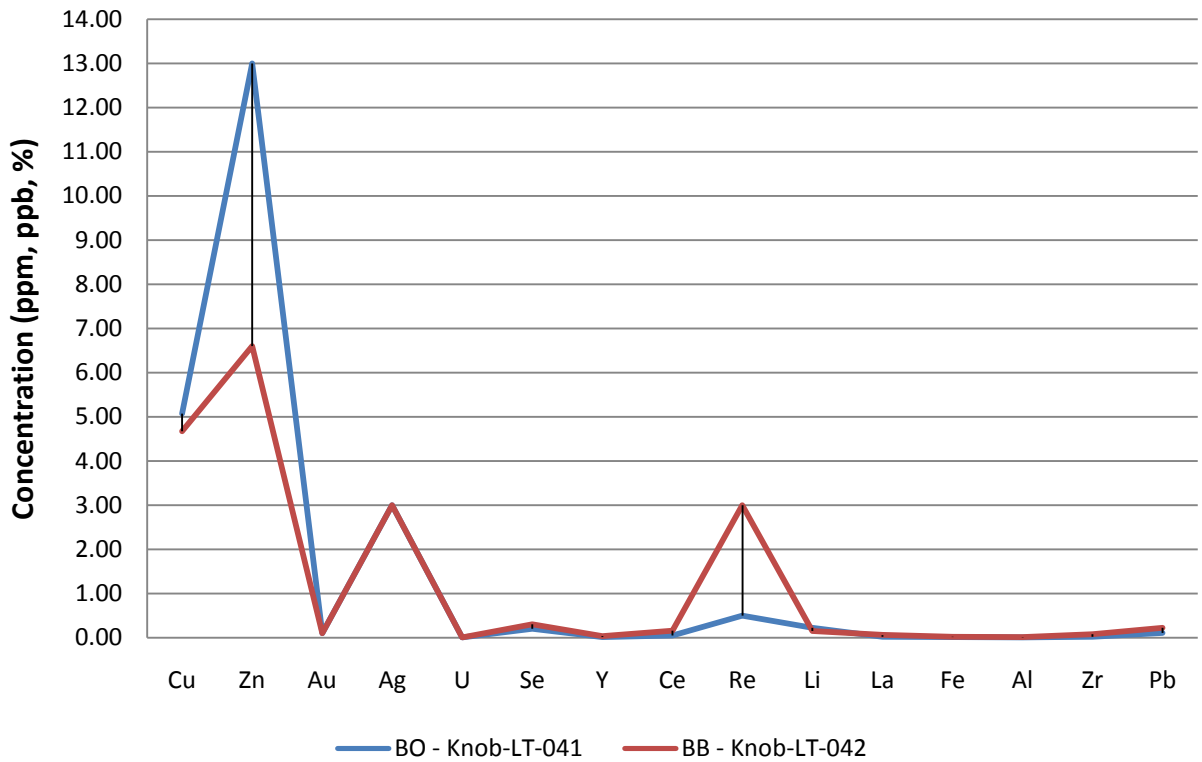— WM - Knob-LT-056   — BB - Knob-LT-058
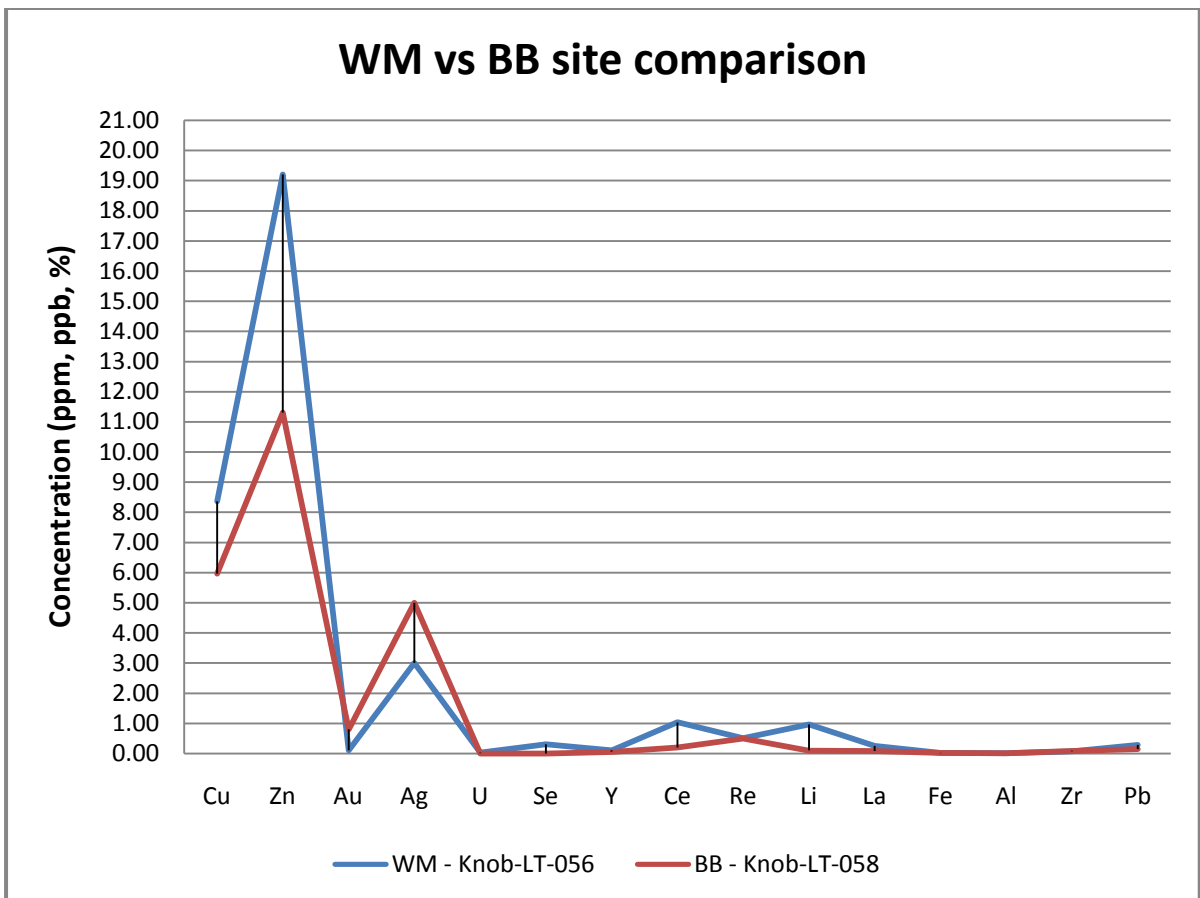
WM vs BB site comparison

WM vs BB site comparison

Blackoak vs. Bluebush site comparisons (BB = red), (BO = Blue)

BO vs BB site comparison

BO - Knob-LT-091 — BB - Knob-LT-070

BO vs BB site comparison

BO - Knob-LT-038 — BB - Knob-LT-037

BO vs BB site comparison

BO vs BB site comparison